THE PROCEEDINGS OF
THE PHYSICAL SOCIETY
Section B

VOL. 65, PART 5 1 May 1952 No. 389 B

The Texture of Diamonds used for Counting α, β or γ Particles as found from Divergent-Beam X-Ray Photographs

BY H. J. GRENVILLE-WELLS
University College, London

Communicated by K. Lonsdale; MS. received 24th October 1951

ABSTRACT. Since the radiation-counting efficiency of diamonds is a structure-sensitive property, x-ray experiments have been undertaken to see whether it is related to crystal texture. A technique for obtaining divergent beam photographs superimposed on Laue photographs has been developed, and results are given for 28 out of 38 colourless octahedral diamonds (edge 1–3 mm) whose ultra-violet transparency, β-particle counting efficiency and fluorescence are known. The relative strength of the anomalous extra x-ray reflections generally found for comparatively perfect diamonds has also been determined for these 38 specimens. Counting efficiency does not seem to be closely related to texture and, in particular, mosaicity is not a necessary condition.

§ 1. INTRODUCTION

It has now been established (Champion 1952) that diamond crystals can count α-, β- and γ-radiation. The counting efficiency, however, like many other properties of diamond, is markedly structure-sensitive, and there is quite a good correlation between β-particle counting efficiency and ultra-violet transparency.

According to Robertson, Fox and Martin (1934) ultra-violet-transparent diamonds are generally mosaic in the x-ray sense, and this was confirmed by Lonsdale (1947) from divergent beam photographs. There has been some speculation, therefore (Lonsdale 1948, Hofstadter 1948), as to whether the counting efficiency is related to the crystal texture. Further, since it has been shown by Lonsdale (1942) that ultra-violet-transparent diamonds do not show the anomalous x-ray streaks characteristic of the more common ultra-violet-opaque diamonds, it appeared possible that there might be an inverse correlation between counting efficiency and these anomalous streaks.

This divergent-beam technique was therefore developed to investigate the correlation, if any, between the mosaicity of diamond and its ability to function as a radiation counter, for, although the possibility that the mobility of electrons in counting diamonds might be connected with submicroscopic cracks and flaws has been discussed, there is as yet no experimental evidence. Information on the presence or absence of extinction—and hence on crystal texture—could be obtained from rotation photographs, but the results are more difficult to extract and less easy to interpret; the quality of the divergent beam photographs obtainable from diamond varies over such a wide range (Lonsdale 1947) that this method appeared to offer the most satisfactory approach.

X-ray measurements were therefore made on 38 specimens from a large collection of colourless octahedral diamonds whose ultra-violet transparency and β-particle counting efficiency have been determined by Dr. F. C. Champion (1952). The octahedral edge length of these specimens was 1–3 mm.

§ 2. GEOMETRICAL CONSIDERATIONS

A photograph of a stationary crystal of suitable size and mosaic texture taken using a divergent beam of X-radiation shows a system of dark and light conics. Lonsdale (1947) has given a comprehensive account of the interpretation of such photographs, particularly as obtained when using a specially constructed wide-angle tube.

The conics observed are actually the intersections with the film of a series of cones, originating at the point of divergence of the X-radiation, directed along the normals to the sets of planes (*hkl*), and having semi-solid angles $[90°-\theta_{hkl}]$, where θ_{hkl} is the Bragg angle. Since the form of the system of conics is dependent on the Bragg angles, different, though analogous, patterns will be obtained from the same crystal when different radiations are used. Such patterns can conveniently be represented on stereograms as in fig. 2(*a*).

§ 3. EXPERIMENTAL TECHNIQUE

A large number of diamonds were examined for differences of texture, most of them somewhat smaller than the optimum size for CuKα divergent beam photographs (Lonsdale 1947); it was therefore to be expected that they would give good FeKα divergent beam photographs, since the mass absorption coefficient of FeKα in carbon is 10·75, as opposed to 5·5 for CuKα. This was very convenient, because fluorescent FeKα radiation can be readily excited by CuKα radiation (Geisler, Hill and Newkirk 1948), and, as copper radiation was being used for most of the extended investigation of diamonds of which this work forms part, it was possible to develop a simple technique for the rapid testing of a number of specimens.

Trial photographs showed that an iron foil 5 μ thick would produce a good divergent beam pattern and still transmit an appreciable quantity of the characteristic CuKα component of the incident beam. This was a necessary condition, as the presence or absence of the anomalous extra reflections could then be determined simultaneously with the divergent beam pattern for appropriate crystal settings.

At first a small piece of iron foil was glued on to the crystal, but it was difficult to cut such small pieces exactly the same size, and the photographs obtained from different diamonds were not strictly comparable, for it was found from a series of photographs taken with the same crystal that the visibility of the conics on photographs of the same exposure time was quite strongly dependent on the size of the foil. Accordingly a piece of iron foil 5 μ thick and 0·5 mm square (the optimum size as determined from the above series of photographs) was stuck on a thin sheet of paper and mounted on a brass cap which fitted the standard Unicam collimator (fig. 1) and thus was almost in contact with the crystal. Since the diameter of the collimator was 1 mm, an appreciable amount of the incident pencil of X-rays actually passed round the foil, and in photographs of sufficiently large crystals hollow Laue spots due to this arrangement can be seen. A typical iron-foil photograph is shown in fig. 2(*b*) (Plate), and the corresponding stereogram is given in fig. 2(*a*), so that the conics associated with the various planes (*hkl*) can be identified. The weak diffraction ring due to the paper on which the foil was glued did not interfere with the pattern obtained, and no better method was found for mounting the foil, since almost anything will give a diffraction ring of some kind. The CuKα and β powder rings from the iron foil can, of course, also be seen. Diamond octahedra of edge 0·5–2·0 mm (approximately) give good FeKα photographs.

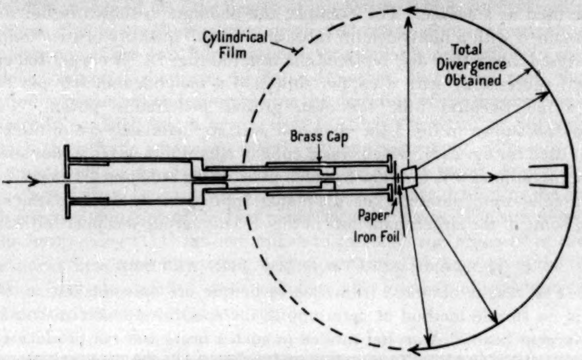

Fig. 1. Experimental arrangement.

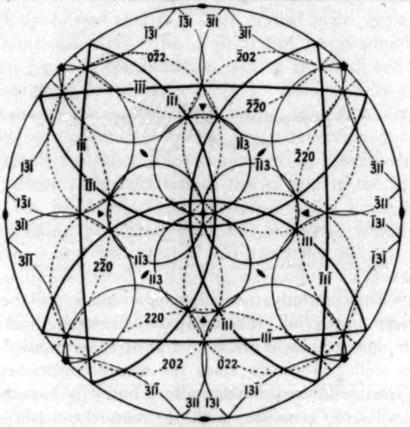

Fig. 2 (*a*). Stereogram showing typical pattern obtained with divergent FeKα radiation and a diamond crystal.

———————— = {111} = conics associated with the form {111}.

- - - - - - - - - = {220} = conics associated with the form {220}.

———————— = {311} = conics associated with the form {311}.

Extension to More Penetrating Radiation

Since this technique only requires that the incident beam should excite fluorescent radiation in a thin foil, it is not confined to a copper x-ray source, and if a more penetrating radiation than FeKα is required, a molybdenum tube can be used as a source. For example, the photograph shown in fig. 3 (Plate) was obtained with a molybdenum tube, and a small quantity of strontium oxide compressed into a thin disc replaced the iron foil (fig. 1). A copper foil can also be used successfully with a copper tube and a molybdenum foil can be used with a molybdenum tube for even greater penetrating power. For the photograph shown in fig. 3 the diamond was approximately 5 mm thick. The crystal used for fig. 2 (*b*), which was a cube of edge 1 mm, gives a poor strontium Kα photograph, as it is too thin for such penetrating radiation. Good strontium photographs were obtained for diamonds approximately 3–8 mm thick. For testing some of the larger diamonds in this 1–3 mm group a copper foil was used.

§4. LIMITATIONS OF THE METHOD

(*a*) The results obtained from this technique are only qualitative, because there is no simple method of determining the spectral intensity distribution in the divergent beam. A crystal rotated in such a beam will not produce a streak in the way that it does in a collimated beam, and although the fluorescent radiation itself will be strictly monochromatic, there will be some scattering of the primary beam in the foil. The comparatively strong background scattering present on Laue photographs of diamond will be superimposed on the divergent beam pattern as well. However, since the measurements required here were essentially comparative, this did not matter; but it is hoped that quantitative measurements will be possible with a monochromatic divergent beam (Grenville-Wells 1951).

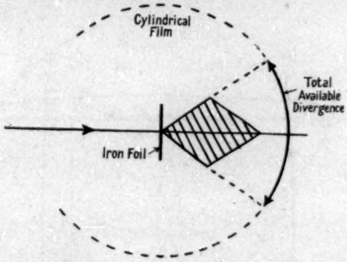

Fig. 4. Unfavourable orientation for an octahedron.

(*b*) In view of the fact that the crystal is much smaller than the diameter of the collimator cap, the total divergence is limited to 180° (fig. 1).

(*c*) The fact that the crystals used were all octahedra had an important bearing on the usefulness of the method for the rapid testing of a number of diamonds, when it was desired to determine from a single photograph both the texture (divergent beam conics) and the presence or absence of extra streaks accompanying the Bragg reflection from the octahedral planes. An octahedral face can be laid flat against the foil as in fig. 1, and the full 180° divergence can then be utilized, but in any other orientation much of the divergence will be wasted, the most unfavourable case for an octahedron being shown in fig. 4. All divergent beam photographs were therefore taken in the optimum orientation, with the beam along [111], which gives a Laue photograph such as that shown in fig. 5 (*a*) (Plate). In this orientation three octahedral planes are near to the Bragg position if CuKα radiation is used, and the degree of mis-setting which results from purely visual orientation of a well-developed octahedral crystal almost invariably means that at least one of the octahedral planes is in a suitable orientation to show the anomalous streaks if they are present. However, it can be seen that this orientation is not nearly so favourable for the detection of the extra reflections as that shown in fig. 5 (*b*), for the crystal used to obtain these two photographs was one which showed the anomalous streaks extremely strongly. The good 'extra effect' orientation of fig. 5 (*b*) is, however, close to the worst divergent beam orientation as defined by fig. 4, and thus cannot be used to determine the strength of both effects simultaneously. This meant that the divergent beam photograph with the beam along [111] did not suffice to establish the presence of the extra streaks unless these were very strong, and an additional photograph in the fig. 5 (*b*) orientation was also needed, thus reducing the number of specimens which could be examined in the time available.

§ 5. DIVERGENT BEAM PHOTOGRAPHS USING THE DIVERGENCE OBTAINABLE WITH A COMMERCIAL X-RAY TUBE

Borrmann (1950) showed that if a large crystal plate was fixed against the window of a commercial x-ray tube, a divergent beam photograph could be obtained by making use of the radiation issuing in all directions through the window (total divergence of the order of 20°). Using a very perfect crystal of calcite, he demonstrated the extremely surprising result that instead of obtaining an *absorption conic* in the direction of the Bragg reflection, there was in fact a *dark line*. The result has since been confirmed by Campbell (1951) using a Geiger counter. Here the perfection of the crystal is the crucial factor; an attempt to find the same effect for diamond failed completely, the usual absorption conics being produced even for a crystal which showed strong anomalous reflections and was opaque to ultra-violet radiation below 3 000 Å, characteristics usually associated with crystal perfection. This cannot perhaps be considered a fair test because the crystal was far too thin for the necessary absorption conditions to be fulfilled. However, Borrmann (private communication) also reports that he was unable to find the effect in diamond, although many specimens were tested.

The diamond photographs are of some interest, however, because whereas the foil technique discussed above requires exposures of the order of two hours, Borrmann's conditions approximate to the method used by Lonsdale (1947) in which the exposure necessary for a diamond about 1·5 mm thick with CuKα radiation is of the order of 5 seconds. In the course of this work, therefore, a rapid test of this kind was evolved and tried on a number of specimens. A series of brass washers fitting over the window of a Machlett tube was made with central holes varying from 2·5 to 5·0 mm in diameter to accommodate diamonds of various sizes; the diameter of the hole thus limits the divergence of the beam, so that the method is only applicable to large crystals.

Two polished diamond plates kindly lent by Mr. B. W. Anderson were tested in this way. One is a Type I and the other a Type II, on the basis of ultra-violet absorption and anomalous x-ray streaks. Both gave equally good divergent beam patterns. This is probably merely an example of the demonstrable inhomogeneity of many large diamonds, since imperfect regions in a predominantly Type I specimen would suffice to produce the divergent beam pattern.

Properties of Diamonds which count β-Particles

(1)	(2)	(3)	(4)	(5)	(6)	(7)	(8)
3½	2255	0	0	0	2	D	0
3½	2260	0	0	0	0	A	0
3	2250	0	½	–	0	B	0
3	2260	0	0	3	2	C	x
3	2250	0	0	3	3	C	0
3	2345	0	3	0	0	B	0
3	2350	1½	0	–	0	A	0
3	2360	3	3	1½	1	C	x
3	2590	0	0	0	0	A	0
3	2620	0	1½	0	1	B	0
2½	2245	0	½	0	½	D	0
2½	2260	0	2½	½	0	A	0
2	2250	0	½	3	2	C	xx
2	2250	0	0	3½	2	C	0
2	2370	0	1½	3	2	C	0
2	2470	0	2	1½	3	C	0
2	2690	0	½	1	2	D	0
2	2700	0	0	2	1	B	0
1½	2660	0	2½	0	1	C	0
1	2100 2900 } split	0	1	0	2	D	0
1	2400	3½	3	1	3	C	xx
1	2400	0	0	–	3	D	xx
1	2725	0	3	1	1	C	0
1	2750	3	½	1½	3	D	0
1	2765	0	½	0	0	D	0
1	2840	0	3	1	0	C	0
0	2890	0	0	–	0	B	0
0	2900	0	3	–	0	A	0
0	2930	0	3½	0	1	B	0
0	2935	0	3	–	0	A	0
0	2940	1½	1½	–	0	A	0
0	2960	1	1	0	2	C	0
0	2960	0	3	½	0	B	0
0	2980	1	1	0	1	B	0
0	2985	0	3	–	0	A	0
0	3000	1½	0	–	0	A	0
0	3040	1½	0	–	0	A	0
0	3080	1	3	1½	3	D	xx

(1) Counting efficiency; (2) u-v absorption edge (Å); (3) fluorescence; (4) extra anomalous x-ray streaks; (5) x-ray divergent beam pattern; (6) anomalous birefringence; (7) morphology; (8) crystalline inclusions.

Symbols :—

Physical properties: 0 = Very weak or absent	Morphology: A = Excellent	Inclusions: 0 = None
1 = Weak	B = Good	x = One
2 = Medium	C = Medium	xx = Several
3 = Strong	D = Bad	
– = Not measured		

§ 6. EXPERIMENTAL RESULTS: DISCUSSION

The experimental results for the 38 diamonds are collected in the table. Since counting ability is the main property under consideration, the specimens have been classified in order of decreasing counting efficiency. Within each group of equal counting efficiency, the specimens are listed according to ultra-violet transparency, the most transparent specimen being listed first. The morphological classification is only intended to give a general indication of the *relative* perfection of the specimens (all of which appear to the naked eye to be well-formed octahedra) when viewed with a magnification of 50 ×. It must be emphasized that, with the exception of the position of the ultra-violet absorption edge, all the statements given here, such as 'good divergent beam pattern' or 'weak x-ray anomalous streaks', are relative values obtained with the particular experimental conditions used, and do not have absolute significance.

There are two main points of interest in these results. The first is the comparative independence of the two x-ray effects considered, namely the divergent beam pattern and the anomalous streaks. From a study of a number of specimens Lonsdale (1942, 1947) had found that diamonds almost always showed one effect or the other; both were not present or absent together. If the specimen was relatively perfect, showing strong primary extinction but no secondary extinction (and hence no divergent beam pattern), then the anomalous streaks would be strong, while if the specimen was a mosaic crystal showing little primary extinction but strong secondary extinction (and hence good divergent beam photographs), then there were no anomalous streaks. Now if such an inverse correlation existed for the specimens considered here, the sum of the numbers in columns (4) and (5) of the table should be 3 for each specimen, and it can be seen that this is far from being the case. In particular, there are specimens in which neither effect occurs.

The second point of interest is that it is the specimens in which neither effect occurs which are the best (grade $3\frac{1}{2}$) counters, proving that neither effect is necessary for radiation counting to be possible. In particular, mosaic structure—as defined by the ability to obtain divergent beam photographs—instead of being the reason for the counting ability of Type II diamonds, tends to be found among the poorer counters. Further, while good counting efficiency seems in general to go with the absence of the anomalous streaks, this rule is by no means hard and fast. It would appear, indeed, that counting efficiency is nearly, if not quite, independent of x-ray texture, but it would be unwise to generalize from the results on these few specimens.

Another point of interest is the lack of correlation between morphology and the type of diamond. In a collection of 175 octahedra, from which these specimens were drawn, 30% had an ultra-violet absorption edge below 2 800 Å, and were hence classified as Type II. This is by far the largest proportion of a single batch of any size ever obtained, and the morphology of many of these, even with a magnification of 50 ×, appeared excellent. It is clear, therefore, that morphology is not a reliable guide in the selection of Type II specimens. It is felt, moreover, that the high proportion of Type II specimens obtained is directly connected with the small size of the specimens, which are probably fairly homogeneous. When, as is usual, larger specimens are tested, the presence of some admixture of Type I would suffice to prevent ultra-violet transparency, and a far smaller number of Type II would be recorded. Unfortunately, the origin of these specimens cannot be ascertained; it is quite possible that they are a mixed batch, and tests on specimens of known origin would be desirable.

ACKNOWLEDGMENTS

I am grateful to the Diamond Corporation for the provision of gem diamonds, and to Industrial Distributors (1946) Ltd. for financial assistance enabling me to undertake the research of which this work forms part. It is a pleasure to thank my supervisor, Professor Kathleen Lonsdale, for continued interest and helpful discussions during the course of the work.

REFERENCES

Borrmann, G., 1950, *Z. Phys.*, **127**, 297.
Campbell, H. N., 1951, *Acta Crystallogr.*, **4**, 180.
Champion, F. C., 1952, *Proc. Phys. Soc.* B, **65**, in the press.
Geisler, A. H., Hill, J. K., and Newkirk, J. B., 1948, *J. Appl. Phys.*, **19**, 1041.
Grenville-Wells, H. J., 1951, *Acta Crystallogr.*, **4**, 563.
Hofstadter, R., 1948, *Phys. Rev.*, **73**, 631.
Lonsdale, K., 1942, *Proc. Roy. Soc.* A, **179**, 315; 1947, *Phil. Trans. Roy. Soc.* A, **240**, 219; 1948, *Phys. Rev.*, **73**, 1467.
Robertson, R., Fox, J. J., and Martin, A. E., 1934, *Phil. Trans. Roy. Soc.* A, **232**, 463.

Non-Linear Amplification in E.M.I. Photomultipliers

By J. F. RAFFLE and E. J. ROBBINS
Nuclear Physics Research Laboratory, University of Liverpool

Communicated by H. W. B. Skinner; *MS received 26th November* 1951

ABSTRACT. The output pulse heights obtained from E.M.I. photomultipliers are found not always to be proportional to the quantity of light incident on the photo-surface of the photomultiplier. The photomultiplier ceases to be a linear amplifier of the incident light pulses when the charge density in the multiplier becomes too great.

The relation between pulse height and energy loss of alpha-particles in various fluorescent materials has been determined at low values of charge density.

During an investigation of the pulse heights produced by alpha-particles in various scintillating crystals in conjunction with an E.M.I. 5311 photomultiplier, it was found that the shape of the curves of pulse height against energy obtained depended on the voltage applied to the multiplier. We have found that the amplification of pulses is modified by the instantaneous charge density in the later stages of the multiplier and is therefore dependent on the magnitude and duration of the light pulses from the crystal and on the applied multiplier voltage.

A collimated beam of alpha-particles from a thin thorium active deposit on a brass plate was allowed to fall on to a thin crystal resting on the surface of the multiplier. The charge generated in the multiplier was integrated by the anode to ground capacity of the tube and amplified by a Los Alamos Type 100 linear amplifier. The two groups of alpha-particles from the ThC and ThC′ produced two groups of pulses, each with an amplitude spread of about 10%, and the mean pulse height of the larger group was determined. The energy lost in the crystal by the alpha-particles was varied by altering the distance between the source and the crystal. By using range–energy curves of alpha-particles in air, correcting for the temperature and pressure of the air, a curve of pulse height against energy loss was constructed. The results for thin crystals of anthracene and potassium iodide (thallium activated) are shown in figs. 1 and 2. Two curves were obtained for each crystal corresponding to about 45 volts/stage and 90 volts/stage applied to the multiplier. The ordinates of the curves were adjusted to coincide at an alpha-particle energy of 8·6 MEV. The pulse heights at the anode of the multiplier produced by alpha-particles of this energy were 10 millivolts and 4 volts respectively. It is seen that the two curves for each crystal do not coincide as they would if the multiplier behaved as a linear amplifier at both applied multiplier voltages.

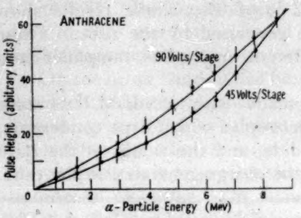

Fig. 1.

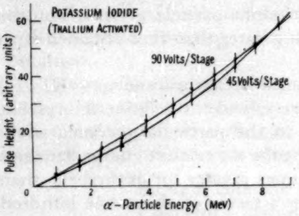

Fig. 2.

Figs. 1 and 2. The shapes of pulse-height–energy curves for alpha-particles obtained at two different voltages applied to an E.M.I. 5311 photomultiplier.

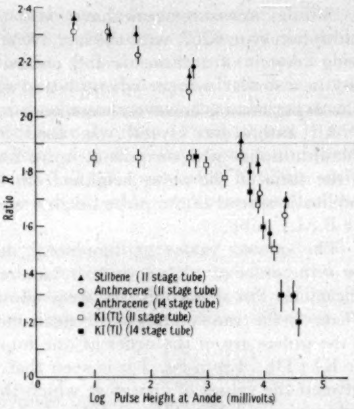

Fig. 3. The variation in the ratio of the output pulse heights from an E.M.I. 5311 photomultiplier obtained from two alpha-particle groups, as a function of the pulse height of the larger group.

In order to investigate this effect further the source was kept at a constant distance from the crystal and the ratios R of the heights of the pulses from the two groups of alpha-particles from ThC and ThC′ were measured for different applied voltages on the tube and hence different magnitudes of output pulse. Figure 3 shows the ratios R plotted against the logarithm of the pulse heights produced by the more energetic group at the anode of the multiplier. It is seen that the ratios fall off as the pulse heights at the anode of the multiplier increase.

The multiplier dynodes were fed from a chain of 47 kΩ resistors and the last three were decoupled with condensers of 150 pF. There was no change in the ratios when the condenser across the last stage was increased to 2000 pF and the two preceding ones to 500 pF, showing the original decoupling to be adequate. When a 100 pF condenser was placed across the 1MΩ anode resistance, the voltage appearing at the anode decreased by a factor of 6. This produced no change in the ratio and indicates that the drop in ratio is not caused by any voltage feedback in the external circuit.

When the initial number of photons reaching the photocathode was reduced by placing absorbing sheets of blue gelatin between the crystal and the multiplier, and maintaining the tube voltage constant, then the ratio of the pulse heights increased: with an anthracene crystal, the output pulse height was decreased by a factor of 8 by placing a gelatin absorber between the crystal and photocathode, and the ratio increased from $2{\cdot}10 \pm 0{\cdot}03$ to $2{\cdot}26 \pm 0{\cdot}03$. These results show that the drop in ratio depends on the charge generated by the tube. These experiments have been repeated with a different multiplier, amplifier and discriminator, with identical results.

Similar measurements have also been made with an E.M.I. 14-stage multiplier, type 6262, with the last five stages decoupled with 250 pF condensers, using crystals of anthracene and potassium iodide, and the values of the ratio vary in a similar manner when plotted against the charge generated in the tube. The experiments, however, were only rough.

An anthracene crystal was used in conjunction with an R.C.A. 931 A photomultiplier with outputs of up to 2 volts. There was no detectable change in the ratio of the pulse heights from the two alpha-particle groups, but the amplitude spread of the pulse heights was much greater than that obtained with the E.M.I. tube.

The quoted values of fluorescent decay times of anthracene and KI (Tl) are of the order of 10^{-8} sec and 10^{-6} sec respectively, and the relative fluorescent efficiencies for alpha-particles were about 1 : 2 in the particular crystals used. Whatever the transit times of the electrons in the tube the relative charge densities in the pulses are of the order of one hundred times greater for anthracene than for KI (Tl). From fig. 3 it is seen that there is a factor of about one hundred between the values of charge at which the ratio begins to fall off in the cases of anthracene and KI (Tl). Similar curves to those in fig. 3 have been obtained with thin crystals of stilbene, 1 : 4 diphenyl butadiene and cadmium tungstate. The two former crystals, with quoted fluorescent decay times of the order of 10^{-8} sec, show similar behaviour to anthracene, while cadmium tungstate shows no drop in ratio up to 4 volts output from the tube.

The E.M.I. tubes employ the Venetian blind type of dynode structure. A grid is stretched over each dynode assembly to screen off the electron accelerating field between it and the previous dynode, for this, if allowed to extend to the secondary emitting surface of the dynodes, would suppress the secondary electrons before they could escape from the surface. The secondary electrons are, therefore, emitted into a region of comparatively field-free space with energies of up to a few volts. It seems likely that, when a pulse of large current density reaches the final stages of amplification, instantaneous space charges may build up in these comparatively field-free regions. It is difficult to estimate the magnitude of the effects of these space charges on the amplification of the pulse. The Coulomb interactions in a space charge are approximately proportional to the square of the number of interacting electrons and may thus cause a reduction in the ratio *R* of the two alpha-particle groups. The space charges may also account for the increased spread in the pulse widths as the applied multiplier voltage increases, as observed by Allen and Engelder (1951) in the E.M.I. 5311 photomultiplier, but the explanation given by these authors, involving an increase in the number of reflected primary electrons as the applied multiplier voltage increases, will not explain a drop in *R*.

If such a space-charge effect occurs for large electron densities then it would be expected that any factor that increases the space charge should cause a further reduction in the ratio. Keeping a constant 80 volts between the dynodes, the voltage between the last dynode and the collector was reduced to 3 volts. This causes a reduction in the ratio of the pulse heights of the two groups from 1·9 to 1·81. By compensating the earth's magnetic field it was shown that the drop in ratio was not produced by losses due to bending of the electrons in the earth's magnetic field.

On the other hand, it has been pointed out to us by Dr. McGee of the E.M.I. Research Laboratories that it may be possible to reduce space charge effects by increasing the voltages applied to the last few dynodes. If the voltages on only the last few dynodes are raised the advantage gained by clearing the space charge more rapidly may be greater than the disadvantage that results from the increased number of electrons. On increasing the voltage between the collector and the last dynode by a factor of 3·1 and between the dynodes 11 and 10, and 10 and 9, by a factor of 2·3 relative to the remaining dynode voltages, we found that the ratio *R* obtained with anthracene did not fall off appreciably until the output pulse became about $\frac{1}{10}$ volt. Thus a considerable improvement has been obtained.

It was also observed that, with the dynode voltages kept constant and the 11th, 10th and 9th dynodes connected successively to the collector and each other, decoupling in each case the last stage of amplification with 150 pF, the ratio of pulse heights with an anthracene crystal increased in the following way:

Ratio at collector	$1{\cdot}80 \pm 0{\cdot}03$
Collector + 11th dynode	$2{\cdot}00 \pm 0{\cdot}03$
Collector + 11th + 10th dynode	$2{\cdot}18 \pm 0{\cdot}03$
Collector + 11th + 10th + 9th dynode	$2{\cdot}27 \pm 0{\cdot}03$

The above results indicate that care should be taken when using photomultipliers of the E.M.I. type. Only at low values of output pulse height will the multiplier be a linear amplifier of the number of photons incident on the photocathode. The value of the output pulse height at which the non-proportionality becomes serious is, in the case of the bombardment of an anthracene crystal by 8 Mev alpha-particles, at about $\frac{1}{10}$ volt. In general it will obviously depend both on the fluorescent decay time of the crystal and the number of electrons released at the photocathode by the light pulse.

The curves of pulse height against energy (figs. 1 and 2), taken at low values of output charge, support the measurements of Taylor, Remley, Jentschke and Kruger (1951) who showed that the relationship between pulse height and energy for heavy particles in NaI and anthracene is a non-linear function of energy. The ratio of the pulse heights from the two groups of alpha-particles is approximately equal to the ratio of the ranges in the case of organic crystals but not in the case of KI (Tl). Preliminary experiments using solutions of *p*-terphenyl in benzene and xylene gave ratios also proportional to the ranges at low values of output charge, indicating a pulse-height–energy distribution similar to that of anthracene.

ACKNOWLEDGMENT

We wish to thank Dr. J. D. McGee, of E.M.I. Research Laboratories, for his useful comments on this communication and also Dr. J. R. Holt, Mr. D. G. E. Martin and Professor H. W. B. Skinner, of the Physics Department, University of Liverpool, for their helpful discussions and interest in the work.

REFERENCES

Allen, J. S., and Engelder, T. C., 1951, *Rev. Sci. Instrum.*, **22**, 401.

Taylor, C. J., Remley, M. D., Jentschke, W. K., and Kruger, P. G., 1951, *Phys. Rev.*, **83**, 169.

On the Measurement of Current Density at the Cathode of a Glow Discharge and Aston's Law at Low Pressures and High Discharge Voltages

By R. M. CHAUDHRI and M. A. BAQUI
Physics Department, Government College, Lahore, Pakistan

MS. received 22*nd October* 1951

ABSTRACT. A method has been described for determining the current density on a plane cathode of a glow discharge over a wide range of pressure and voltage. It is shown that Aston's relation, $V=E+F\sqrt{i}/P$, holds good down to as low a pressure as 2×10^{-2} mm Hg and up to as high a voltage as 3000 volts. The work of the earlier investigators extends up to a voltage of about 1000 volts and a pressure not much below 10^{-1} mm Hg. It is also seen from these experiments that the distribution of current over a plane cathode is a function of the discharge pressure and is in general independent of voltage and current.

§1. INTRODUCTION

The distribution of current over the cathode of a glow discharge, although of fundamental importance for the theory of the negative end of the discharge, has been studied very incompletely. Wilson (1902) made measurements with cathodes in the form of a wire and determined the current density by assuming that it was uniform over that area of the electrode which was covered by negative glow. This method is not suited for plane electrodes. Aston (1907, 1912) used a guard ring type of plane cathode and assumed that the current density was uniform over a large area of the electrode. Experiments of Childs (1930) with a cathode consisting of a central disc surrounded by a number of concentric rings showed, however, that this assumption is not always valid.

The work of Aston and Childs was confined to a narrow range of voltage and no data were obtained for very low pressures and for voltages higher than 1000 volts. In the work described here investigations have been carried over a wide range of discharge voltage, current and pressure, and the method used is free from objections which existed in the experiments of previous workers.

The distribution of current over the cathode has been taken to be proportional to the current received by an auxiliary electrode set behind a small hole in the cathode. This current consists mainly of the positive ions coming from the discharge and the secondary electrons assumed to be proportional to the intensity of the ion beam which causes their emission from the walls and the edges of the hole while passing through it (Oliphant 1928, 1930). The current densities so obtained have been used in a new test of Aston's empirical law $V=E+F\sqrt{i}/P$ for the relation between current, pressure and cathode fall, which can be assumed without appreciable error to be identical with the tube voltage.

§ 2. APPARATUS

The discharge passed between two parallel plane circular electrodes, each 3·98 cm in diameter and 10 cm apart, housed in a cylindrical Pyrex glass tube, 4·2 cm in diameter and 18 cm long. The electrode K, fig. 1, consisted of a solid brass cylinder 8·5 cm long and 4·5 cm in diameter, hollowed out at the bottom to a depth of 6 cm, leaving a wall thickness of about 2 mm over this length. A circular cavity 2·5 mm deep and 3 mm wide was made all round on the top of the electrode near its edges, leaving a plane central surface 3·98 cm in diameter to act as the cathode. The cavity served as a seat for the discharge tube which was waxed to the electrode. The cathode was provided with an eccentric conical groove 2·5 cm deep, 2·36 cm and 2·80 cm diameter at the top and bottom respectively, and a well-ground solid brass cylinder C supported on a metal plate P, screwed to the lower face of the cathode and closely fitted into it giving a smooth cathode surface. The cylinder C could be rotated freely in the groove with the help of a rod R while the system remained air tight. A fine hole H 0·066 cm in diameter was bored in the rotating cylinder 1·0 mm from its edge. A hollow nickel cylinder F, open at the top, 3·6 cm in diameter and 5 cm long was placed about 2 mm below the cathode and collected the ions flowing out of the cathode hole H. The rod R rigidly fixed to the bottom of the rotating cylinder and sealed with wax to the ground glass joint J passed out of the bottom of F, through the opening O, 0·8 cm in diameter. A pointed T fixed to the ground glass joint moved on a graduated scale S and indicated the position of H relative to the cathode centre. The hole H described a circle 2·16 cm in diameter on the cathode surface and was at a minimum distance of 3·3 mm from the cathode centre when the pointer read zero on the scale S, and at a maximum distance of 18·3 mm from it on the diametrically opposite side, when the pointer read 180°. The distance of the hole H from the cathode centre could thus be varied at will from 3·3 mm to 18·3 mm.

The electrode A, a plane circular brass disc 3·98 cm in diameter and 3 mm thick, served as the anode.

The cathode was kept water cooled during the experiment.

The voltage for the discharge was obtained from a d.c. motor generator set and the discharge was stabilized by putting a diode valve in series with the tube. The voltage was measured with electrostatic voltmeters having ranges 0–750 and 500–3 000 volts.

The current flowing to the collector F, which was maintained 40–60 volts negative with respect to the cathode, was measured with a moving-coil mirror galvanometer G having a current sensitivity of about 10^{-10} amp/mm, and varying the distance of the hole H from the cathode centre.

The apparatus was exhausted with a single stage Gaede's all-steel mercury diffusion pump backed by a Cenco Hyvac pump through wide-bore glass tubes. Since the gas leaked from the discharge to the analysing chamber only through the hole H a very low pressure could be maintained behind the cathode while working over a suitable range of discharge pressure. Experiments were performed with air only which entered the tube through a fine glass capillary leak open to the atmosphere. The pressure in the discharge as well as behind the cathode was measured with a McLeod gauge.

§ 3. RESULTS

A large number of curves, relating the current to F with the distance of hole H from the cathode centre were obtained over a pressure range of $1{\cdot}83 \times 10^{-2}$ to $2{\cdot}64 \times 10^{-1}$ mm Hg with the discharge voltage varying from 380 to 3 000 volts and the discharge current varying from 0·30 to 8·0 mA. Only typical curves are given here.

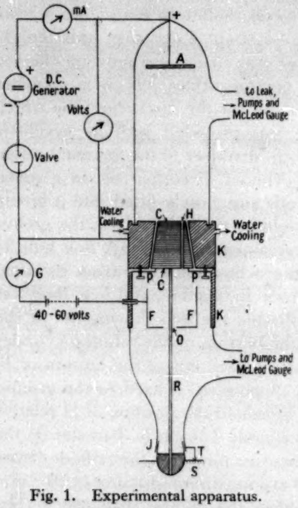

Fig. 1. Experimental apparatus.

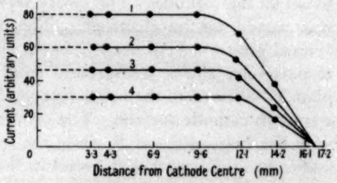

Fig. 2. Current plotted against distance from cathode centre.
Pressure $= 3{\cdot}08 \times 10^{-2}$ mm Hg.
Discharge voltage and current:
1. 1800 v, 2·4, 2·3 mA; 2. 1575 v, 2·0 mA;
3. 1375 v, 1·7 mA; 4. 1250 v, 1·3 mA.

Figure 2 shows curves which are typical for the low pressure range of $2{\cdot}18 \times 10^{-2}$ to $5{\cdot}08 \times 10^{-2}$ mm Hg, while results at comparatively higher pressure are typified by curves in fig. 3. Curves have also been obtained at constant discharge currents with varying voltages and pressures and also at constant voltages with other factors varying. Figure 4 shows the relation between the discharge voltage and the current density at the cathode at different discharge pressures.

The results were strictly reproducible even after several weeks if the discharge conditions were kept the same.

It is evident from the figures that there is always a central portion of the cathode over which the current is uniform. The area of this portion is, in general, dependent upon the discharge pressure alone. It is, however, observed that at low pressures the area over which the current is uniform diminishes as the voltage and current increase. Beyond this area the current falls regularly towards the edges of the cathode and appears to fall almost to zero at a finite distance from its outer boundary. The thickness of the outer ring of the cathode over which there is practically no current depends mainly upon the discharge pressure. The drop in current towards the cathode boundary is linear but its rate of fall at any one constant pressure depends upon the voltage and the current through the discharge.

The total area of the cathode covered by the discharge at a constant pressure is a function of pressure alone and is independent of voltage and current and increases with the pressure. At the lowest pressure used ($1{\cdot}83 \times 10^{-2}$ mm Hg), however, the current gets spread over a larger area with increasing voltage and current. The curves at this pressure have pronounced tails which in each case cover an area comparable with that under the uniform current. The total current under the tails is, in general, found to be too small to be taken into account in calculating the current density but this is not so at very low pressures.

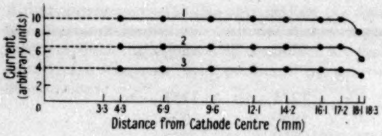

Fig. 3. Current plotted against distance from cathode centre. Pressure$=2{\cdot}64 \times 10^{-1}$ mm Hg. Discharge voltage and current:
1. 425 v, 3·6 mA; 2. 400 v, 2·6 mA;
3. 300 v, 1·65 mA.

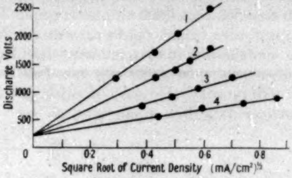

Fig. 4. Discharge volts plotted against square root of current density.
1. $2{\cdot}18 \times 10^{-2}$ mm Hg;
2. $3{\cdot}08 \times 10^{-2}$ mm Hg;
3. $5{\cdot}08 \times 10^{-2}$ mm Hg;
4. $9{\cdot}24 \times 10^{-2}$ mm Hg.

At low pressures the area of the cathode over which the current is uniform increases rapidly with the rise of pressure but the increase in the total area engaged in the discharge is not so pronounced. At pressures higher than 10^{-1} mm Hg the increase with pressure in the area over which the current is uniform is gradual while the total active area shows very little change indeed. At the highest pressure ($2{\cdot}64 \times 10^{-1}$ mm Hg) used, the uniform current spreads up to a distance of only 18·1 mm from the cathode centre, and is never observed to cover the entire surface of the cathode under the conditions of the discharge studied.

Every experimental curve obtained can be divided into two nearly straight lines, one parallel and the other inclined to the distance axis, the slope of the latter depending upon the discharge current, voltage and pressure. With the first line we determine the area over which the current is uniform while with the other we find the area over which the current falls from the maximum value to zero.

Now suppose that a current density i is uniform over the cathode up to a a distance r_1 cm from its centre and that it drops linearly to zero at a distance r_2 cm from it. It can be shown that

$$i = \frac{I}{A + \frac{1}{3}\pi(r_2 + 2r_1)(r_2 - r_1)}$$

where I is the total discharge current and A is the area of the cathode over which the current density i is uniform.

From the current density thus measured the discharge potential has been calculated from Aston's law, $V = E + F\sqrt{i}/P$ and the values obtained are given in column 4 of the table. E and F are constants and are taken to be 220 and 750 respectively for air (expressing $\sqrt{i}$ in $(\text{mA/cm}^2)^{1/2} \times 10$ and P in hundredths of mm Hg), i is the current density at the cathode and V and P stand for the discharge voltage and pressure respectively.

Pressure (mm Hg)		Discharge Current (mA)	Discharge Volts Observed	Discharge Volts Calculated
$2{\cdot}18 \times 10^{-2}$				
,, ,,	(*a*)	1·4	2550 2500	2387
,, ,,	(*b*)	1·0	2050 2000	1974
,, ,,	(*c*)	0·85	1675	1699
,, ,,	(*d*)	0·50	1260	1252
$3{\cdot}08 \times 10^{-2}$				
,, ,,	(*a*)	2·4 2·3	1800	1742 1752
,, ,,	(*b*)	2·0	1575	1559
,, ,,	(*c*)	1·75 1·70	1375	1437
,, ,,	(*d*)	1·3	1250	1266
$5{\cdot}08 \times 10^{-2}$				
,, ,,	(*a*)	4·25	1275	1253
,, ,,	(*b*)	3·0	1050	1076
,, ,,	(*c*)	2·1	910	940
,, ,,	(*d*)	1·35	780	781
$9{\cdot}24 \times 10^{-2}$				
,, ,,	(*a*)	8·0 7·5	880	918
,, ,,	(*b*)	5·5	805	820
,, ,,	(*c*)	3·45	730	707
,, ,,	(*d*)	2·4	590	577

The table shows a good agreement between the calculated and the observed values of the discharge potentials over the entire pressure range used; the slight divergence between them is probably due to experimental error. It can be inferred from this that Aston's law $V = E + F\sqrt{i}/P$ holds good even when the pressure is very low and the discharge voltage is about 100 times as large as the ionization potential of the gas, i.e. even under strongly abnormal conditions of the discharge. The law is valid for that portion of the discharge over which the current is uniformly distributed.

ACKNOWLEDGMENTS

It is a pleasure to record our thanks to Professor M. L. E. Oliphant for his interest in this work. Our thanks are also due to Professor K. G. Emeléus for his helpful suggestions given in writing this paper.

REFERENCES

Aston, F. W., 1907, *Proc. Roy. Soc.* A, **79,** 80; 1912, *Ibid.*, **86,** 168.
Childs, E. C., 1930, *Phil. Mag.*, **9,** 529.
Oliphant, M. L. E., 1928, *Proc. Camb. Phil. Soc.*, **24,** 451; 1930, *Proc. Roy. Soc.* A, **127,** 373.
Wilson, H. A., 1902, *Phil. Mag.*, **4,** 608.

The Theory of Gaseous Arcs: I
The Fundamental Relations for the Positive Columns

By K. S. W. CHAMPION
Electron Physics Department, University of Birmingham

Communicated by J. Sayers; MS. received 28*th August* 1951, *and in amended form* 7*th January* 1952

ABSTRACT. It is postulated that the five fundamental relations, stated by Tonks and Langmuir to be sufficient to describe fully a low pressure positive column, also apply to high pressure positive columns. Previously, only two of these relations had been applied to high pressure columns. A 'natural arc radius' is postulated for low pressure arcs when the boundaries are removed an indefinite distance. Previous theories of low pressure arcs always assumed that the arc completely filled the cross section of its containing vessel, and thus did not apply to low pressure arcs in large chambers or arcs at intermediate pressures.

The theory of low pressure arcs with high electron densities in which ionization by stages is important is developed. It is then shown that by taking recombination into account this theory may be applied to intermediate and high pressure arcs with a high degree of ionization. A first approximation is also obtained for the theory of high pressure arcs in which there is a low degree of ionization. All the theory presented includes the effect of a longitudinal magnetic field, and the no-field conditions are included as a special case. It is found that the effects of a magnetic field predicted by the theory are in agreement with experimental observations.

---

§ 1. INTRODUCTION

HITHERTO the theories of low and high pressure arcs have been considered to be quite distinct, but actually the same five fundamental relations apply throughout the pressure range. The only difference is that the relative importance and detailed statement of these equations changes through the pressure range. That five equations are necessary and sufficient for a full description of the positive column of a low pressure arc was first stated by Tonks and Langmuir (1929). The fundamental relations are:

1. The plasma balance equation.
2. The ion generation equation.
3. The lateral ion current equation.
4. The arc current equation.
5. The energy balance equation.

The plasma balance equation for the low pressure case states the adjustment of electron temperature to ion generation which just fits the plasma into the space available for it (i.e. the tube cross section). This equation and the ion generation equation constitute a pair of simultaneous equations in ionization constant λ_i and electron temperature T_e. From these equations it can be shown that, for a given set of conditions, T_e diminishes as the tube radius a is increased. This process continues until T_e does not greatly exceed the gas temperature T_g, the latter having been increased by elastic electron collisions. If the tube radius is further increased, the arc no longer fills the cross section but retains a constant radius which in this paper is termed the 'natural arc radius'. This, of course, is the usual radius of a high pressure arc, except in a capillary when the conditions are somewhat similar to those for a low pressure arc in a confined space. Note that for an arc with its natural radius, T_g is slightly less than T_e only if the gas is atomic; if the gas is in a molecular state radiation will keep the value of T_g appreciably below that of T_e. Also, for a low-pressure arc with its natural radius the difference between T_e and T_g is small only if the length of the arc is considerably greater than one mean free path. Otherwise T_g is considerably less than T_e.

The lateral ion current equation gives the current of positive ions drifting to the tube wall, where, in the case of a non-conducting wall, they recombine with electrons which reach the wall because of their large random motion. As the concentration of charged particles is increased and/or the tube radius increased, volume recombination becomes appreciable, and eventually its effect is much greater than that of wall (or boundary) recombination, and sometimes the latter may become negligible. This occurs under some conditions with arcs with their natural radii, in which case the arcs are in equilibrium in a lateral direction and the positive ion current in this direction is negligible. (The effect of increasing the tube radius on volume recombination is not only direct, through the walls becoming more remote, but indirect, through the electron temperature becoming lower.)

When the arc current is considered, a slight approximation is usually made by neglecting the positive ion contribution. This equation relates the current to the electron concentration, mobility, longitudinal gradient and the actual arc radius. The energy input per unit length of the positive column is equated to the energy losses in the energy balance equation. Suits (1939) has given a good approximation for this equation for arcs which do not fill their containing tube. Suits' treatment is based on comparison of the losses from such an arc with those from a hot solid cylinder in a gas. A complete statement of the energy balance equation for arcs which completely fill their containing tube is still awaited. For high pressure arcs relations 4 and 5 together give an expression for the longitudinal electric gradient in terms of the current and other parameters which are related by relations 1 and 2. The same could be deduced for low pressure arcs if an accurate energy balance equation were known. However, a method of investigation first suggested by Schottky (1924), and later developed by several authors, including Wasserrab (1950), involves the equivalent of an energy balance relation, and thus the longitudinal electric gradient of a low pressure arc can be explicitly expressed.

§ 2. THE POSITIVE COLUMN OF LOW PRESSURE ARCS

The theory of low pressure arcs has been dealt with at length by a number of authors, including Tonks and Langmuir (1929) and Tonks (1939). Several additions to this theory are made below. The relations first considered are the simultaneous plasma balance and ion generation equations. From these relations important information can be deduced with regard to the lateral conditions of the arc, viz. the distribution of particles and the lateral variation of potential. For generality the equations which follow are written in a form to include the effect of a uniform longitudinal magnetic field but, unless otherwise specified, they apply equally well in the absence of a magnetic field merely by using the appropriate values of the quantities involved.

Tonks and Langmuir obtained solutions for plasma using the following assumptions and approximations: (i) Long mean free paths and rate of ionization (*a*) uniform throughout the plasma, (*b*) proportional to electron density. (ii) Short mean free paths, with collisions so frequent that the energy gained by an ion between collisions is small compared with the thermal energy of the atoms and ionization (*a*) uniform throughout the plasma, (*b*) proportional to electron density. (iii) Conditions intermediate between (i) and (ii) such that the ion temperature is determined more by the energy acquired in a free path than by the gas temperature and ionization (*a*) uniform throughout the plasma, (*b*) proportional to electron density. (Solutions (iii) are only approximate.)

In 1939 Tonks considered the effect on the plasma of a uniform longitudinal magnetic field. Because of the curvature, and hence the increased length of the electron and ion paths caused by the magnetic field, the number of collisions occurring in unit volume of the discharge per second is greatly increased. Thus case (ii) conditions will usually apply, although with low pressure discharges in weak fields case (iii) may apply. For case (ii) the radial ion drift velocity in a cylindrical tube is

$$u_{\mathrm{p}} = -D_{\mathrm{p}}\left(\frac{\partial(\ln n_{\mathrm{p}})}{\partial r} - \frac{\boldsymbol{e}}{\boldsymbol{k}T_{\mathrm{p}}}\frac{\partial V}{\partial r}\right), \qquad \ldots\ldots(1)$$

where D_{p} is the positive ion diffusion coefficient, n_{p} the density of positive ions and V the plasma potential. For strong magnetic fields eqn. (1) requires to be modified to take into account the effect of the magnetic field on the lateral drift of the ions. This correction, neglected by Tonks, is important when the Larmor radii of the ions are smaller than the dimensions of the containing vessel. With typical conditions this occurs with magnetic fields of the order of 1 000 gauss, which are small compared with fields of up to 25 000 gauss used in recent research.

Thus, when there is axial symmetry,

$$u_{\mathrm{p}} = -D_{\mathrm{p}}\alpha_{\mathrm{p}}\left(\frac{\partial(\ln n_{\mathrm{p}})}{\partial r} - \frac{\boldsymbol{e}}{\boldsymbol{k}T_{\mathrm{p}}}\frac{\partial V}{\partial r}\right), \qquad \ldots\ldots(2)$$

where, for small values of magnetic field strength H,

$$\alpha_{\mathrm{p}} \simeq 1 - H^2\boldsymbol{e}^2 l_{\mathrm{p}}^2/2\boldsymbol{k}T_{\mathrm{p}}m_{\mathrm{p}} \qquad \ldots\ldots(3)$$

and, for large values of H,

$$\alpha_{\mathrm{p}} \simeq \frac{4\boldsymbol{k}T_{\mathrm{p}}m_{\mathrm{p}}}{H^2\boldsymbol{e}^2 l_{\mathrm{p}}^2}, \qquad \ldots\ldots(4)$$

where l_{p} is the mean free path of the ion and m_{p} its mass. Expressions (3) and (4) represent limiting values and are not accurate for intermediate magnetic field strengths. They are adapted from the corresponding expressions for electrons given by Tonks and Allis (1937), who based their derivation on the Maxwellian velocity distribution as modified by a magnetic field. From eqn. (3) it can be seen that for small magnetic fields α_{p} is not very different from unity, and its value can be taken to be such. For strong fields α_{p} approximately equals $\alpha_{\mathrm{e}}m_{\mathrm{p}}/m_{\mathrm{e}}$.

The density of electrons in a plasma in the presence of a longitudinal magnetic field is given by

$$n_{\mathrm{e}} = n_0 \exp(-\boldsymbol{e}V/\boldsymbol{k}T_{\mathrm{e}}\tau), \qquad \ldots\ldots(5)$$

where n_0 is the density at the axis and n_{e} is the density at a region in the plasma where the potential differs by V from that at the axis. Also

$$\tau = \frac{\alpha_{\mathrm{e}}D_{\mathrm{e}} - \mu\alpha_{\mathrm{p}}D_{\mathrm{p}}}{\alpha_{\mathrm{e}}D_{\mathrm{e}} + \mu\alpha_{\mathrm{p}}D_{\mathrm{p}}T_{\mathrm{e}}/T_{\mathrm{p}}} \qquad \ldots\ldots(6)$$

with μ defined by the equation

$$u_{\mathrm{e}} = \mu u_{\mathrm{p}}, \qquad \ldots\ldots(7)$$

where u_e is the radial electron drift velocity. When the discharge tube has non-conducting walls μ is always unity, but when the tube has conducting walls the value of μ is controlled by the wall potential.

If τ becomes zero with increasing magnetic field strength the radial plasma field must also be zero, and if τ becomes negative the plasma field changes its direction. Now

$$\frac{D_e}{D_p}=\frac{l_e m_p^{1/2} T_e^{1/2}}{l_p m_e^{1/2} T_p^{1/2}} \quad \text{and} \quad \lim_{H\to\infty} \frac{\alpha_p}{\alpha_e}=\frac{l_e^2 m_p T_p}{l_p^2 m_e T_e},$$

and thus

$$\lim_{H\to\infty} \tau=\frac{1-\mu\kappa T_p^{3/2}/T_e^{3/2}}{1+\mu\kappa T_p^{1/2}/T_e^{1/2}}, \qquad \text{......(8)}$$

where

$$\kappa=l_e m_p^{1/2}/l_p m_e^{1/2}. \qquad \text{......(9)}$$

When $\mu \geqslant 1$ $\lim_{H\to\infty}\tau \simeq -T_p/T_e$ since generally $\kappa T_p^{1/2}/T_e^{1/2} \gg 1$. ($\kappa \simeq 250$ for a proton and is larger for other ions.) However, this does not hold when $\mu<1$ and, in particular, when $\mu\to 0$ $\lim_{H\to\infty}\tau=1$*. Thus, even in the limit, the plasma field is not always reversed in direction or even zero.

When the magnetic field is zero, $\alpha_e=\alpha_p=1$ and $\tau=(D_e-\mu D_p)/(D_e+\mu D_p T_e/T_p)$. On the other hand, Boltzmann's equation for a plasma with no magnetic field requires that $\tau=1$. However, the reason for this is that Boltzmann's usual equation only applies when there is thermal equilibrium, in which case the radial electron drift velocity is zero, i.e. $u_e=0$, and hence $\mu=0$ and $\tau=1$. It is interesting to note that when the plasma is in thermal equilibrium (i.e. $\mu=0$) the ordinary Boltzmann equation ($\tau=1$) still holds in a magnetic field. However, when $\mu\neq 0$ τ may differ from unity, even when there is no magnetic field, but the difference is usually small since $D_p \ll D_e$. In this case the addition of a magnetic field further reduces the value of τ.

The physical interpretation of these results is as follows. When the tube walls are non-conducting, the radial potential gradient is such that the radial electron and ion drift velocities are equal. The addition of a weak magnetic field tends to reduce u_e more than u_p and the radial plasma gradient adjusts itself to compensate for the change. With a strong magnetic field the Larmor radii for both electron and ion are small compared with the tube dimensions. When this occurs the radial gradient should remain constant with increasing field strength as the coefficients of radial drift are proportional to the Larmor radii, and these have a constant ratio. That this is true is shown by the limiting value of τ with strong magnetic fields.

In the case of a tube with conducting walls at a fixed potential the radial potential drop V is held constant, and this quantity determines μ. However, when a magnetic field is applied u_e is reduced more than u_p, i.e. μ is reduced, but, for similar reasons to those above, μ and hence τ tend to limits with strong magnetic fields.

Now the ion generation equation for the present case (ion production proportional to electron concentration) is

$$\frac{\partial(n_p u_p r)}{\partial r}=r\lambda n_e \,\dagger \qquad \text{......(10)}$$

---

* Tonks' approximate expression for τ is accurate when $\mu \gg 1$ but not when $\mu<1$, and when $\mu\to 0$ the limiting value is indeterminate.

† Actually the complete ion generation relation involves another equation for λ in terms of the gas temperature, pressure and ionization potential and the energy of the electrons, see eqn. (24).

and solution of the appropriate equations for n_e as a function of r gives

$$n_e = n_0 J_0(\beta r) \qquad \ldots\ldots(11)$$

where

$$\beta = \left(\frac{\lambda T_p}{D_p \alpha_p (T_p + T_e \tau)}\right)^{1/2}. \qquad \ldots\ldots(12)$$

Assuming that the arc fills the tube $n_e = 0$ when $r = a$, and hence, from eqn. (11),

$$\beta a = 2{\cdot}405. \qquad \ldots\ldots(13)$$

From eqns. (12) and (13) the plasma balance equation is obtained:

$$\frac{2{\cdot}405}{a} = \left(\frac{\lambda T_p}{D_p \alpha_p (T_p + T_e \tau)}\right)^{1/2}. \qquad \ldots\ldots(14)$$

Note on the Electron Velocity Distribution

The electron velocity distribution assumed in this paper is that of Maxwell or, where applicable, the Maxwell distribution as modified by a magnetic field. It is not claimed that this distribution accurately represents the electron velocity distribution in a gaseous arc under all conditions. However, it is considered that under most conditions the error introduced by assuming a Maxwell velocity distribution will be relatively small and that, until the present theory has been thoroughly investigated experimentally, the refinement of using special velocity distributions for various conditions is not justified.

Tonks and Allis (1937) claim that the Maxwell distribution applies to low pressure arcs in which electrons lose energy by inelastic impacts with atoms and by direct interchange between themselves. However, with the relatively large values of E/p in these arcs this is not immediately obvious. If the collisions were elastic it would be expected that the distribution would be that of Druyvesteyn, and a large proportion of inelastic collisions is likely to further increase the deficiency of high energy electrons unless the cross section for electron–atom collisions decreases rapidly with increasing energy. In high current arcs another factor operates, viz. the electrostatic interaction between the charged particles. Cahn (1949) has evaluated this effect for high current discharges in which the field strength is small and all collisions are assumed to be elastic. He showed that the distribution is Maxwellian if the cross section varies inversely with the electron velocity. On the other hand, if the cross section is independent of electron energy, the distribution is Maxwellian for high electron densities (10^{11} per cm^3 or more) but tends to that of Druyvesteyn for low electron densities (10^6 per cm^3 or less). Thus, for high current discharges the distribution will be Maxwellian in either case. Cahn's deduction is based on a paper by Landau which has been criticized by Allis (1949) and later defended by Landau (1950). However, even if Allis's criticism is correct, the effect on Cahn's deduction is not likely to be large.

At present there is no derivation of the corresponding distribution when the field strength is not small. However, it seems likely that it will be similar to the Druyvesteyn distribution. Thus it is probable that the actual velocity distribution in a low pressure arc will lie between those of Maxwell and Druyvesteyn. At high pressures (e.g. above 10 mm) E/p will be small (1·3 at 10 mm for hydrogen) and nearly all the collisions will be elastic. Thus the velocity distribution will be Maxwellian.

§3. LOW PRESSURE POSITIVE COLUMNS WITH IONIZATION BY STAGES

With high current arcs the types of ion production previously considered do not apply and a more accurate assumption is that ion production is proportional to the square of electron concentration. This is due to multi-stage ionization processes in which an atom becomes ionized by low energy electrons via one or more excited states*. Thus the ion generation equation is

$$\frac{\partial(n_p u_p r)}{\partial r} = r\lambda_2 n_e^2. \qquad \text{......(15)}$$

It should be noted that the ionization process represented by eqn. (15) differs from the process termed 'thermal ionization' in high-pressure arcs. Thermal ionization requires high gas density but not necessarily a high density of charged particles. The energy is fed into the arc column by accelerating the electrons and ions, but the collision frequency of these particles is high so that they continuously lose this energy in small amounts (i.e. by elastic collisions) to neutral particles, whose temperature is thus raised almost to that of the charged particles. Because collisions between neutral particles are so much more frequent than those between one neutral and one charged particle a large proportion of the excited and ionized atoms are produced by such collisions.

However, the ionization process postulated above requires a high electron concentration and hence high current density. If the tube radius is somewhat smaller than the natural arc radius the gas temperature will be considerably lower than the electron temperature and, in any event, the number of ions produced at low pressures by collisions of neutral particles will be negligible compared with the number produced by collisions with electrons. Further, photo-ionization probably plays an important part in the ionization mechanism of high-pressure arcs. However, at low pressures the probability of a photon being absorbed by the arc gas is considerably smaller, and photo-ionization plays a much smaller part.

Inserting in eqn. (15) the values of u_p from eqn. (2) and of the resultant space derivatives of V from eqn. (5), we find, after rearrangement,

$$\frac{\partial^2(n_e/n_0)}{\partial r^2} + \frac{1}{r}\frac{\partial(n_e/n_0)}{\partial r} + \frac{\lambda_2 n_0}{M}\left(\frac{n_e}{n_0}\right)^2 = 0, \qquad \text{......(16)}$$

where

$$M = D_p \alpha_p (1 + T_e \tau / T_p). \qquad \text{......(17)}$$

Now put

$$s = \beta r, \qquad \text{......(18)}$$

where β is such that $\lambda_2 n_0 / M = 1$ when s is substituted for r,

i.e.

$$\beta = \left(\frac{\lambda_2 n_0}{M}\right)^{1/2} = \left(\frac{\lambda_2 n_0 T_p}{D_p \alpha_p (T_p + T_e \tau)}\right)^{1/2} \qquad \text{......(19)}$$

and

$$\frac{\partial^2(n_e/n_0)}{\partial s^2} + \frac{1}{s}\frac{\partial(n_e/n_0)}{\partial s} + \left(\frac{n_e}{n_0}\right)^2 = 0.$$

Using Frobenius' method, a solution of this equation can be obtained in the form of a series, viz.: $n_e/n_0 = a_0 + a_2 s^2 + a_4 s^4 + \ldots + a_n s^n + \ldots$, n always even, where $a_n = -(2a_0 a_{n-2} + 2a_2 a_{n-4} + 2a_4 a_{n-6} + \ldots)/n^2$. The final term will be $2a_{\frac{1}{2}n-2} a_{\frac{1}{2}n}$ or $(a_{\frac{1}{2}n-1})^2$, according as $\frac{1}{2}n$ is even or odd. The first few terms of the series are

---

* The life of a normal excited state is about 10^{-8} sec, and thus multi-stage ionization processes are usually only appreciable when the collision frequency is 10^8 per sec or more. However, the lives of some metastable states are as long as 0·1 sec, and in such gases this causes some lowering of the required collision frequency.

$$n_e/n_0 = 1 - 0{\cdot}25 s^2 + 3{\cdot}125 \times 10^{-2} s^4 - 3{\cdot}472 \times 10^{-3} s^6 + 3{\cdot}526 \times 10^{-4} s^8 - 3{\cdot}418 \times 10^{-5} s^{10} + 3{\cdot}206 \times 10^{-6} s^{12} - 2{\cdot}939 \times 10^{-7} s^{14} + 2{\cdot}646 \times 10^{-8} s^{16} - 2{\cdot}352 \times 10^{-9} s^{18} + \ldots \qquad \ldots\ldots(20)$$

This series converges when $s < 3{\cdot}4$ but, as s_0 (the value of s corresponding to the first zero of n_e/n_0) is 3·03, the series converges within the range required by the physical problem.

Assuming that the arc fills the tube, $\beta a = 3{\cdot}03$, and the plasma balance equation is

$$\frac{3{\cdot}03}{a} = \left(\frac{\lambda_2 n_0 T_p}{D_p \alpha_p (T_p + T_e \tau)} \right)^{1/2}. \qquad \ldots\ldots(21)$$

In fig. 1 n_e/n_0 is plotted as a function of r/a for case (ii), with three different types of ion production: (*a*) uniform ($n_e/n_0 = 1 - \frac{1}{4}s^2$, Tonks and Langmuir 1929), (*b*) proportional to the electron density (eqn. (11)), and (*c*) proportional to the square of the electron density (eqn. (20)). Thus accurate observation of the radial variation of electron density should shed light on the actual ionization process taking place in a particular arc. In general, the type of ion production changes from (*a*) to (*b*) and (*b*) to (*c*) as the number of collisions suffered per second by electrons in unit volume of an arc is increased. Thus, indirectly, a longitudinal magnetic field may cause a slight constrictive effect on the plasma of a low pressure arc by increasing the number of collisions as a result of the curvature of the paths of the electrons.

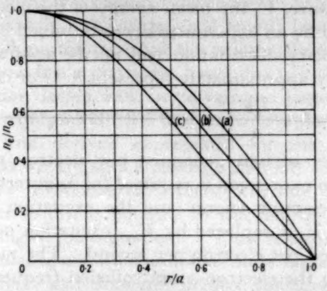

Fig. 1. n_e/n_0 as a function of r/a for arcs in which the mean free paths are short and ion production is : (*a*) constant, (*b*) proportional to n_e, (*c*) proportional to n_e^2.

With arc currents of the order of 2 amperes in the ion source of the Birmingham University cyclotron the beam current of alpha-particles is found to be approximately proportional to the square of the arc current, the arc voltage remaining sensibly constant. This suggests that the rate of ionization may be approximately proportional to the square of the electron density and that the ions may be produced via excited states by electron collisions.

(i) *Lateral Ion Current Equation*

Neglecting the ion contribution to the arc current, the number of ions reaching unit wall area per second is the number generated per second in the volume subtended by that area. Thus, for a cylindrical tube, the lateral ion current

$$I_{\mathrm{p}}=\frac{1}{a}\int_0^a N_r \mathbf{e} r\,dr,$$

where N_r is the number of ions generated per unit volume per second at a distance r from the axis. For case (ii) (*a*)

$$I_{\mathrm{p}}=0{\cdot}5\mathbf{e}aJ, \qquad \ldots\ldots(22)$$

where J is the number of ions generated per unit volume per second. For case (ii) (*b*)

$$I_{\mathrm{p}}=\frac{\lambda\mathbf{e}}{a}\int_0^a n_{\mathrm{e}} r\,dr=0{\cdot}216\,\mathbf{e}an_0\lambda, \qquad \ldots\ldots(23)$$

where λ is the number of ions generated per electron per second, each ion being produced by a single collision. If the velocity distribution is Maxwellian,

$$\lambda=6{\cdot}7\times10^7\beta_{\mathrm{T}}(p/T_{\mathrm{g}})V_{\mathrm{e}}^{3/2}(2+3V_1/2V_{\mathrm{e}})\exp(-3V_1/2V_{\mathrm{e}}), \qquad \ldots\ldots(24)$$

where p is the gas pressure, V_{e} the mean energy of the electrons in volts, V_1 the ionization potential and β_{T} an experimentally determined constant. In a strong magnetic field the velocity distribution will not be accurately Maxwellian, and expression (24) will only approximately represent λ. For case (ii) (*c*)

$$I_{\mathrm{p}}=\frac{\lambda_2\mathbf{e}}{a}\int_0^a n_{\mathrm{e}}^2 r\,dr=0{\cdot}104\,\mathbf{e}an_0^2\lambda_2, \qquad \ldots\ldots(25)$$

where λ_2 is the number of ions generated per electron per electron per unit volume per second. An expression is required for λ_2 in terms of the gas pressure and temperature, the electron energy and the excitation potential of the gas. Expression (24) where V_1 is replaced by V_{ex} (excitation potential) will give the number of atoms excited per electron per second. The number of these which are ionized depends on the electron–atom collision frequency as well as on the distribution of electron energies. Wasserrab (1950) considered the energy lost by electrons in inelastic collisions, and it should be possible to extend his theory to obtain an approximate expression for λ_2.

The quantity $n_0\lambda_2$ is analogous to λ, and it is obvious that λ_2 is much smaller than λ. This is borne out by the values obtained from the respective plasma balance equations (21) and (14). Note that for (ii) (*b*) conditions $T_{\mathrm{e}}\gg T_{\mathrm{p}}$ and for (ii) (*c*) conditions $T_{\mathrm{e}}>T_{\mathrm{p}}$. Substituting for λ and λ_2 respectively,

$$I_{\mathrm{p}}=C\frac{\alpha_{\mathrm{e}}\alpha_{\mathrm{p}}D_{\mathrm{e}}D_{\mathrm{p}}(T_{\mathrm{e}}+T_{\mathrm{p}})}{\alpha_{\mathrm{e}}D_{\mathrm{e}}T_{\mathrm{p}}+\mu\alpha_{\mathrm{p}}D_{\mathrm{p}}T_{\mathrm{e}}}\frac{\mathbf{e}n_0}{a}, \qquad \ldots\ldots(26)$$

where C is 1·248 or case (ii) (*b*) and 0·955 for case (ii) (*c*).

(ii) *Arc Current Equation*

The arc current equation is $i=2\pi\int_0^a jr\,dr$, where the current density at a distance r from the axis $j=n_{\mathrm{e}}\mathbf{e}K_{\mathrm{e}}E$, where K_{e} is the electron mobility, E is the positive column gradient and the ion contribution is neglected. Assuming that the electron mobility and arc gradient do not depend on r, for case (ii)

$$i=\gamma_{\mathrm{c}}\pi a^2\mathbf{e}n_0K_{\mathrm{e}}E \qquad \ldots\ldots(27)$$

where $\gamma_{\mathrm{c}}=0{\cdot}5$, 0·432 and 0·346 for conditions (ii) (*a*), (*b*) and (*c*) respectively. Thus accurate measurement of the parameters in eqn. (27) should permit the deduction of the type of ionization in a particular arc.

(iii) *Energy Balance Equation*

Klarfeld in 1937 measured the power released at the walls of discharges in mercury vapour by a probe method and found that, at a pressure of $2{\cdot}2 \times 10^{-4}$ mm Hg, this power was 86% of the total power expended in the positive column. An increase in pressure caused a decrease in this percentage along a complicated curve and, as would be expected, an increase in the discharge current was accompanied by increased losses at the walls. Approximate calculations showed that at pressures of 10^{-4} to 10^{-3} mm about 4 to 7% of the total power losses in the discharge were due to collisions of excited atoms with the walls.

Klarfeld's experiments suggest that most of the energy of a low pressure discharge is lost in a transverse direction. Tonks and Langmuir in 1929 compared the power input per unit length of positive column Ei with $2\pi a I_p(V_i + 8T_e/11600)$. The latter expression accounts for the kinetic energy of the electrons striking the walls and for the energy of recombination. However, in a typical case this is only 30% of the total energy loss. Thus there must be added further terms taking into account the energy gained by the ions from the longitudinal gradient and lost at the walls, losses due to collisions of excited atoms with the walls, radiation losses and, in polyatomic gases, additional losses due to dissociation in the column followed by re-association at the walls.

Schottky (1924) first derived expressions for the longitudinal potential gradient of a low pressure arc and Wasserrab in 1950 developed a similar, but more accurate, theory. In Wasserrab's theory the rate of loss of energy by an electron in inelastic collisions is equated to the rate of gain of energy by the electron from the longitudinal gradient. This relation is equivalent to an approximate energy balance equation and, like Suits' equation for a high pressure arc, relates overall effects and does not involve consideration of the individual processes involved.

§4. THE POSITIVE COLUMN OF HIGH PRESSURE ARCS

Now for low pressure arcs the particle temperatures T_e, T_p and T_g, although different, are each approximately constant throughout the arc. For high pressure arcs T_e, T_p and T_g are very nearly the same and, with large currents in dissociating gases, the temperatures are nearly constant in the body of the arc and fall sharply at the boundaries. However, arcs in monatomic gases exhibit a considerable lateral variation of temperature (Suits 1939). From the foregoing it seems reasonable to assume that the particle temperatures are approximately constant in the body of arcs in dissociating gases at intermediate pressures. Hence the preceding analysis, in which it has been implicitly assumed that the particle temperatures are constant throughout the arc,[*] still applies approximately to arcs in dissociating gases at intermediate and high pressures. Conditions (ii) (*c*) are most likely to apply, and do when the current density is high and the number of ions produced by collisions of neutral atoms is relatively small. At high pressures a very high degree of ionization is required for electron ionization to exceed ionization by collisions of neutral atoms. However, since $T_e \simeq T_p$ ions are likely to make an appreciable contribution to the production of ions, and the essential nature of the (ii) (*c*) conditions is unaltered since $n_e = n_p$.

[*] In the analysis referred to, $\lambda n_0/M$ has been assumed independent of r, and as both λ and M depend on T_e and T_p it has been implicitly assumed that they are independent of r.

Finally, photo-ionization may be important under these conditions. It may be of two kinds. In the first kind ionization is produced by single photons and as, in general, only photons emitted during recombination will have sufficient energy to do this, this type of ionization will be proportional to the rate of recombination. Secondly, there is ionization by cumulative excitation by lower energy photons emitted by excited atoms. The number of such photons produced is approximately proportional to n_e (the number of excited atoms is proportional to n_e), and the chance of the photons being absorbed is approximately proportional to n_g. Thus the rate of cumulative ionization is proportional to $n_e^2 n_g$, and, if the temperature in the body of the plasma is constant, n_g is constant and the rate is proportional to n_e^2.

(i) *Temperature Constant throughout the Arc*

In the preceding analysis λ must be replaced by $\lambda_i - \lambda_r$, where λ_i is the rate of ionization and λ_r is the rate of recombination. λ_i corresponds to λ_2, and is thus a function of T_e which increases with T_e, and λ_r is a function of T_e which decreases as T_e increases. Thus, for some intermediate pressure arcs eqn. (20) still holds, but the value of β is changed to

$$\beta = \left(\frac{(\lambda_i - \lambda_r) n_0 T_p}{D_p \alpha_p (T_p + T_e \tau)} \right)^{1/2}. \qquad \ldots\ldots(28)$$

As the pressure is increased, $\lambda_i - \lambda_r$ decreases, and so, in general, does β. Hence r_0, corresponding to s_0 ($r_0 = s_0/\beta$), increases and becomes greater than the tube radius. Under these conditions the arc radius does not necessarily coincide with the tube radius, but is such that the sectional area can carry the arc current

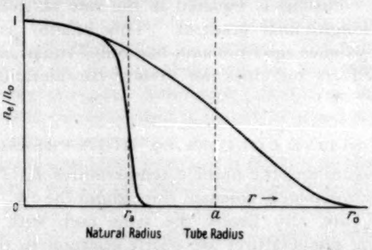

Fig. 2. Electron distribution in an arc at moderately high pressure.

$$i = 2\pi \mathbf{e} K_e E \int_0^{r_a} n_e r \, dr, \qquad \ldots\ldots(29)$$

where r_a is the natural arc radius. At the boundary of the arc eqn. (20) no longer gives the particle density, as the Poisson term in the plasma equation can no longer be neglected. In the bounding sheath $\lambda_i - \lambda_r$ may even be negative as λ_i is small, and recombination of particles drifting from central regions of the arc causes λ_r to be still appreciable. Figure 2 gives qualitatively the radial distribution of charged particles in an arc at a moderately high pressure.

Now for high pressure arcs $T_e \simeq T_p$, and experiment shows that in dissociating gases the temperature is nearly constant in the body of the arc, but falls rapidly at the boundary. This is due to the sharp drop in the thermal conductivity of such gases at lower temperatures. Thus eqn. (20) still holds and

$$\beta=\{(\lambda_i-\lambda_r)n_0/D_p\alpha_p(1+\tau)\}^{1/2} \text{ where } \tau=(\alpha_e D_e-\mu\alpha_p D_p)/(\alpha_e D_e+\mu\alpha_p D_p). \quad ..(30)$$

Further, for a high pressure arc, when $r_a<a$, volume recombination is considerably more important than boundary recombination and $\lambda_i-\lambda_r$ will be small. There is little radial drift of charged particles, and consequently no radial potential gradient. $\beta\to 0$, and thus $s\simeq 0$ for all values of r. In other words, $n_e/n_0\simeq 1$ for all r except at the boundary of the arc. As the discharge is approximately in equilibrium in both radial and longitudinal directions, the value of n_e can be calculated from Saha's equation:

$$\log\frac{n_e^2 n_g}{n_g^2-n_e^2}=-\frac{5\,050V_i}{T_e}+1{\cdot}5\log T_e+15{\cdot}385, \qquad ......(31)$$

where n_g is the total concentration of particles, both charged and uncharged. Unless there is a high percentage of ionization, n_e^2 in the denominator of the first term can be neglected and the term then becomes $\log(n_e^2/n_g)$.

(ii) *Arc Temperature a Function of Radial Position*

However, Koch (1949) has shown experimentally for the special case of a wall-stabilized arc that, even at pressures of the order of 1 atmosphere, a 3 ampere arc in mercury vapour possesses an appreciable radial variation of temperature, and comments that arcs in which the temperature is almost constant over the whole section appear only at higher currents. Thus the previous theory is reconsidered for the more general case when the particle temperatures are a function of the radial distance from the axis of the arc. Equation (16) becomes

$$\begin{aligned}&\frac{\partial^2(n_e/n_0)}{\partial r^2}rD_p\alpha_p(T_p+T_e\tau)+\frac{\partial^2(T_e\tau)}{\partial r^2}rD_p\alpha_p\frac{n_e}{n_0}\ln\frac{n_e}{n_0}\\&\quad+\frac{\partial(n_e/n_0)}{\partial r}\left\{\frac{\partial(D_p\alpha_p)}{\partial r}r(T_p+T_e\tau)+\frac{\partial(T_e\tau)}{\partial r}rD_p\alpha_p\left(2+\ln\frac{n_e}{n_0}\right)\right.\\&\quad\left.-\frac{\partial T_p}{\partial r}rD_p\alpha_p\frac{T_e\tau}{T_p}+D_p\alpha_p(T_p+T_e\tau)\right\}\\&\quad+\frac{\partial(T_e\tau)}{\partial r}\frac{n_e}{n_0}\left(\ln\frac{n_e}{n_0}\right)\left\{\frac{\partial(D_p\alpha_p)}{\partial r}r-\frac{\partial T_p}{\partial r}\frac{rD_p\alpha_p}{T_p}+D_p\alpha_p\right\}\\&\quad+rT_p\lambda(r)n_0\left(\frac{n_e}{n_0}\right)^2=0. \qquad ......(32)\end{aligned}$$

It is impracticable to solve eqn. (32) for the general case, but it is possible to solve it for at least some particular cases. Consider the case of a high-pressure arc ($T_e\simeq T_p$) with no longitudinal magnetic field ($\alpha_p=1$, $\tau=1$), then eqn. (32) reduces to

$$\begin{aligned}&\frac{\partial^2(n_e/n_0)}{\partial r^2}+\frac{\partial^2 T}{\partial r^2}\frac{n_e}{n_0 2T}\ln\frac{n_e}{n_0}+\frac{\partial(n_e/n_0)}{\partial r}\left\{\frac{\partial(\ln D_p)}{\partial r}+\frac{\partial(\ln T)}{\partial r}\frac{1}{2}\left(1+\ln\frac{n_e}{n_0}\right)+\frac{1}{r}\right\}\\&\quad+\frac{\partial(\ln T)}{\partial r}\frac{n_e}{2n_0}\left(\ln\frac{n_e}{n_0}\right)\left\{\frac{\partial(\ln D_p)}{\partial r}-\frac{\partial(\ln T)}{\partial r}+\frac{1}{r}\right\}+\frac{\lambda(r)n_0}{2D_p}\left(\frac{n_e}{n_0}\right)^2=0. \qquad (33)\end{aligned}$$

The dependence of D_p on T_p can be obtained from kinetic theory and, when T is known as a function of r, eqn. (33) can be solved for n_e/n_0 as a function of r. However, the same general conclusions, drawn for the case when the particle temperatures are constant in the body of the arc, still apply, and the natural arc radius is given by the solution of the equation

$$i=2\pi eE\int_0^{r_a} n_e K_e r\,dr, \qquad \ldots\ldots(34)$$

where K_e is a function of temperature and hence of the radial distance from the axis.

(iii) *Fundamental Relations for High Pressure Arcs with a High Degree of Ionization*

The following are the fundamental relations for high pressure arcs in which there is a relatively high degree of ionization, that is, for arcs in which the degree of ionization is higher than about 1%.

(*a*) *The plasma balance equation.* Two versions of the plasma balance equation are given in eqns. (28) and (30) for arcs in which the temperature is constant and $T_e \neq T_p$ or $T_e = T_p$ respectively. The arc temperature adjusts itself so that $\lambda_i - \lambda_r$ has the appropriate value.

(*b*) *The ion generation equation.* This is similar to that for case (ii) (*c*) low-pressure arcs.

(*c*) *The lateral ion current equation.* When $\lambda_i=\lambda_r$ the lateral ion current is zero, and when $\lambda_i>\lambda_r$ the current reaching the wall is still zero if $a>r_a$. Thus, only when $a<r_a$ (as for capillary arcs) does a lateral current reach the walls, and then

$$I_p=(\lambda_i-\lambda_r)\frac{e}{a}\int_0^a n_e^2 r\,dr. \qquad \ldots\ldots(35)$$

If the arc temperature is a function of position a slightly different expression for I_p is obtained.

(*d*) *The arc current equation.* This is given by eqn. (29) or (34), depending on whether or not the particle temperatures are constant in the body of the arc. For a high pressure arc with $\lambda_i=\lambda_r$, and hence $n_e/n_0=1$ in the body of arc,

$$i=\pi eK_e E n_0 r_a^2. \qquad \ldots\ldots(36)$$

(*e*) *The energy balance equation.* This is considered in detail in Part II of this paper (Champion 1952), where Suits' theory of the high pressure arc is further developed.

§ 5. HIGH PRESSURE POSITIVE COLUMNS WITH A LOW DEGREE OF IONIZATION

In high pressure arcs in which $\lambda_i \simeq \lambda_r$ and the arc is very nearly in thermal equilibrium the ionization is, of course, 'thermal', that is, the ion density corresponds to the temperature of the arc. With the usual conception of thermal ionization, the rate of ionization is not necessarily proportional to the square of the electron concentration as required by the preceding theory. However, owing to the considerably greater electron velocity and, hence, collision frequency, when the electron density is 1% of the gas density, the rate of ionization by electron collisions is of the same order as that by collisions between neutral atoms. Thus, as already pointed out, when there is a relatively high percentage of ionization the rate of ionization is approximately proportional to the square of the electron density.

On the other hand, the rate of ionization for low percentages of ionization is not known, but some information may be obtained from the fact that the mean rates of ionization and recombination over the cross section of the arc must be the same (neglecting the positive ion contribution to the arc current). Normally, recombination is proportional to the square of the electron density, but the conditions at present being considered are abnormal. In particular, owing to the high gas temperature, the gas is almost completely dissociated into atoms and thus dissociative recombination is very improbable. Also, because of the energies of the atoms and electrons, electrons will rarely attach themselves to atoms, that is, there will be practically no negative ions. Recombination is thus simplified under these conditions, and the only known processes which can take place are volume and preferential electron recombination. By preferential recombination is meant recombination of an electron with its parent ion to re-form the original atom. In general, in this process the electron will suffer one and possibly more collisions with neutral atoms before recombining.

Volume electron recombination is proportional to the square of the electron concentration, and no doubt accounts for most of the recombination when there is a moderate percentage of ions. However, when there is a low percentage of ions, preferential recombination may be more important or even predominate. Now the rate of preferential recombination depends greatly on the gas density since it depends on the frequency of collision of the electrons with neutral atoms. Thus, over a certain range of gas density and ionization density, preferential recombination is approximately proportional to the product $n_e n_g$. Also, with such conditions, the rate of ionization is approximately proportional to $(n_e/n_g)n_g^2 = n_e n_g$. The factor n_e/n_g is a measure of the energy input per neutral atom (since the total energy input is proportional to n_e) and n_g^2 is a measure of the rate of ion production by collisions between atoms (including both neutral and ionized atoms). Again, when there is a low percentage of ions, photo-ionization by cumulative excitation will be negligible. However, ionization produced by photons liberated during recombination can still occur and, of course, this type of ionization will be proportional to the rate of recombination.

Consequently, as required by the condition of equilibrium, the rates of ionization and recombination under the present conditions are of the same form. It may again be pointed out that both the existence of preferential recombination and the application of Saha's equation require that the conditions closely approach those for equilibrium—in other words, require E/p to be small.

If the temperature is constant in the body of the arc so also is n_g. In that case both the rates of ionization and recombination would be approximately proportional to n_e only, and (ii) (*b*) conditions would apply.

Fundamental Relations for High Pressure Arcs with a Low Degree of Ionization

The temperature is assumed to be constant in the body of the arc.

1. *The plasma balance equation.* $\beta = \{(\lambda_i - \lambda_r)/D_p \alpha_p (1+\tau)\}^{1/2}$ where $\lambda_i \simeq \lambda_r$, and hence $\beta \simeq 0$ when $a > r_a$.

2. *The ion generation equation.* Equation (24) for ionization by a single collision does not hold and the precise nature of the required equation has yet to be established.

3. *The lateral ion current equation.* I_p is given by

$$I_p = (\lambda_i - \lambda_r)\frac{e}{a}\int_0^a n_e r \, dr,$$

but when $a > r_a$ the current reaching the wall is zero. However, for capillary arcs ($a < r_a$) I_p is not negligible when $\lambda_i > \lambda_r$. In any measurement of I_p in a capillary arc great care would be required to ensure that no part of the longitudinal drift current were included.

4. *The arc current equation.* } The same equations apply as
5. *The energy balance equation.* } for a high degree of ionization.

It must be pointed out that the above theory is only a first approximation for the theory of high pressure arcs with a low degree of ionization.

§6. SOME PRACTICAL IMPLICATIONS OF THE THEORY OF ARCS

(i) *The Variation of β with Pressure*

Useful information can be obtained from consideration of the plasma balance equation and, in particular, of the variation of β with pressure, where $\beta = s_0/r_0$ with s_0 invariant for a given set of basic conditions. Assuming (ii) (*c*) conditions expression (28) applies, and if there is no magnetic field $\alpha_p = 1$ and $\tau = 1$. At low pressures the arc generally fills the tube, $r_0 = a$ the tube radius and λ_r is negligible. Now λ_i (i.e. λ_2) depends on T_e and also on n_0 unless n_0 is very high and the rate of ionization is accurately proportional to n_0^2. For relatively low values of n_0, when the rate of ionization is proportional to n_0, it is λ (i.e. $\lambda_2 n_0$), which is constant when n_0 is varied over a small range. Thus, for intermediate values of n_0, λ_2 diminishes as n_0 is increased but it asymptotically approaches a limiting value for sufficiently large values of n_0. Now, in general, n_0 increases with pressure and T_e decreases. Thus at first λ_i diminishes rapidly with increase in pressure, but its variation due to n_0 ceases if the latter becomes sufficiently large, and its variation due to T_e becomes small at intermediate pressures when T_e becomes (to a first approximation) independent of pressure. In addition, D_p diminishes and n_0 and T_p increase with pressure to an extent to maintain β constant while low pressure conditions exist.

Now volume electron recombination is independent of pressure but does depend on electron temperature and $\lambda_r \propto 1/T_e^c$, where the exact value of the exponent c is open to some doubt. Loeb (1939) claims from theoretical deductions that $c = 3/2$, but Sayers (1950) obtained experimental results which suggest that $c \simeq 1$ when $T_e \sim 400°$ K and rapidly falls to 0·5 when $T_e \sim 1\,000°$ K. If these results can be extrapolated to the values of electron temperature found in arcs, then c will be very small, say about 0·1. In either case λ_r increases as T_e decreases with increasing pressure. It is postulated that, when there is appreciable volume recombination (which is defined to occur when λ_r is no longer negligible compared with λ_i), r_0 no longer coincides with, but in fact exceeds, a. This hypothesis seems to be founded on sound physical principles, as the existence of volume recombination will obviously affect the radial distribution of particles and, as s_0 is invariant for a given type of ion production, r_0 must change. Again, the change in r_0 must be an increase since the volume recombination will cause the radial potential gradient to be less—in other words, to correspond to that in a discharge with no volume recombination in a larger diameter tube.

The pressure at which λ_r is appreciable compared with λ_i and r_0 first exceeds a is taken to mark the beginning of the transition to high pressure conditions and probably occurs at about 10 mm Hg pressure, although the exact pressure depends on the arc current and tube radius. As the pressure is further increased, $\lambda_i - \lambda_r$ diminishes until, at high pressures in dissociating gases, it is probable that $\lambda_i \simeq \lambda_r$ and hence $\beta \simeq 0$.

Thus, if the present theory is correct, $\lambda_i \simeq \lambda_r$ for high pressure arcs in nitrogen. From experimental results for arcs in nitrogen at pressures of one atmosphere and above (Cobine 1941, p. 327) it can be seen that T increases approximately as the logarithm of the pressure. This variation in T will cause λ_i to increase but λ_r to decrease very slightly. Now there are three factors which could cause a small increase in T as the pressure is increased. The first is the observed fact that radiation losses (neglected in the preceding theory) are not negligible with such arcs and increase with pressure. Secondly, the density of ions increases with pressure, and it is possible that λ_i is still decreasing slightly with increasing ionization density. Finally, it is possible that under such conditions some other form of recombination supplements volume electron recombination. Negative ions could not be formed and hence ionic recombination is out of the question. Dissociative recombination is a possible process, but it does not seem likely that this process will occur when the atoms have energies as high as those in high pressure arcs. However, owing to the high concentration of particles, some other form of three-body recombination may take place. The first of these three factors, which could cause T to increase with pressure, certainly does operate, and it is likely that either or both the second and third factors also operate.

(ii) *The Variation of β with Tube Radius*

The variation of β at low pressures with tube radius a is of some importance. For small values of a, β is constant, T_e and λ_i are large, T_p is small and λ_r is negligible. When a is increased, T_e and λ_i decrease, T_p increases and λ_r becomes appreciable, and for sufficiently large values of a, β starts to decrease. Eventually T_p approaches the value of T_e, and λ_r approaches λ_i, the corresponding tube radius being called the natural arc radius r_a. If the tube radius is further increased, the arc retains its natural radius. If the temperature is constant across the body of the arc, r_a is determined by eqn. (29), but if the temperature is a function of the radial distance from the axis, r_a is determined by eqn. (34) in which n_e is given by the solution of eqn. (33).

(iii) *The Effect of a Longitudinal Magnetic Field*

Consider the effect of a longitudinal magnetic field on a high pressure arc for which $T_e \simeq T_p$ (and both are constant across the arc) and $\lambda_i \simeq \lambda_r$. Preferential recombination is probably increased and, if this occurs, λ_i must be increased to maintain its equality with λ_r by an increase in arc temperature. Thus n_0 and K_e are increased and E changed slightly. From eqn. (36) it can be seen that under these circumstances r_a will be decreased.

Considering a low pressure arc for which T_e, T_p are constant across its section, the plasma balance equation is given by (28). A magnetic field reduces τ and α_p slightly and, as a result of an increased number of collisions, T_e and hence λ_i are reduced, T_p and, hence, D_p are slightly increased and λ_r may no longer be negligible. In general, these changes tend to reduce β when the tube radius is of the same order or greater than the natural radius of the arc. Thus a magnetic field generally reduces the natural radius of a low pressure arc but, if $r_a \gg a$, there will be no change in the radial distribution of charged particles* in a tube of radius a, although the radial potential gradient will be reduced. Also, since at low pressures T_e and the loss of energy to the walls are reduced by a magnetic field, it follows from the energy balance relation for low pressure arcs that E will be reduced.

The above conclusions are consistent with the experimental results of Cummings and Tonks (1941) for low pressure arcs in weak magnetic fields. Massey *et al.* (1949, p. 202), on the other hand, found that even at $1{\cdot}4 \times 10^{-3}$ mm Hg an appreciable constriction effect was produced by magnetic fields of thousands of gauss, although this was probably largely a cathode effect transmitted through the relatively short arc. However, if the magnetic field does reduce r_a to a value less than the tube dimensions a constriction effect will be obtained.

REFERENCES

ALLIS, W. P., 1949, *Phys. Rev.*, **76**, 146.
CAHN, J. H., 1949, *Phys. Rev.*, **75**, 293.
CHAMPION, K. S. W., 1952, *Proc. Phys. Soc.* B, **65**, 345.
COBINE, J. D., 1941, *Gaseous Conductors* (New York and London : McGraw-Hill).
CUMMINGS, C. S., and TONKS, L., 1941, *Phys. Rev.*, **59**, 514.
KLARFELD, B., 1937, *Techn. Phys. U.S.S.R.*, **4**, 44.
KOCH, O., 1949, *Z. Phys.*, **126**, 507.
LANDAU, L., 1950, *Phys. Rev.*, **77**, 567.
LOEB, L. B., 1939, *Fundamental Processes of Electrical Discharges in Gases* (New York : John Wiley).
MASSEY, H. S. W., BOHM, D., BURHOP, E. H. S., and WILLIAMS, R. W., 1949, *The Characteristics of Electrical Discharges in Magnetic Fields* (New York and London : McGraw-Hill).
SAYERS, J., 1950, *Proc. Conf. Ionos. Phys.*, State Coll., Pennsylvania.
SCHOTTKY, W., 1924, *Phys. Z.*, **25**, 342.
SUITS, C. G., 1939, *J. Appl. Phys.*, **10**, 730.
SUITS, C. G., and PORITSKY, H., 1939, *Phys. Rev.*, **55**, 1184.
TONKS, L., 1939, *Phys. Rev.*, **56**, 360.
TONKS, L., and ALLIS, W. P., 1937, *Phys. Rev.*, **52**, 710.
TONKS, L., and LANGMUIR, I., 1929, *Phys. Rev.*, **34**, 876.
WASSERRAB, T., 1950, *Z. Phys.*, **127**, 324, **128**, 312.

---

* Similarly, when $r_a \gg a$, an increase in pressure, which reduces r_a, produces no change in the radial distribution of charged particles in a tube of radius a.

The Theory of Gaseous Arcs : II
The Energy Balance Equation for the Positive Columns*

By K. S. W. CHAMPION
Electron Physics Department, University of Birmingham

Communicated by J. Sayers ; *MS. received* 19*th October* 1951

ABSTRACT. The theory of arcs is developed further by investigating the energy balance equation for high pressure positive columns. The energy balance equation put forward by Suits and based on the Nusselt relation is considered and some refinements in his analysis result in better agreement between theory and experiment. This theory only takes into account energy losses due to convection and conduction, but the neglect of radiation losses is justified for a wide range of conditions by reference to experimental values of radiation efficiencies.

The effect of a longitudinal magnetic field on high pressure arcs is then investigated. From the point of view of the energy balance equation the action of a magnetic field is to reduce the contributions of the charged particles to the conduction and convection losses from the column. Horizontal and vertical arcs are considered separately, as the nature of the convection, and hence the effect of a magnetic field, is not the same in the two cases.

The theory predicts that the action of a magnetic field will tend to a limit with sufficiently strong fields, and certain simple relations are deduced which should apply in this case. According to the theory, when the radius of a high pressure arc is reduced by a magnetic field the arc temperature must rise (incidentally, only by a relatively small amount) and the positive column gradient may increase or decrease, depending on certain relations which are specified. There are virtually no experimental data available for these conditions, but the scant data available are in general agreement with the theory.

.B
5
2

§ 1. THE ENERGY BALANCE EQUATION FOR HIGH PRESSURE POSITIVE COLUMNS

A great advance can be made in the theory of high pressure arcs when the energy balance equation is considered. The exact form of this equation in terms of the processes actually occurring is very difficult to formulate, but Suits and Poritsky (1939) have shown that the energy losses from a high pressure arc can be represented with reasonable accuracy by comparison with those from a hot solid cylinder in a gas. The heat lost from a solid cylinder by conduction and natural convection is given by Nusselt's expression, and hence the energy balance equation for the positive column of a high pressure arc may be written as

$$Ei = \text{const.}\ (k\Delta T)\left(\frac{D^3 M_{\mathrm{g}}^2 p^2 \mathbf{g} \Delta T}{\eta^2 \boldsymbol{R}^2 T^3}\right)^{\nu} \qquad \ldots\ldots(1)$$

where ΔT is the difference between the ambient and arc temperatures, k is the thermal conductivity at the mean film temperature ($T_{\text{ambient}} + \frac{1}{2}\Delta T$), D is the arc diameter (equals $2\,r_{\mathrm{a}}$), M_{g} is the molecular weight of the gas, $\mathbf{g}$ is the acceleration due to gravity, η is the viscosity and $\boldsymbol{R}$ the gas constant. The exponent ν has values lying in the range 0·04 to 0·25 for a solid cylinder. (ν is given by the slope of the dotted curve in fig. 100 of McAdams (1933).)

---

* Part I of this paper (Champion 1952) will be referred to as I ; symbols used there are not in general re-defined here.

Equation (1) applies to conditions where natural convection exists, and thus will be most accurate when the arc chamber is sufficiently large for convection to take place freely. Also, as Suits points out, this relation is based on natural convection around solids at whose surface there is no flow, but at the boundary of an arc the gas flow will be a maximum or nearly so. However, measurements of the heat convected upwards inside the body of an arc have shown that it is usually a relatively small quantity and can be neglected without gross error but, if required, the accuracy can be improved by employing in eqn. (1) an 'effective arc diameter' which is smaller than the actual arc diameter by an amount calculated to make the arc and solid convection processes correspond more closely.

Finally, from the above it can be seen that radiation losses are neglected in this theory. This procedure is justified for a wide range of conditions by experimental observations, including those of Suits (1939). From his measurements it is possible to deduce approximate values for the proportion of power lost in the form of radiation from the positive columns of arcs in various gases at high pressure. It is found that radiation is a maximum (excluding vapours) for polyatomic gases, for which it consists mainly of band spectra. For example, approximately 1% of the energy in a 1-atmosphere nitrogen arc is lost as radiation, but at 100 atmospheres it is approximately 10%. However, only 0·1% is lost from helium and argon at 1 atmosphere and 0·6% from helium at 50 atmospheres. The radiation losses from hydrogen arcs are exceptionally low (since the hydrogen is largely dissociated and with the present conditions the ionized hydrogen atom will not radiate), and at 1 atmosphere only 0·0001% of the energy is lost in this way. These radiation efficiencies were obtained with currents of 5 amperes.

Höcker and Finkelnburg (1946) comment that radiation losses from arcs in air at 1 atmosphere are small, even when the power dissipation* is as high as 2 kw/cm of column, and they neglect radiation losses in the theory they develop for these arcs. On the other hand, vapours such as mercury and sodium have relatively high radiation efficiencies, and it is not claimed that the present theory can usefully be applied to high power arcs in vapours. However, Elenbaas (1951 and references contained therein) and Francis (1946, 1949) have derived suitable theories for such arcs, although their theories contain a number of approximations. The calculations of Francis (1949) for helium and mercury provide an example of the relative efficiencies of permanent gases and vapours as radiators. He found that a power dissipation of 10^4 watts per cm of arc column would be required in helium to produce conditions (including radiation efficiency) similar to those in mercury with 10 to 100 w/cm.

Thus it is seen that over a wide range of conditions energy is lost almost exclusively from the positive column of a high pressure arc in a permanent gas by conduction and convection. Consequently, in the following theory attention is concentrated on representing these losses as accurately as possible.

Assuming that the arc temperature does not vary with current, Suits deduced from eqns. I (36) and (1) that, at a given pressure,

$$E = \text{const.}\, i^{-n} \qquad \ldots\ldots(2)$$

where $n = (2-3\nu)/(2+3\nu)$). ν is used in this context to represent Suits' α. When the temperature remains constant, from Saha's eqn. I (31) $n_0 = \text{const.}\, p^{0\cdot5}$, but if the arc temperature depends on pressure $n_0 = \text{const.}\, p^{\beta_s}$, where β_s is obtained from experimental results. Suits then deduced that, when the current was constant,

---

* It is found that the radiation efficiency of a high pressure arc increases approximately linearly with the power dissipation per unit length of positive column.

$$E = \text{const.}\, p^{m};\quad r_a = \text{const.}\, p^{-\gamma} \qquad \ldots\ldots(3)$$

where

$$m = -\nu[3(\beta_s - 1) - 4]/(3\nu + 2)$$

and

$$\gamma = (\beta_s + 2\nu - 1)/(3\nu + 2). \qquad \ldots\ldots(4)$$

In the table, experimentally determined values of n, m and γ are compared with those calculated from Suits' expressions. The table applies to nitrogen data—Suits and Poritsky (1939).

Exponent		n	m	γ	ρ†
Experimental					
Arc current	1 A	0·60	0·29	0·30	0·5 (approx.)
	10 A		0·32	0·38	
Theoretical					
Suits and Poritsky—independent of current		0·74	0·12*	0·28	(0·87)
Author–current	1 A	0·78	0·20	0·34	0·46
	10 A	0·75	0·21	0·35	0·45

* Suits and Poritsky incorrectly state the expression for m as $-\{\nu[3(\beta_s - 1) + 4]\}/(3\nu - 2)$, which gives $m = 0\cdot31$ in this example.

† ρ is defined in eqn. (15).

Better agreement is obtained if the variation of arc temperature with current is taken into account in the arc current equation, as well as the dependence of the Nusselt relation on arc temperature. For this purpose it is more convenient to represent n_0 by the expression

$$n_0 = \text{const.}\, p^{0\cdot5} T^{\delta}, \qquad \ldots\ldots(5)$$

which is a more general version of Suits' expression for n_0. δ is obtained from experimental results and Saha's equation. For example, for nitrogen $V_i = 14\cdot5$ volts and for currents of 1 to 10 amp in the 1 to 30 atmosphere pressure range the temperature lies in the range 5 000° to 8 000° K and $\delta = 13\cdot6$. A further experimental relation between T and p is required, and for the nitrogen data $T = \text{const.}\, p^{0\cdot07}$. Equation (5) also gives the variation of n_0 with current (via the dependence of T) for constant pressure.

If $T \gg T_{\text{ambient}}$, $\Delta T \simeq T$, $\eta \simeq \text{const.}\, T^{0\cdot7}$ and $k \simeq \text{const.}\, T^{0\cdot7}$. Also, $K_e \simeq \text{const.}\, T^{0\cdot7}/p$.

Thus

$$\frac{di}{i} = 2\frac{dr_a}{r_a} + \frac{dE}{E} - \frac{1}{2}\frac{dp}{p} + (\delta + 0\cdot7)\frac{dT}{T} \qquad \ldots\ldots(6)$$

and

$$\frac{dE}{E} + \frac{di}{i} = 3\nu\frac{dr_a}{r_a} + 2\nu\frac{dp}{p} + 1\cdot7(1 - 2\nu)\frac{dT}{T}. \qquad \ldots\ldots(7)$$

Consider the case of constant current and eliminate dE/E from eqns. (6) and (7),

$$\frac{dr_a}{r_a} + \left(\frac{2\nu - \frac{1}{2}}{3\nu + 2}\right)\frac{dp}{p} + \left(\frac{\delta + 2\cdot4 - 3\cdot4\nu}{3\nu + 2}\right)\frac{dT}{T} = 0,$$

from which $r_a = \text{const.}\, p^{(1-4\nu)/(6\nu+4)}\, T^{-(\delta + 2\cdot4 - 3\cdot4\nu)/(3\nu+2)}$ ......(8)

The first part of this expression corresponds with that of Suits, but the factor $T^{-(2\cdot4-3\cdot4\nu)/(3\nu+2)}$ constitutes a correction. With pressure constant, the plasma gradient as a function of current as deduced from eqns. (6) and (7) is

$$\frac{dE}{E}+\left(\frac{2-3\nu}{3\nu+2}\right)\frac{di}{i}=\frac{dT}{T}\left(\frac{3\cdot4-8\cdot9\nu-3\nu\delta}{3\nu+2}\right)$$

i.e. $$E=\text{const.}\,i^{(3\nu-2)/(3\nu+2)}\,T^{(3\cdot4-8\cdot9\nu-3\nu\delta)/(3\nu+2)} \qquad \ldots\ldots(9)$$

(The factor in T constitutes a correction to the expression obtained by Suits.)

If Saha's equation is used instead of the approximate relation (5) the following expression is obtained

$$E=\text{const.}\,i^{(3\nu-2)/(3\nu+2)}\,T^{(3\cdot4-9\cdot65\nu)/(3\nu+2)}\,10^{\{(5\cdot050V_i)/T\}\,\{6\nu/(3\nu+2)\}}. \qquad \ldots\ldots(10)$$

For the nitrogen data this becomes $E=\text{const.}\,i^{-0\cdot68}10^{j}$, where $j=\text{const.}/i^{0\cdot06}$. Equation (10) gives approximately the same variation of gradient with arc current as eqn. (9) but is less convenient to use.

When the current is constant, by eliminating dr_a/r_a from eqns. (6) and (7) and integrating the resultant differential equation

$$E=\text{const.}\,p^{11\nu/(6\nu+4)}T^{(3\cdot4-8\cdot9\nu-3\nu\delta)/(3\nu+2)} \qquad \ldots\ldots(11)$$

The correction factor in this expression is $T^{(3\cdot4-8\cdot9\nu)/(3\nu+2)}$.

Values of n, m and γ calculated from the corrected expressions are given in the table for the nitrogen data. The new values of m and γ are appreciably closer to the experimental values than were the original theoretical values, but the agreement between the values for n is not quite as good. The reason for this is not obvious, but the experimental value of n may be open to a little doubt.

In general, any discrepancies still remaining between the experimental and theoretical values of the constants must be due to (i) limitations of the model used for the energy losses or (ii) lack of accuracy in the experimental results. In the former case errors can arise due to the neglect of radiation and losses at the ends of the tube. Also, the use of eqn. I (36) for the arc current implies that throughout the body of the arc the temperature is constant and $\lambda_l=\lambda_r$, that is, that the arc is in equilibrium in a lateral direction and there is no transverse current. If the temperature is a function of radial position eqn. I (34) must be used, but this will cause little difference in the general trend of the results. However, if $\lambda_l>\lambda_r$ in the body of the arc there will be a transverse current and the energy losses will be increased. In monatomic gases the additional loss is mainly due to liberation of energy of recombination at the bounding sheath, and in gases which dissociate there is the additional liberation of reassociation energy.

In many high pressure arcs these losses will not be important since λ_l very nearly equals λ_r but where this is not the case the additional losses can readily be included in the preceding theory. Following Höcker and Finkelnburg* (1946) the conductivity k can be considered to consist of components $k_a+k_e+k_i+k_d$. k_a corresponds to the transport of translation energy of the molecules, atoms and ions, k_e to the corresponding transport of electron energy and k_i and k_d are due to ions and atoms forming in the interior of the arc and recombining and re-associating respectively at the boundary. The viscosity may be dealt with in the same way. However, when k_e, k_i and k_d are appreciable compared with k_a, it will be necessary to use the mean values of k and η over the temperature range from that of the arc to ambient instead of the values at the mean film temperature. The approximations for these quantities used in eqns. (6) and (7) will no longer be accurate and, if the same form of representation is retained, the exponent 0·7 will need to be replaced by a quantity which, in general, will be larger than 0·7 and will also be temperature dependent.

---

* The values of the components of the conductivity are corrected in a later paper by Höcker and Schulz (1949).

By combining eqns. (9) and (11)

$$E = \text{const.}\, i^{(3\nu-2)/(3\nu+2)} p^{11\nu/(6\nu+4)} T^{(3{\cdot}4-8{\cdot}9\nu-3\nu\delta)/(3\nu+2)}, \qquad \ldots\ldots(12)$$

where T is now a function of both i and p. Also, from eqns. (8) and (11), if r_{a1} and E_1 correspond to pressure p_1, and likewise for pressure p_2,

$$(E_2/E_1)^{\delta+2{\cdot}4-3{\cdot}4\nu}(r_{a2}/r_{a1})^{3{\cdot}4-8{\cdot}9\nu-3\nu\delta} = (p_2/p_1)^{0{\cdot}85-0{\cdot}3\nu+2\nu\delta}, \qquad \ldots\ldots(13)$$

which gives a relation between the changes caused in E and r_a when the pressure is changed from p_1 to p_2. For the nitrogen data this becomes

$$\left(\frac{E_2}{E_1}\right)^{15{\cdot}66}\left(\frac{r_{a2}}{r_{a1}}\right)^{-1{\cdot}57} = \left(\frac{p_2}{p_1}\right)^{3{\cdot}54} \quad \text{or} \quad \frac{E_2}{E_1} = \left(\frac{p_2}{p_1}\right)^{0{\cdot}23}\left(\frac{r_{a2}}{r_{a1}}\right)^{0{\cdot}10}.$$

The last factor in the final expression is approximately unity.

Another relation which can be derived from eqns. (6) and (7) is that expressing the arc radius as a function of current

$$r_a = \text{const.}\, i^{2/(3\nu+2)}\, T^{-(\delta+2{\cdot}4-3{\cdot}4\nu)/(3\nu+2)}. \qquad \ldots\ldots(14)$$

This may be written in the form

$$r_a = \text{const.}\, i^{\rho} \qquad \ldots\ldots(15)$$

where the exponent ρ includes the effect of the dependence of the arc temperature on the current.

Suits has not derived an expression corresponding to eqn. (15), but with his assumptions it would be

$$r_a = \text{const.}\, i^{2/(3\nu+2)} \qquad \ldots\ldots(16)$$

From experiment it is found that for most gases the current density I is almost independent of the current i, and thus $r_a \simeq \text{const.}\, i^{0{\cdot}5}$. Values of ρ for the nitrogen data, calculated from eqns. (14) and (16), are included in the table. The big improvement in the corrected value can readily be seen.

By combining eqns. (8) and (14)

$$r_a = \text{const.}\, i^{2/(3\nu+2)} p^{(1-4\nu)/(6\nu+4)} T^{-(\delta+2{\cdot}4-3{\cdot}4\nu)/(3\nu+2)} \qquad \ldots\ldots(17)$$

where T is now a function of both i and p. Also, from eqns. (9) and (14),

$$\left(\frac{E_2}{E_1}\right)^{\delta+2{\cdot}4-3{\cdot}4\nu}\left(\frac{r_{a2}}{r_{a1}}\right)^{3{\cdot}4-8{\cdot}9\nu-3\nu\delta} = \left(\frac{i_2}{i_1}\right)^{1-3{\cdot}4\nu-\delta} \qquad \ldots\ldots(18)$$

which gives a relation between the changes in E and r_a caused when the current is changed from i_1 to i_2. For the nitrogen data

$$E_2/E_1 = (i_2/i_1)^{-0{\cdot}83}(r_{a2}/r_{a1})^{0{\cdot}10}.$$

The Value of ν

The value of ν is given by the slope of the dotted curve in fig. 100 of McAdams (1933), and thus depends on the value of $D^3 M_g^2 p^2 \boldsymbol{g} \Delta T/\eta^2 \boldsymbol{R}^2 T^3$, which in the following is denoted by z. Now, for currents for which there is no selfconstriction effect (up to quite high currents at high pressure), $r_a \simeq \text{const.}\ i^{0{\cdot}5}$. If the variation of arc temperature with current is also taken into account ($T = \text{const.}\ i^{0{\cdot}06}$ for nitrogen at 1 atmosphere) it is found that $z \propto i^{1{\cdot}3}$. Consequently, for the present example, if the *current* is increased from 1 to 10 amperes, ν is increased from 0·1 to 0·13. The corresponding values of the exponents are shown in the table, and it can be seen that their variation with current is very small.

When only the *pressure* is varied, $z \propto p^{0{\cdot}74}$ for the nitrogen arc and thus, at a pressure of 100 atmospheres, ν is still only 0·13 for a 1 ampere arc, showing that the exponents are still less dependent on the pressure than on the arc current.

The value of ν also depends on the *atomic weight* of the gas. For example, for arcs of 1 ampere at 1 atmosphere in hydrogen $\nu \simeq 0{\cdot}03$, whereas for similar arcs in mercury $\nu \simeq 0{\cdot}15$. For hydrogen $T \simeq \text{const.}\ i^{0{\cdot}1}$ and, taking into account the ionization potential of hydrogen in estimating δ, a value of 0·81 is obtained for n. This is in good agreement with the experimental value of 0·82 for n in the vicinity of 2 amperes current.

§ 2. POSITIVE COLUMNS IN THE PRESENCE OF A UNIFORM LONGITUDINAL MAGNETIC FIELD

Of the two fundamental equations (6) and (7), that is, the arc current and energy balance equations, the former is unchanged except that the arc temperature T is now a function of the magnetic field strength as well as of current and pressure. Nusselt's equation (1) still holds, but the differential equation (7) is inadequate. This is because the thermal conductivity k and viscosity η can be affected by a magnetic field. The case of a horizontal arc is considered first, in which case the contributions of the charged particles to both k and η are affected by a longitudinal magnetic field.

(i) *Horizontal Arcs*

The modified version of eqn. (7) becomes

$$\frac{dE}{E} + \frac{di}{i} = 3\nu\frac{dr_a}{r_a} + 2\nu\frac{dp}{p} + (1-2\nu)\frac{dT}{T} + \frac{dk}{k} - 2\nu\frac{d\eta}{\eta}. \quad \ldots\ldots(19)$$

The portions of k and η due to charged particles are each reduced by a magnetic field and, since these contributions vary rapidly with temperature, it is necessary to use the mean values of these quantities over the temperature range from that of the arc to ambient. The precise effect of a magnetic field will depend on the particular properties of individual arcs, as it will depend on the relative magnitudes of the components of k and η. However, for a wide range of conditions, particularly for arcs with a high temperature, the predominant contribution of the charged particles to k will be k_e. Thus, only the effect of a magnetic field on k_e will be considered. In a magnetic field it is reduced by a factor $1/(1+\omega_e^2\tau_e^2)$ where $\omega_e = \boldsymbol{e}H/m_e$ and $\tau_e = m_m m_e n[D_e]_1/\rho_g \boldsymbol{k}T$ where m_m is the mean mass of the molecules and atoms, ρ_g is the gas density and $[D_e]_1$ is the first theoretical approximation to D_e, the diffusion coefficient (Chapman and Cowling 1939).

Assuming a relatively low degree of ionization, the effect of the ions compared with that of the molecules and atoms can be neglected. Thus the force between the electrons and gas particles can be represented by κ_e/r^σ, where σ will be considerably greater than 2, the value for an electrostatic force, and may be of the order of 11, which is the value for the particles of the light gases. With the above assumption

$$[D_{\mathrm{e}}]_1 = \frac{3}{8nA_1(\sigma)\Gamma\{3-2/(\sigma-1)\}}\left(\frac{\boldsymbol{k}T(m_{\mathrm{m}}+m_{\mathrm{e}})}{2\pi m_{\mathrm{m}}m_{\mathrm{e}}}\right)^{1/2}\left(\frac{2\boldsymbol{k}T}{\kappa_{\mathrm{e}}}\right)^{2/(\sigma-1)}$$

$$= \text{const.}\,\frac{T^{1/2}}{n}\left(\frac{T}{\kappa_{\mathrm{e}}}\right)^{2/(\sigma-1)} \qquad \ldots\ldots(20)$$

where m_{e} is neglected relative to m_{m} and it is assumed that σ is a constant. The composition of the gas (i.e. the relative proportions of atoms and molecules) is temperature dependent, and this can affect κ_{e}. However, the variation of κ_{e} with temperature will probably be small and, particularly as it is raised to the $-2/(\sigma-1)$ power, it can be neglected. Thus

$$[D_{\mathrm{e}}]_1 = \text{const.}\ T^{\{3/2+2/(\sigma-1)\}}/p \text{ and } \tau_{\mathrm{e}} = \text{const.}\ T^{\{1/2+2/(\sigma-1)\}}/p. \qquad \ldots\ldots(21)$$

There is little evidence as to the value of σ for collisions between electrons and atoms and molecules, but a value of 11 will be provisionally assumed. In this case $\tau_{\mathrm{e}} = \text{const.}\ T^{0{\cdot}7}/p$.

If, on the other hand, there is a very high degree of ionization in the arc, electrostatic forces will play a dominant part in collisions. The force between the electrons and ions will then be $e_{\mathrm{i}}\boldsymbol{e}/r^2$. Since these forces only fall off according to an inverse square law, the fields due to a number of particles will appreciably overlap when there are large concentrations of particles as in high pressure arcs. Thus 'collisions' will no longer be binary, and the theory with such conditions is not straightforward. However, if the gas pressure is considerably less than 1 atmosphere the collisions can be considered, with sufficient accuracy, to be binary and in eqn. (20) $e_{\mathrm{i}}\boldsymbol{e}$ can be substituted for κ_{e} and 2 for σ. Therefore

$$[D_{\mathrm{ie}}]_1 = \frac{3}{8nA_1(2)}\left(\frac{\boldsymbol{k}T(m_{\mathrm{i}}+m_{\mathrm{e}})}{2\pi m_{\mathrm{i}}m_{\mathrm{e}}}\right)^{1/2}\left(\frac{2\boldsymbol{k}T}{e_{\mathrm{i}}\boldsymbol{e}}\right)^2 = \text{const.}\,\frac{T^{7/2}}{p} \text{ and } \tau_{\mathrm{e}} = \text{const.}\,\frac{T^{5/2}}{p}. \qquad \ldots\ldots(22)$$

Thus, with the appropriate conditions, $\omega_{\mathrm{e}}^2\tau_{\mathrm{e}}^2 = A_1H^2T^{1{\cdot}4}/p^2$ or $A_2H^2T^5/p^2$ or, more generally,

$$\omega_{\mathrm{e}}^2\tau_{\mathrm{e}}^2 = AH^2T^u/p^2 \qquad \ldots\ldots(23)$$

where A is a constant depending on κ_{e} and σ and u represents $1+4/(\sigma-1)$. Thus the values of k and η transverse to a magnetic field are obtained by multiplying the no-field values by

$$F \equiv (1+BH^2T^u/p^2)/(1+AH^2T^u/p^2)^* \qquad \ldots\ldots(24)$$

where B is a function of the relative values of k_{a} and k_{e}. When $k_{\mathrm{e}} \ll k_{\mathrm{a}}$, $B \to A$, when $k_{\mathrm{e}} \gg k_{\mathrm{a}}$, $B \to 0$, and when $k_{\mathrm{e}} = k_{\mathrm{a}}$, $B = \frac{1}{2}A$. In other words, when there is a very high degree of ionization B tends to zero, and when there is a very low degree of ionization B tends to A.

---

[*] In the case of a very high degree of ionization k_{a} is almost entirely due to the positive ions and consequently is reduced in a magnetic field by a factor $(1+\omega_{\mathrm{i}}^2\tau_{\mathrm{i}}^2)^{-1} = (1+\omega_{\mathrm{e}}^2\tau_{\mathrm{e}}^2Cm_{\mathrm{e}}^2/m_{\mathrm{i}}^2)^{-1}$, where C denotes the order of ionization (usually predominantly unity). Now $\omega_{\mathrm{e}}^2\tau_{\mathrm{e}}^2Cm_{\mathrm{e}}^2/m_{\mathrm{i}}^2 \simeq 10^{-7}\omega_{\mathrm{e}}^2\tau_{\mathrm{e}}^2$, and thus, generally, the reduction in k_{a} can be ignored compared with that in k_{e}. However, if $\omega_{\mathrm{e}}^2\tau_{\mathrm{e}}^2$ is extremely large the reduction in k_{a} can be included by suitably modifying the value of B.

When H/p is small F is very little less than unity, but for sufficiently large values of H/p F tends to the limit B/A. Now the differential equation for η and k in the presence of a magnetic field is

$$\frac{d\eta_H}{\eta_H}=\frac{dk_H}{k_H}=0{\cdot}7\frac{dT}{T}+\frac{dF}{F}.^{*} \qquad \ldots\ldots(25)$$

Substituting in eqn. (19),

$$\frac{dE}{E}+\frac{di}{i}=3\nu\frac{dr_a}{r_a}+2\nu\frac{dp}{p}+1{\cdot}7(1-2\nu)\frac{dT}{T}+(1-2\nu)\frac{dF}{F}, \qquad \ldots\ldots(26)$$

where the additional term to the no-field expression is a function of H/p and T and depends on the gas.

From eqns. (6) and (26)

$$E=\text{const.}\ i^{(3\nu-2)/(3\nu+2)}p^{11\nu/(6\nu+4)}F^{(2-4\nu)/(2+3\nu)}T^{(3{\cdot}4-8{\cdot}9\nu-3\nu\delta)/(3\nu+2)}, \qquad \ldots\ldots(27)$$

where T is a function of i, p and H. Similarly,

$$r_a=\text{const.}\ i^{2/(3\nu+2)}p^{(1-4\nu)/(4+6\nu)}F^{(2\nu-1)/(3\nu+2)}T^{-(\delta+2{\cdot}4-3{\cdot}4\nu)/(3\nu+2)}, \qquad \ldots\ldots(28)$$

where again T is a function of i, p and H. If in these equations i and p are kept constant

$$E=\text{const.}\ F^{(2-4\nu)/(2+3\nu)}T^{(3{\cdot}4-8{\cdot}9\nu-3\nu\delta)/(3\nu+2)} \qquad \ldots\ldots(29)$$

and

$$r_a=\text{const.}\ F^{(2\nu-1)/(3\nu+2)}T^{-(\delta+2{\cdot}4-3{\cdot}4\nu)/(3\nu+2)} \qquad \ldots\ldots(30)$$

where T now depends only on H.

It is interesting to note that Suits' approximate theory, in which variations of η and k are neglected, predicts that a longitudinal magnetic field will have no effect on the positive column of a high pressure arc.

The above theory assumes that k_i+k_d are small compared with k_a+k_e, and this will be accurate for many high pressure arcs in which the transverse current is very small. However, if this is not the case, the influence of the magnetic field on the ambipolar diffusion of the ions and electrons must be taken into account. Now $k_i \propto D_a$ and $D_a=(b_pD_e+b_eD_p)/(b_p+b_e)$ with $b=\boldsymbol{e}\lambda/2\boldsymbol{mv}$, where the free path is denoted by λ. D_e is reduced in a magnetic field by a factor $1/(1+\omega_e^2\tau_e^2)$ and D_p is reduced by the corresponding factor. The relative values of the b's may also be affected. D_a is not much larger than D_p, and its reduction by a magnetic field will not be much greater than that in D_p, thus resulting in a relatively small reduction in k_i. Basically similar considerations apply to the effect of a magnetic field on k_d.

(ii) *Vertical Arcs*

Without a magnetic field the equations are formally the same as for a horizontal arc, but ν has a different value; in particular, corresponding to conditions for which $\nu=0{\cdot}25$ in the horizontal case, $\nu=0{\cdot}33$ in the vertical case. Thus it seems likely that for a vertical arc ν will be approximately four-thirds of its value for the corresponding horizontal arc.

To a first approximation η is not affected by a longitudinal magnetic field when the arc is vertical, since most of the convection is parallel to the magnetic field. Again to a first approximation, it is assumed that k is reduced to the same extent by a magnetic field as for a horizontal arc. The energy losses can still be represented by Nusselt's relation but a more general form than that in eqn. (1) is required as the Prandtl number $c_p\eta/k$ assumed constant therein will not remain constant for a vertical arc in a magnetic field. Thus

---

* When k_a does not exceed $k_e+k_i+k_d$ the coefficient of dT/T will no longer be 0·7 (see p. 349).

$$Ei = \text{const.}\,(k\Delta T)\left(\frac{r_a^3 M_g^2 p^2 \mathbf{g}\Delta T}{\eta^2 \mathbf{R}^2 T^3}\right)^{\nu}\left(\frac{c_p\eta}{k}\right)^{\nu}, \qquad \ldots\ldots(31)$$

from which

$$\frac{dE}{E} + \frac{di}{i} = 3\nu\frac{dr_a}{r_a} + 2\nu\frac{dp}{p} + (1-2\nu)\frac{dT}{T} + (1-\nu)\frac{dk}{k}$$

$$= 3\nu\frac{dr_a}{r_a} + 2\nu\frac{dp}{p} + (1{\cdot}7 - 2{\cdot}7\nu)\frac{dT}{T} + (1-\nu)\frac{dF}{F}. \qquad \ldots\ldots(32)$$

It can be shown that

$$E_v = \text{const.}\ F^{(2-2\nu)/(2+3\nu)}T^{(3\cdot4-7\cdot5\nu-3\nu\delta)/(2+3\nu)} \qquad \ldots\ldots(33)$$

and

$$r_{av} = \text{const.}\ F^{(\nu-1)/(2+3\nu)}T^{-(\delta+2\cdot4-2\cdot7\nu)/(2+3\nu)} \qquad \ldots\ldots(34)$$

where the subscript v denotes that the quantities refer to a vertical arc.

As $F \equiv (1 + BH^2T^u/p^2)/(1 + AH^2T^u/p^2)$ tends to the limit B/A when H tends to infinity,* corresponding to zero energy transport across the magnetic field due to charged particles, and as any other direct effect of the magnetic field will also tend to a limit, it would be expected that T will tend to a limit as H tends to infinity. This means that E and r_a must also tend to limits.

However, it has been found experimentally by Massey *et al.* (1949) that the transport of charged particles across a strong magnetic field is considerably greater than predicted by theory, and it may never become zero no matter how strong the magnetic field. The reason for the unduly high transverse transport appears to be connected with the drift induced by the magnetic field perpendicular to the radius and axis of the arc. If the radial drift were zero this latter drift should be in concentric circles round the arc. However, due to plasma oscillations, the equipotentials can be distorted, allowing particles to progress further from the arc, and if the positions of the equipotentials fluctuate with time at least some of the particles will possess a net outward radial drift. This effect has so far only been observed at low pressures, and it seems reasonable to expect that the effect will be less at higher pressures. Thus, if E and r_a do not tend to exact limits, their rate of change with field strength for very strong fields must be very small.

§ 3. THE EFFECT OF A VERY STRONG MAGNETIC FIELD

It is an experimental fact that, at intermediate pressures, the positive column of an arc with cathode of limited area is constricted by a uniform longitudinal magnetic field (Cummings and Tonks 1941, Reichrudel and Spiwak 1941, and others). Whether this constriction is fundamentally due to the action of the magnetic field on the positive column or whether it is due to the field collimating the electrons from the cathode, an effect which is transmitted through the positive column (Tonks 1941), may not be clear, but the present theory has the merit that it applies to any arc in a uniform longitudinal field provided the arc does not fill the tube.

For a given current and pressure, when the temperature is constant across the body of the arc

$$r_a = \text{const.}\left(\frac{1}{n_0 K_e E}\right)^{1/2} = \text{const.}\ T^{-(\delta+0\cdot7)/2}E^{-1/2}. \qquad \ldots\ldots(35)$$

---

* In general, at high pressures, the larger p the larger the value of H before the limit is reached.

Thus, if r_a is reduced by a magnetic field, $T^{\delta+0\cdot 7}E$ is increased and hence, since $\delta > 0$, either or both of T and E are increased.

A more general relation between the changes caused in r_a and E when a magnetic field is applied can be obtained from eqns. (29) and (30). If subscripts 0 refer to values with no magnetic field and subscripts H to values with a field of magnitude H,

$$\left(\frac{E_H}{E_0}\right)^{\delta+2\cdot 4-3\cdot 4\nu}\left(\frac{r_{aH}}{r_{a0}}\right)^{3\cdot 4-8\cdot 9\nu-3\nu\delta}=\left(\frac{1+BH^2T^u/p^2}{1+AH^2T^u/p^2}\right)^{(1-2\nu)(\delta+0\cdot 7)} \qquad \ldots\ldots(36)$$

If, now, the subscript '$\boldsymbol{H}$' is used to denote the values for a very strong magnetic field (i.e. the limiting values) then

$$\left(\frac{E_{\boldsymbol{H}}}{E_0}\right)^{\delta+2\cdot 4-3\cdot 4\nu}\left(\frac{r_{a\boldsymbol{H}}}{r_{a0}}\right)^{3\cdot 4-8\cdot 9\nu-3\nu\delta}=\left(\frac{B}{A}\right)^{(1-2\nu)(\delta+0\cdot 7)}. \qquad \ldots\ldots(37)$$

The corresponding versions of eqns. (29) and (30) are

$$E_{\boldsymbol{H}}=E_0\left(\frac{B}{A}\right)^{(2-4\nu)/(2+3\nu)}\left(\frac{T_{\boldsymbol{H}}}{T_0}\right)^{(3\cdot 4-8\cdot 9\nu-3\nu\delta)/(2+3\nu)} \qquad \ldots\ldots(38)$$

and

$$r_{a\boldsymbol{H}}=r_{a0}\left(\frac{B}{A}\right)^{(2\nu-1)/(2+3\nu)}\left(\frac{T_{\boldsymbol{H}}}{T_0}\right)^{-(\delta+2\cdot 4-3\cdot 4\nu)/(2+3\nu)} \qquad \ldots\ldots(39)$$

In handling eqns. (37), (38) and (39) it must be remembered that they apply *only* to the limiting conditions with zero and very strong fields respectively.

Both the exponents in eqn. (39) are negative and $B/A<1$. Hence, if r_a is reduced by a magnetic field then T is increased and

$$\frac{T_{\boldsymbol{H}}}{T_0}>\left(\frac{B}{A}\right)^{-(1-2\nu)/(\delta+2\cdot 4-3\cdot 4\nu)} \qquad \ldots\ldots(40)$$

From eqn. (38) it can be seen that $E_{\boldsymbol{H}}<E_0$ when $3\cdot 4-8\cdot 9\nu-3\nu\delta\leqslant 0$. However, the inequality $E_{\boldsymbol{H}}<E_0$ still holds when $3\cdot 4-8\cdot 9\nu-3\nu\delta>0$ provided that

$$\frac{T_{\boldsymbol{H}}}{T_0}<\left(\frac{B}{A}\right)^{-(2-4\nu)/(3\cdot 4-8\cdot 9\nu-3\nu\delta)}. \qquad \ldots\ldots(41)$$

Otherwise E remains constant or is increased by a magnetic field.

The equations corresponding to (38) and (39) for a vertical arc are

$$E_{\boldsymbol{H}\mathrm{v}}=E_{0\mathrm{v}}\left(\frac{B}{A}\right)^{(2-2\nu)/(2+3\nu)}\left(\frac{T_{\boldsymbol{H}}}{T_0}\right)^{(3\cdot 4-7\cdot 5\nu-3\nu\delta)/(2+3\nu)} \qquad \ldots\ldots(42)$$

and

$$r_{a\boldsymbol{H}\mathrm{v}}=r_{a0\mathrm{v}}\left(\frac{B}{A}\right)^{(\nu-1)/(2+3\nu)}\left(\frac{T_{\boldsymbol{H}}}{T_0}\right)^{-(\delta+2\cdot 4-2\cdot 7\nu)/(2+3\nu)}. \qquad \ldots\ldots(43)$$

The only change from the equations for a horizontal arc is a small difference in the value of each exponent. Thus the preceding considerations for a horizontal arc apply to a vertical arc with only the requisite minor changes in the values of the exponents.

Another useful relation can be obtained by squaring eqn. (39) and multiplying by the respective sides of eqn. (38). The result reduces to

$$\left(\frac{E_{\boldsymbol{H}}}{E_0}\right)\left(\frac{r_{a\boldsymbol{H}}}{r_{a0}}\right)^2=\left(\frac{T_{\boldsymbol{H}}}{T_0}\right)^{-(\delta+0\cdot 7)}. \qquad \ldots\ldots(44)$$

thus giving a relation between the respective changes caused by a very strong magnetic field in arc radius, voltage gradient and temperature. From eqns. (42) and (43) it can be shown that the same relation exists between the appropriate quantities for a vertical arc.

Comparison of the Theory with Experimental Results

There are virtually no experimental results to which the theory developed in this section for the action of a longitudinal magnetic field on arcs at medium or high pressures can be applied. However, it is interesting to consider some results of Reichrudel and Spiwak (1938) in the light of the present theory. According to their results, with low pressures of mercury vapour (~0·001 mm) a longitudinal field reduces the positive column gradient in a 2·5 amp arc, but as the pressure is increased the reduction becomes less until at 0·06 mm there is practically no change on application of a magnetic field. Again, with a 40 mA discharge in argon at 0·096 mm there is a slight increase in potential gradient when a magnetic field is applied, but with higher currents (up to 400 mA) the increase is much greater. Magnetic fields up to 130 gauss were used and, although these fields probably caused some distortion of the probe measurements from which the gradients were calculated, the general nature of the results should be accurate.

The above results are consistent with the theoretical prediction that the positive column gradient of a low pressure arc is reduced by a longitudinal magnetic field. They also suggest that a magnetic field increases the positive column gradient in high pressure arcs in mercury vapour or argon. From the theory a requirement for this is that $3{\cdot}4-8{\cdot}9\nu-3\nu\delta>0$. Now, for a 2·5 amp mercury arc at several millimetres pressure ν is approximately 0·12, and hence $\delta<6{\cdot}5$. Similarly, ν is approximately 0·07 for 0·1 amp argon discharges at several millimetres pressure, and thus $\delta<13{\cdot}2$. The values of δ to satisfy the inequalities seem reasonable, remembering that the low ionization potential of mercury will cause δ to be considerably lower for that vapour for a given temperature range than for, say, argon.

With regard to the present theory, it is interesting to consider some results of Earhart (1914), although his measurements were made with glows, where the processes involved are probably not exactly the same as in arcs. Earhart found, using dried air at 0·24 mm Hg pressure, that a longitudinal magnetic field up to 1 400 gauss reduced the potential across the discharge, but that a stronger field increased it again. The magnetic field had little effect with pressures about 1 mm Hg, but with somewhat higher pressures all values of the field increased the discharge potential. Earhart showed that the effect was in the positive column by using chambers of different length. In particular, with a short (5 mm) discharge a magnetic field had practically no effect. Thus the cathode and anode falls must have remained unchanged, as would be expected with Earhart's conditions, in which the electrons did not have to cross lines of magnetic force in leaving the cathode or reaching the anode. He obtained similar results with hydrogen and carbon dioxide.

Although the conditions in the above experiments only border on those assumed in the theory, they nevertheless suggest that the theory is physically sound. However, the subject of medium and high pressure arcs in magnetic fields is almost untouched, and a considerable amount of experimental data has to be obtained before the theory can be thoroughly tested.

ACKNOWLEDGMENTS

The author wishes to thank Professor J. Sayers for his encouragement in this work, which was made possible by the award of a Research Fellowship by the Australian National University.

REFERENCES

The following references are additional to those listed in Champion (1952):

CHAMPION, K. S. W., 1952, *Proc. Phys. Soc.* B, **65**, 329.

CHAPMAN, S., and COWLING, T. G., 1939, *The Mathematical Theory of Non-Uniform Gases* (Cambridge: University Press).

EARHART, R. F., 1914, *Phys. Rev.*, **3**, 103, and **4**, 135.

ELENBAAS, W., 1951, *The High Pressure Mercury Vapour Discharge* (Amsterdam: North-Holland Publishing Company).

FRANCIS, V. J., 1946, *Phil. Mag.*, **37**, 433, 653; 1949, *Ibid.*, **40**, 435, 1063.

HÖCKER, K. H., and FINKELNBURG, W., 1946, *Z. Naturforsch.*, **1**, 305.

HÖCKER, K. H., and SCHULZ, P., 1949, *Z. Naturforsch.*, **4a**, 266.

MCADAMS, W. H., 1933, *Heat Transmission* (New York and London: McGraw-Hill).

REICHRUDEL, E., and SPIWAK, G., 1938, *C. R. Acad. Sci. U.R.S.S.*, **18**, 177; 1941, *J. Phys. U.S.S.R.*, **4**, 211.

TONKS, L., 1941, *Phys. Rev.*, **59**, 522.

Observations on Radio-Frequency Oscillations in Low-Pressure Electrical Discharges

BY N. R. LABRUM AND E. K. BIGG*

Division of Radiophysics, Commonwealth Scientific and Industrial Research Organization, Australia

Communicated by J. L. Pawsey; MS. received 27th July 1951, *and in amended form 18th December* 1951

ABSTRACT. The generation of high-frequency energy by electrical discharges in air at low pressures has been investigated by observations with several types of discharge tube, at frequencies near 200 Mc/s and below 2 Mc/s.

Random noise of high intensity was observed in both these frequency ranges, and was found to be associated with a field reversal in the discharge.

Coherent oscillations were also observed at the lower frequencies, and there was evidence that these were the cause of the striations of the positive column.

§ 1. INTRODUCTION

It has long been known that radio-frequency oscillations can often be detected in electrical discharges in gases at low pressures. This phenomenon was observed by Penning (1927); subsequently it was more thoroughly investigated by Tonks and Langmuir (1929), who found that the hot-cathode mercury vapour arc used by them generated a wide variety of oscillations, ranging in frequency from 1 Mc/s to 1 000 Mc/s. They also showed theoretically that vibrations could take place at those frequencies in the ionized plasma of the discharge; their theory in its original form, however, did not indicate any mechanism by which energy could be supplied to maintain such oscillations.

---

* Now at Meteorological Department, Imperial College, London.

More recently it has been shown by Bailey (1948), and also by Böhm and Gross (1949), that in an ionized medium which contains well-defined streams of charged particles it is possible for an initial small disturbance to 'grow' by the conversion of some of the kinetic energy of the ions into high-frequency energy. In conditions favourable to processes of this kind, sustained 'plasma oscillations' are evidently possible.

Many experimental investigations have confirmed in general the results obtained by Tonks and Langmuir. Cobine and Gallagher (1947) found evidence that the oscillations were generated near the cathode in the discharge which they examined. Neill and Emeléus (1951) obtained similar results, and also showed that these disturbances produced a velocity modulation of the primary electron beam, and so were transmitted to other parts of the discharge.

The present paper describes an experimental investigation of the radio-frequency energy emitted by certain special types of glow discharge in air, and an attempt to establish what are the essential conditions for the production of such radiation. It was found that the effects which were observed fell into two distinct categories, which will be discussed separately. It will be shown that the first type of oscillation had the properties of electrical 'noise' of high intensity and that its occurrence depended on the geometry of the discharge. A possible explanation of this will be advanced.

The second effect was the generation of coherent oscillations at low radio frequencies, which appeared to be associated with the striations of the positive column. Whilst the observations were made only under restricted conditions, the discussion of them leads to some general speculation as to the origin of the striations. These, whilst very tentative, will be shown to be consistent both with the present work and with previously published data.

§ 2. APPARATUS

(i) *Discharge Tubes*

A typical tube used in the study of high-frequency electrical energy originating in glow discharges is shown in fig. 1. This glass-walled tube had two cathodic electrodes C and A_1, consisting of flat zigzags of 0·0012 inch diameter tungsten wire lying in planes 3 mm apart, and could be used for examining both self-sustaining and hot-cathode discharges. For reasons which will be explained later, the discharge column, immediately in front of the electron gun, was usually enclosed by a nickel cylinder N. The main anode A_2 was a small nickel or molybdenum disc. The glass envelopes ranged in diameter from

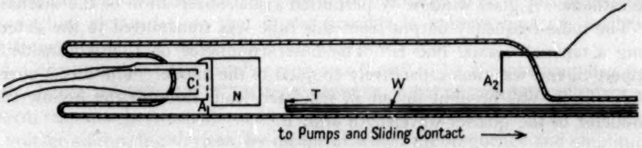

Fig. 1. Hot-cathode discharge tube with movable probe.

1·5 cm to 3 cm; the distance between the main anode and the electrode gun was about 20 cm. One of the hot-cathode tubes was fitted with a movable probe (also shown in fig. 2), for the examination of the potential distribution. This probe consisted of the exposed tip T (fig. 1) of a thin tungsten wire W, the remainder of which was covered by a glass insulating sleeve. The probe could be moved along by a magnetic device (not shown in the diagram), electrical contact being provided through a rail along which the end of the probe structure was made to slide.

When somewhat more detailed probe measurements became necessary in connection with the study of the low-frequency oscillations, these were made on a cold-cathode tube with glass walls 3 cm in internal diameter, along the side of which were sealed 19 probes, spaced 1 cm apart. Each probe consisted of a 0·005 inch diameter tungsten wire, which extended about 0·8 cm into the tube; all but the tip of each wire was enclosed in glass. Whilst it should be pointed out that the use of such small probes may possibly lead to errors at the highest pressures used (see Sloane and Emeléus 1933), this disadvantage is outweighed by the convenience of the method, in view of the approximate nature of this investigation.

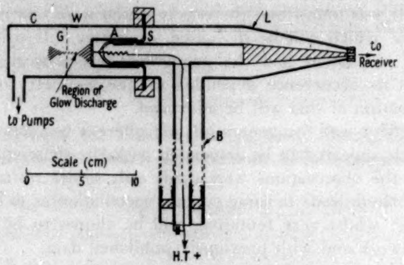

Fig. 2. Metal discharge tube used in preliminary experiments.

A cold-cathode tube of another type is shown in fig. 2. This had a special electrode structure for conveying high-frequency signals from the discharge to a receiver. The anode was a copper sleeve A, closed at one end, which fitted over a glass support S. The latter was waxed in position upon the end of the copper cylinder C, which together with a grid G (of 0·2 cm mesh) formed the cathode. A glass window W permitted visual observation of the discharge.

The radio-frequency output from this tube was transmitted to the detector along a tapered coaxial line L. The inner conductor of L fitted inside the support S, and was thus capacitively coupled to the anode. The direct current anode supply was brought in, on an insulated lead, through the hollow inner conductor of the quarter-wavelength stub B.

(ii) *Radio-frequency Measuring Equipment*

Measurements of oscillations generated in gas discharges were in the main confined to frequencies below 2 Mc/s, and a band centred at 200 Mc/s.

For the higher frequencies a conventional superheterodyne receiver was used. The tuning range of this extended from 180 Mc/s to 220 Mc/s and the bandwidth was approximately 1 Mc/s. The minimum detectable signal was found by tests with a standard signal generator to be 2×10^{-13} watts. This power distributed over a 1 Mc/s band would be equal to that received from a resistance at 2000° K, matched to the receiver input; however, except under certain special conditions, noise was in fact not detected in gas discharges in which the mean electron energy was certainly equivalent to a temperature many times this value (in calculating equivalent temperatures from noise intensities, it has been assumed that 'thermal' noise is entirely due to the random motion of electrons in the discharge). This indicated that a large mismatch occurred, either in the coupling system or (more probably) between the coupling and the discharge column. The energy generated by the discharge was, therefore, always greater by an unknown factor than that available at the receiver input, and values for the effective temperature deduced from noise measurements must accordingly be regarded merely as lower limits.

The method of coupling the output from the discharge tube shown in fig. 2 to this receiver is clear from the diagram. In the case of the hot-cathode tubes the coupling unit shown in fig. 3 was used. The discharge tube T was mounted transversely between two copper discs D, attached to the ends of a pair of copper rods C, 6 mm in diameter. The latter formed a parallel-conductor transmission line, which could be tuned to the same frequency as the receiver by moving the short-circuiting bar S. This bar also carried a coupling loop L, the output from which was taken through a coaxial line A to the receiver. The size of this loop was not at all critical, and it could be left fixed after a preliminary adjustment. The position of the bar S, however, needed adjusting for each observation, owing to variations in the impedance presented by the discharge. This type of coupling had the advantage that any part of the discharge could be placed between the coupling electrodes, so that it was possible to observe how the available high-frequency output varied along the axis of the tube.

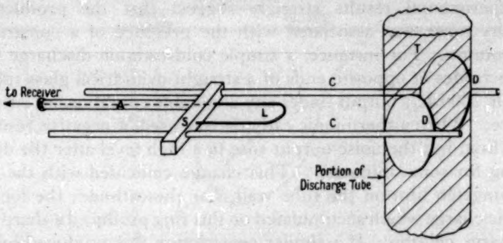

Fig. 3. Coupling unit, used with hot-cathode discharge tube (schematic).

A Cossor double-beam oscillograph was found to be a convenient detector for the lower frequencies. This instrument included an amplifier with nearly uniform response between about 50 c/s and 1 Mc/s, and was also fitted with time and voltage calibrating devices, by means of which the frequency and amplitude of the signal could be determined. In using the oscillograph, the radio-frequency voltage between any two electrodes was applied to the amplifier input; in most cases simple filter circuits were necessary to remove a 50 c/s component, due to ripple on the d.c. supply to the discharge tube, and also to avoid the production of spurious circuit oscillations.

§ 3. EXPERIMENTAL

(i) *Observations of High-frequency Noise*

Experiments conducted with the equipment described above showed that, under suitable conditions, electrical discharges in air can produce high-frequency oscillations of considerable intensity, with the characteristics of electrical noise. For example, the measurements with the tube shown in fig. 1 indicated that the radio-frequency energy generated in the discharge was uniformly distributed over the frequency range of the receiver (180–220 Mc/s); some rough tests with a second receiver showed that the signal also extended over the range 400–800 Mc/s. The spectrum had therefore the continuity which is typical of 'noise' as distinct from coherent oscillations. Similar results were obtained with the cold-cathode tube shown in fig. 2. The power available at the receiver input was usually of the order of 10^{-12} watt per c/s of bandwidth; it was found to be greatest at pressures of about 10 microns Hg, and to fall off rapidly when the pressure was increased above 100 microns. Although the noise output varied as current and voltage were changed, there were indications that the noise-generating process did not depend directly on these parameters but on other properties of the discharge which changed when the operating conditions were altered.

The experimental results strongly suggest that the production of this high-intensity noise was associated with the presence of a constriction of the discharge column. For instance, a simple cold-cathode discharge between the two disc electrodes at opposite ends of a straight cylindrical glass tube produced no detectable 200 Mc/s output under any attainable conditions of current, voltage and pressure. When a thermionic cathode was used, a negative result was again obtained at first, but the noise output rose to a high level after the discharge had been passing for some minutes. This change coincided with the deposit of a sputtered tungsten film on the tube wall near the cathode; the focusing action of the electric charge which accumulated on this ring produced a sharp constriction of the discharge column. If a similar constriction was produced by means of a metal ring (N in fig. 1) at cathode potential, it was found that noise was generated, even when the tubes were new, as soon as the discharge was started.

Further evidence on the effect of a constriction of the discharge was provided by observations with the cold-cathode tube shown in fig. 2. The structure in this case was such that the discharge column was brought to a very sharp focus in the region of the grid. When the anode voltage of this tube was gradually decreased, a point was reached at which the noise output rose abruptly from below the threshold sensitivity of the receiver to an intensity about 70 db above that level. It was noticed that when the discharge was in the 'silent' condition the positive column extended to the cathode side of the constriction, but that when noise was being generated the negative glow extended into the anode–grid space. From this experiment it therefore appears that 200 Mc/s noise was only generated when the negative glow, rather than the positive column, of the discharge was constricted. The behaviour of the other types of tube was consistent with this hypothesis, since in them the constriction invariably occurred near the cathode end of the discharge.

In the case of the discharges in glass tubes, it was found that the maximum high-frequency output was obtained when the coupling electrodes were placed near the constriction. Other much smaller maxima were observed at the heads of the striations when these were present in the positive column. The noise output always appeared simultaneously at all these points, the positions of which were independent of frequency over the range 200 to 600 Mc/s.

Finally, the influence of the constriction of the discharge column upon the axial potential gradient was examined by measuring the floating potential of the moving probe shown in fig. 1.* These observations, which were made for a wide variety of operating conditions, all indicated that noise was generated only when a pronounced reversal of the axial electric field occurred in the discharge near the cathode. When no noise could be detected, this field reversal was invariably found to be either absent or much less marked. Figure 4 shows the results of two typical measurements of floating potential.

The main results of the observations described in this section can, then, be summarized as follows: discharges in air at pressures below 100 microns have been shown to produce electrical noise in the 200 Mc/s region with intensity of the order of 10^{-12} watt per c/s. This effect appeared to be dependent upon the presence of a constriction of the negative glow portion of the discharge column; high intensity noise was only generated when such a constriction caused a reversal of the axial electric field in the discharge.

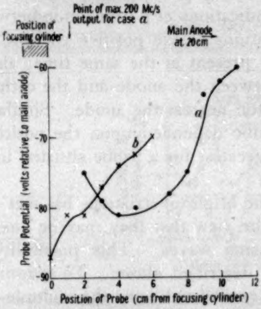

Fig. 4. Floating potential of probe in hot-cathode discharge.
a. Current to main anode = 80 mA.
Noise input to 200 Mc/s receiver = 10^{-9} watt per c/s.
b. Current to main anode = 40 mA.
Noise input to receiver $< 2 \times 10^{-13}$ watt per c/s.
Air pressure = 10 microns (approx.).

(ii) *Low-frequency Noise*

It seemed likely that the high-frequency noise which was observed might be due to some kind of electronic oscillation. If this were the case, an analogous positive-ion effect might reasonably be expected to give rise to noise at much lower frequencies. A search was accordingly made for electrical noise in the region of 1 Mc/s. The cathode-ray oscillograph was used as a detector of the radio-frequency voltages between the cathode and the anode of the tube. It was found that a signal was frequently present which, from its appearance on the oscillograph, closely resembled thermal noise. This low-frequency output was most intense under conditions which favoured the production of 200 Mc/s noise.

---

* It must be recognized that this method does not give dependable values for the space potential. It can, however, be expected to give a rough indication of the general nature of the axial potential gradient, which is all that was required in these experiments.

The amplitude was about 0·1 volt at the amplifier input, where the impedance was 1 000 ohms. If the detector bandwidth is taken as being 2 Mc/s, this corresponds to 5×10^{-12} watt per c/s.

(iii) *Coherent Oscillations*

In addition to the low-frequency noise, it was found that the oscillograph frequently indicated the presence in the discharge of a coherent oscillation at a frequency of the order of 200 kc/s. This occurred, over a wide range of discharge currents, with pressure less than about 150 microns, in various discharge tubes with either hot or cold cathodes. It was quite distinct from the random noise, which was often simultaneously present in the same frequency band; it was, in fact, most readily observed at low pressures and current densities, under which conditions the level of the low-frequency random noise was low. The frequency of the oscillation was independent of the circuit constants but varied with pressure and discharge current. It may therefore be concluded that the phenomenon was a characteristic of the discharge alone, and was not dependent on the external circuit. The amplitude was very variable; the signal voltage induced on a probe maintained at approximately the space potential was in some cases as high as 1 volt.

There were several indications of a connection between these low-frequency oscillations and the striations of the positive column. For example, the two phenomena were usually present at the same time; also, the amplitude of the oscillations developed between the anode and the cathode was correlated with the position of the striation nearest the anode. Similarly, the radio-frequency voltage induced on a probe depended upon the position of the latter relative to the striations; it was greatest for a probe situated in the luminous part of a striation.

Whilst no theory of the origin of striations has met with general acceptance, Loeb (1939) inclines to the view that they may be due to nodes and antinodes set up by invisible plasma waves. This possibility is supported by the preliminary observations described above. To examine it further a series of probe measurements was carried out using the multiple-probe cold-cathode tube described in §2 (i). Voltage–current characteristics of a number of the probes were determined; from these, using as a first approximation the assumption that there was a Maxwellian distribution of electron energies, it was possible to find the average electron temperature, the space potential and the variation of electron concentration (see, for example, Loeb 1939). However, in the positive column the current to the probes was very small, and here the accuracy of readings was so low that only space potentials could be satisfactorily determined. The average electron temperature in this region was roughly 2×10^5 deg. K. The space potential in the positive column is plotted in fig. 5 (*a*). Figure 5 (*b*) shows the space potential, electron concentration and electron temperature in the Faraday dark space, where more accurate measurements were possible. The electron temperatures there were not sufficiently high to excite visible striations.

These measurements show that the space potential went through a maximum at the brightest part of each striation (fig. 5 (*a*)), and that the voltage maxima also corresponded to points of maximum electron temperature and minimum electron concentration (fig. 5 (*b*)). References to many measurements of this type by earlier workers are given by Thomson and Thomson (1933). The results obtained are in general agreement with those of the experiments described above.

If, as has already been suggested, the striations are caused by the oscillations, it should be possible to modify them by applying a sufficiently large radio-frequency voltage to the discharge. To test this prediction, a signal with a frequency variable between 200 kc/s and 800 kc/s was applied to a probe near the cathode end of the tube. The peak amplitude as measured between the probe and the cathode was about 50 volts; however, the voltage actually effective in modifying the discharge was probably only a small fraction of this owing to the screening action of the ion-sheath surrounding the probe. The probe was biased to prevent the alternating voltage from driving it sufficiently positive to draw appreciable current. It was found that the spacing of the striations varied considerably with the frequency of this signal, decreasing as the frequency increased. Thus in one case there were four striations in the absence of any external signal and ten (in the same total length of positive column) when a signal of 800 kc/s was injected at the probe. The oscillation generated in the discharge had in this instance a frequency of 200 kc/s. For some frequencies of the applied voltage, it was noticed that the striations became irregularly spaced; for others the contrast between the dark and luminous bands was considerably reduced. These changes in appearance were quite different from those observed when the anode potential was varied, and are evidently not, therefore, due to rectification of the signal applied to the probe.

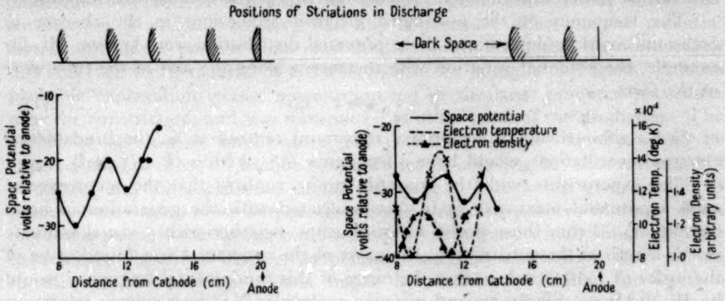

(*a*) *above*: Positions of striations in discharge. *below*: Variation of space-potential in positive column. Discharge current = 1·2 mA.

(*b*) *above*: Positions of striations in discharge. *below*: Variation of space-potential and electron-temperature and density in dark space. Discharge current = 3·5 mA.

Fig. 5. Data from probe measurements in cold-cathode discharges.

§ 4. DISCUSSION

(i) *The Mechanism of Noise Generation in the Discharge*

An attempt will now be made to explain the production of high-intensity noise by electrical discharges under the conditions described above. The experimental evidence is given in § 3 (i). It must first be remarked that the high noise intensities which were observed could not be of thermal origin, for a thermal source generating 10^{-12} watt per c/s would have a temperature of about 10^{11} deg. K, whereas the electron temperature in the discharges was known to be less than 10^{6} deg. K.

An alternative explanation is suggested by the correlation between the generation of high intensity noise and the occurrence of a constriction of the discharge column accompanied by a reversal of the axial potential gradient. It seems possible that electrons which had insufficient energy to carry them right through this potential maximum would perform oscillations resembling the electron oscillations in the Barkhausen–Kurz oscillator; positive ions would oscillate in the same way near the adjacent potential minimum. This hypothesis is open to the objection that it implies that high-frequency oscillations would be generated in any discharge in which a field reversal occurred, e.g. in any striated positive column. It is, however, possible that potential maxima of this type are usually too small to 'capture' electrons entering them, so that oscillations do not, in fact, take place. A further difficulty arises in explaining the apparent failure of a constriction of the positive column to cause noise to be generated. It may be that in some cases the positive column was so nearly a neutral plasma that a distortion of it had little effect upon the potential gradient; however, this does not apply to a striated positive column, most parts of which are by no means neutral. Further experimental evidence on this point is evidently desirable.

The frequency of the postulated electron oscillations in the absence of collisions could be determined if the potential distribution were known. If, for example, the potential variation with distance x along the axis of the tube were of the form

$$V = V_0 - k(x - x_0)^2 \qquad \ldots\ldots(1)$$

in the neighbourhood of a potential maximum centred at x_0, the fundamental electronic oscillations would have a frequency $9{\cdot}5\sqrt{k}$ Mc/s (k in v/cm^2).

The experiments with the movable probe confirm that the occurrence of such a potential maximum is in fact associated with the generation of noise (see fig. 4). From these probe measurements, together with a visual estimate of the length of the constriction, the value of the constant k was found to be of the order of 1–10 v/cm^2, so that the range of this fundamental frequency would be 10–30 Mc/s. Singly ionized nitrogen molecules N_2^+ in a voltage minimum of similar dimensions would have oscillations in the range 50–150 kc/s.

In this discussion it has so far been assumed that the ions were free to move under the influence of the electric field alone; in practice, however, the oscillatory motion must, clearly, have been modified by collisions with gas molecules. The effect of this would be to break up the otherwise steady oscillation of an electron or positive ion into a series of short pulses, each lasting for a time equal to the interval between successive collisions. The mean collision frequency for electrons in air at the pressures used (5–10 microns) is of the order of 10^8 per second (for an electron energy of 10 ev); for positive ions, the corresponding collision frequency is 5×10^4 per second. The output would, therefore, have consisted of a series of very short pulses of oscillation, and so would have resembled random electrical noise. Since the average duration of these pulses was only of the order of one cycle of oscillation, the resultant spectrum would be extremely broad. The collisions, by frequently interrupting the electron motion, would also reduce any tendency for the oscillations of the individual electrons to be brought into synchronization with each other by a 'bunching' process. Thus the effects of collisions account for the observed facts that the radio-frequency output has a very wide, uniform, spectral distribution, that, in the low-frequency case at least, it resembles electrical noise, and that it has appreciable components at frequencies many times the value calculated for the fundamental electron oscillations.

It has already been pointed out that the mechanism of noise generation which has been suggested is analogous to that of the Barkhausen–Kurz oscillator. In the latter, the electrons oscillate in the potential maximum set up by the application of a positive voltage to the grid of the triode valve. Similar suggestions have also been made by Ballantine (1933) to explain spurious oscillations in radio valves which contained traces of gas, and by Armstrong (1947) in connection with microwave oscillations which he detected in gas-filled thermionic diodes. In all these cases, however, collisions of the oscillating particles with neutral molecules either did not take place, or occurred at intervals of time which were long compared with the frequency of oscillation. Consequently, the oscillatory motion was in each case orderly, and coherent oscillations, rather than noise, were produced.

The observation that high-frequency noise sometimes appeared at the heads of the striations is not easily explained. This effect occurred only when the discharge was constricted near the electron gun. Therefore, since this constriction is unlikely to have had any appreciable effect on the potential distribution in the positive column, it does not seem likely that the noise which was observed was generated by electron oscillations in the latter region. A more probable explanation is that noise originated in the large potential maximum near the constriction, and was transmitted to other parts of the discharge. The variations of electron temperature and concentration (see fig. 5) would be expected also to cause a variation in the degree of coupling between the external electrodes and the oscillations in the discharge. This would give a series of points of maximum noise output, distributed along the positive column. It is, of course, possible that under conditions other than those which obtained in the experiments described above, the potential maxima which have been shown to exist in the positive column might be sufficiently intense for electron oscillations of appreciable amplitude to be set up in them.

(ii) *Low-frequency Oscillations in the Discharge*

It has already been shown that the experiments described in § 3 (iii) indicate that the striations are related to the coherent low-frequency oscillations which were detected in the discharge, and that this correlation may mean that the striations are the visible effect of a standing wave set up in the discharge column. In order to put this hypothesis on a firmer basis, it is first necessary to show that an appropriate mode of propagation through the discharge does, in fact, exist.

Among the 'plasma waves' which, according to Tonks and Langmuir (1929), can exist in a gas discharge, only one has a non-zero group velocity, i.e. is capable of propagating in space; for this mode, both space and group velocities are approximately equal to v cm/sec, where

$$v = 3{\cdot}9 \times 10^5 (T_e M_e / M_p)^{1/2}. \qquad \ldots\ldots(2)$$

Here, T_e is the electron temperature in degrees K, and M_e, M_p are the masses of the electrons and positive ions respectively.* From the probe measurements described above, the average value of T_e in the positive column was found to be about 2×10^5 deg. K; if nitrogen ions N_2^+ are assumed to be the predominant positive ions in the plasma, $M_e/M_p=2\times10^{-5}$. Hence from eqn. (1), $v=0{\cdot}8\times10^6$ cm/sec.

---

* v is strictly the velocity of waves with zero frequency only. It is however a good approximation, provided that $\lambda \gg 25(T_e/n)^{1/2}$, where n is the number of electrons per cm^3 and λ the wavelength of the plasma wave. In the example used here, this condition is satisfied if $n > 10^8$, which is likely to have been the case in the positive column.

Now, in a typical experiment the frequency of the oscillation was found to be $2{\cdot}5\times10^5$ c/s when the distance between striations was 3 cm. On a standing-wave hypothesis, the striation spacing must clearly be a half-wavelength, so in this case the wavelength was 6 cm and the velocity $v=1{\cdot}5\times10^6$ cm/sec. In view of the lack of precision in the calculation, and the effect of tube boundaries on the actual wavelength, this order-of-magnitude agreement is fairly satisfactory.

Confirmatory evidence is provided by the experiments in which the striations were modified by an injected radio-frequency voltage. These support the hypothesis that there is an intimate connection between the striations and the low-frequency oscillations; in addition, they provide another measurement of the velocity of propagation. Thus, in the case quoted in § 3 (iii), the striation spacing, and therefore the wavelength in the plasma, decreased in the ratio of 5 : 2 when the frequency was increased from 200 kc/s (for the oscillation already present) to 800 kc/s (for the injected signal). Thus it appears that the velocity of propagation of the 800 kc/s signal was about 1·6 times that of the 200 kc/s oscillation (the simple theory deliberately neglects dispersion and also disregards the influence of boundaries, which may account for the discrepancy).

Finally, the results of the various probe measurements are also consistent with the explanation which has been put forward. The observations of radio-frequency output from probes indicated that this output was highest when the probe was located in the bright part of a striation. This may be taken to mean that these points were the voltage antinodes of the standing wave, which is in agreement with the fact that the latter are points of maximum electron temperature (as shown both by the probe measurements and, more simply, by the higher luminosity of the plasma). It is also to be expected that the electrons would, on the average, tend to crowd together near the nodes, since near the antinodes they would be alternately accelerated towards the next node and repelled towards the preceding one. The high electron concentrations near the nodes would tend to cause minima of space potential at those points. These deductions are confirmed by the data from probe measurements which are plotted in fig. 5 (*b*).

It can therefore be stated that all the experimental evidence is in accordance with the suggestion that the oscillations set up standing waves which are the cause of the striations of the discharge column.

It should be mentioned that various other attempts have been made to explain striations (see, for example, Compton, Turner and McCurdy 1924). Schumann (1943) has shown that ions and electrons moving freely in opposite directions under the influence of an electric field tend to produce a space potential with the type of variation actually observed in striated gas discharges. The 'wavelength' of the predicted fluctuation is of the order of magnitude which is found experimentally. It is doubtful, however, whether this theory is applicable to a discharge in a tube since it neglects the effects of boundaries, electrodes and collisions. Moreover, it does not explain the observed fact that striations do not occur in pure monatomic gases.

Since the coherent oscillations did not always occur simultaneously with the high-frequency noise, and did not appear to depend upon a constriction of the discharge column, it appears that they must have been produced by some mechanism other than the ionic oscillations to which the latter have been ascribed. It has in any case been shown that, with collision frequencies such as occurred in these experiments, such ionic vibrations would produce noise rather than coherent oscillations.

A possible alternative explanation is suggested by Bailey's (1948) prediction of the propagation in ionized media of 'growing waves', i.e. waves the amplitude of which increases during transmission. Haeff (1949) and others have independently investigated a particular example of this phenomenon, and have shown that it is possible for a 'growing wave' to exist in a medium consisting of two streams of charged particles with different velocities. Haeff's work indicates that the existence of such waves is favoured by high charge densities in both streams, and a low value of the difference between the two velocities.

Now, in a gas discharge, the electrons and positive ions have drift velocities determined by the field strength and their respective masses. Thus there will be a number of streams of charged particles each with a well-defined peak in its velocity distribution. Interaction between electron and positive ion streams is unlikely to produce growing waves because of the great difference in mean velocities; however, in discharges in a gas such as air, in which more than one kind of positive ion is produced, there are streams of particles with comparable velocities. The latter conditions would evidently favour the propagation of Haeff's growing wave.

This suggestion is very tentative; it is, however, interesting to find that striations appear in discharges in precisely those gases in which this growing-wave mechanism could take place. Loeb (1939), in a survey of the experimental evidence upon striations, concludes that the inert gases and mercury—all of which have only one kind of positive ion under the conditions of low electron energy which usually exist in the positive column (with the possible exception of Hg_2^+)—do not produce striations when very pure but that other gases may show them. Again, Compton, Turner and McCurdy (1924) found that striations could be induced in a discharge in mercury vapour by the admixture of a very small quantity of hydrogen, although much larger amounts of helium were needed to produce any such effect. This is readily explicable, since the mercury and helium ions would move with drift velocities so different (because of their very unequal masses) that 'growing-wave' interaction between the two streams would be unlikely to take place (except possibly when the plasma frequency was very high for both kinds of ion). Hydrogen, however, forms positive ions of two kinds, H^+ and H_2^+, so that streams of these could act independently of the much slower mercury ions.

§ 5. CONCLUSIONS

The radio-frequency oscillations generated in electrical discharges in air at pressures of the order of 10 microns and with the various types of discharge tube used in these experiments were of two distinct kinds: random noise and coherent oscillations.

Noise was present at frequencies near 200 Mc/s with an intensity of the order of 10^{-12} watt per c/s of receiver bandwidth. This value is high enough to preclude the possibility that it is of thermal origin; all the observed effects were consistent with the hypothesis that it was due to electron oscillations, analogous to those in the Barkhausen–Kurz oscillator, in a region where the potential on the axis of the discharge passed through a maximum value. In particular, noise was only generated in discharges in which, owing to a constriction, such a reversal of potential gradient did in fact occur. The noise-like character of the output can be ascribed to the effect of collisions, in breaking up the oscillations into a series of short pulses. Effects observed at frequencies near 1 Mc/s were consistent with the occurrence of analogous positive-ion oscillations.

A coherent oscillation at a frequency of 200–300 kc/s is also often present in such discharges. There is considerable evidence that the striations, under the particular conditions of these experiments, were a visible effect of standing waves set up in the discharge column by the oscillations. It is suggested that the latter were generated by a 'growing-wave' process. This may explain the fact that striations have been found by various workers to occur only in those gases or gaseous mixtures which would be expected to favour such a mechanism.

ACKNOWLEDGMENTS

The authors desire to acknowledge the assistance of Messrs. H. Flood and L. J. Smith, who constructed most of the apparatus used in the experiments. They are indebted to Dr. J. L. Pawsey of this Laboratory, and to Mr. J. M. Somerville of New England University College, Armidale, New South Wales, for valuable discussions during the preparation of this paper.

REFERENCES

Armstrong, E. B., 1947, *Nature, Lond.*, **160**, 713.
Bailey, V. A., 1948, *Aust. J. Sci. Res.* A, **1**, 351.
Ballantine, S., 1933, *Physics*, **4**, 294.
Böhm, D., and Gross, E. P., 1949, *Phys. Rev.*, **75**, 1851, 1864.
Cobine, J. D., and Gallagher, C. J., 1947, *J. Appl. Phys.*, **18**, 110.
Compton, K. T., Turner, L. A., and McCurdy, W. H., 1924, *Phys. Rev.*, **24**, 597.
Haeff, A. V., 1949, *Proc. Inst. Radio Engrs., N.Y.*, **37**, 4.
Loeb, L. B., 1939, *Fundamental Processes of Electrical Discharges in Gases.* (New York : John Wiley).
Neill, T. R., and Emeléus, K. G., 1951, *Proc. R. Irish Acad.*, **53 A**, 197.
Penning, F. M., 1927, *Nature, Lond.*, **118**, 301.
Schumann, W. O., 1943, *Z. Phys.*, **21**, 112.
Sloane, R. H., and Emeléus, K. G., 1933, *Phys. Rev.*, **44**, 333.
Thomson, J. J., and Thomson, G. P., 1933, *Conduction of Electricity through Gases*, **2.** (Cambridge : University Press).
Tonks, L., and Langmuir, I., 1929, *Phys. Rev.*, **33**, 195.

An Improved Frequency Equation for Contour Modes of Square Plates of Anisotropic Material

By R. BECHMANN
Post Office Research Station, Dollis Hill, London

MS. received 22nd October 1951

ABSTRACT. An improved approximation, based on previous work, has been derived for the frequency equation covering the four contour modes of vibration of square plates of anisotropic material. The modes consist of three longitudinal and one shear mode. An X-cut quartz, a Y-cut EDT and Yψ-cut lithium sulphate plates have been used as examples. The equation has been used to determine the elastic coefficients s_{55} and s_{13} of EDT and lithium sulphate monohydrate.

§ 1. INTRODUCTION

In an earlier paper (Bechmann 1951) the four isolated contour modes of vibration of free square plates were discussed, using the solutions given by Ekstein (1944) for the three longitudinal modes and the solution for the shear mode given by Mähly and Trösch (1947). The same notation for the modes (longitudinal modes 1, 2, 3 and shear mode) is used in this paper. In general, these modes are coupled with each other in materials with low symmetry.

The first attempt to analyse these coupled modes of square and rectangular plates was made by Bechmann (1941, 1942). The theory was based on the assumption of three degrees of freedom: two longitudinal and a shear vibration. The frequency equation obtained is an approximation since the postulated boundary conditions are not fulfilled in all cases. However, measurements on quartz plates showed that the agreement was usually quite satisfactory, although some systematic differences were found. An equation covering the three longitudinal modes was derived by Ekstein (1944) for the condition when there is no coupling with the shear mode. An improved equation for the isolated shear mode of square plates was given by Mähly and Trosch (1947). The solutions were discussed by Bechmann (1951). The frequency calculated for longitudinal mode 2 differed from measurements, but the agreement was improved by a correction derived experimentally. Earlier investigations by Mähly (1945) had shown that mode 3 also needed a correction for the frequency equation. A general survey of the methods of approximating the characteristics of elastic vibrations of anisotropic bodies has been given recently by Mähly (1951).

Based on previous work an improved frequency equation for the four contour modes of square plates of anisotropic material has been obtained and details are given. This frequency equation is still an approximation with empirical corrections but is in a suitable form for practical application.

§ 2. FREQUENCY EQUATION FOR CONTOUR MODES OF SQUARE PLATES OF ANISOTROPIC MATERIAL

(i) *Transformation of the Frequency Equation* (*Bechmann* 1942)

Before discussing the new frequency equation, the earlier equation covering three modes (longitudinal modes 1, 3 and shear mode) given in 1942 is considered. Using a square plate cut perpendicular to the Z axis, with sides parallel to the X and Y axes as described in the previous paper (Bechmann 1951), this approximate frequency equation is

$$\begin{vmatrix} s_{11}-s & s_{12} & s_{16} \\ s_{12} & s_{22}-s & s_{26} \\ s_{16} & s_{26} & s_{66}-2a^2s \end{vmatrix} = 0 \qquad \ldots\ldots(1)$$

which can be written

$$\begin{vmatrix} \tfrac{1}{2}(s_{11}+s_{22}-2s_{12})-s & \tfrac{1}{2}(s_{11}-s_{22}) & \dfrac{1}{2a}(s_{16}-s_{26}) \\ \tfrac{1}{2}(s_{11}-s_{22}) & \tfrac{1}{2}(s_{11}+s_{22}+2s_{12})-s & \dfrac{1}{2a}(s_{16}-s_{26}) \\ \dfrac{1}{2a}(s_{16}-s_{26}) & \dfrac{1}{2a}(s_{16}+s_{26}) & \dfrac{s_{66}}{2a^2}-s \end{vmatrix} = 0. \qquad \ldots\ldots(2)$$

For this particular orientation, the three roots of the equation are expressed in terms of the six elastic coefficients, s_{ik} $(i, k=1, 2, 6)$.

The original empirical coefficient a in the expression for the shear mode has been evaluated by Ekstein (1944) and improved by Mähly and Trösch (1947). Instead of the scheme of elastic coefficients, s_{ik} $(i, k=1, 2, 6)$, the elements of the reciprocal matrix, the elastic moduli γ_{ik} $(i, k=1, 2, 6)$ can be introduced (Ekstein 1944, Bechmann 1951):

$$\begin{vmatrix} s_{11} & s_{12} & s_{16} \\ s_{12} & s_{22} & s_{26} \\ s_{16} & s_{26} & s_{66} \end{vmatrix} \quad \ldots\ldots(3) \qquad \begin{vmatrix} \gamma_{11} & \gamma_{12} & \gamma_{16} \\ \gamma_{12} & \gamma_{22} & \gamma_{26} \\ \gamma_{16} & \gamma_{26} & \gamma_{66} \end{vmatrix}. \quad \ldots\ldots(3\,a)$$

The coefficients γ_{ik} expressed in terms of s_{ik} are

$$\left.\begin{aligned} \Pi\gamma_{11} &= s_{22}s_{66} - s_{26}^2 & \Pi\gamma_{12} &= s_{16}s_{26} - s_{12}s_{66} \\ \Pi\gamma_{22} &= s_{11}s_{66} - s_{16}^2 & \Pi\gamma_{16} &= s_{12}s_{26} - s_{16}s_{22} \\ \Pi\gamma_{66} &= s_{11}s_{22} - s_{12}^2 & \Pi\gamma_{26} &= s_{12}s_{16} - s_{26}s_{11} \end{aligned}\right\} \quad \ldots\ldots(4)$$

$$\Pi = s_{11}s_{22}s_{66} - (s_{11}s_{26}^2 + s_{22}s_{16}^2 + s_{66}s_{12}^2) + 2s_{12}s_{16}s_{26}$$

and similar formulae exist for s_{ik} in terms of γ_{ik}. The following relationship holds between the s_{ik} and γ_{ik}

$$\Sigma s_{ik}\gamma_l = \begin{cases} 1 & k=l \\ 0 & k\neq l \qquad i, k, l=1, 2, 6. \end{cases} \quad \ldots\ldots(5)$$

Multiplying eqn. (1) with the determinant (3 a), the following equation is obtained

$$\begin{vmatrix} \gamma_{11}-\gamma & \gamma_{12} & \gamma_{16} \\ \gamma_{12} & \gamma_{22}-\gamma & \gamma_{26} \\ \gamma_{16} & \gamma_{26} & \gamma_{66} - \dfrac{1}{2a^2}\gamma \end{vmatrix} = 0, \quad \ldots\ldots(6)$$

where $\gamma = 1/s$. This equation can be written as

$$\begin{vmatrix} \frac{1}{2}(\gamma_{11}+\gamma_{22}-2\gamma_{12})-\gamma & \frac{1}{2}(\gamma_{11}-\gamma_{22}) & a(\gamma_{16}-\gamma_{26}) \\ \frac{1}{2}(\gamma_{11}-\gamma_{22}) & \frac{1}{2}(\gamma_{11}+\gamma_{22}+2\gamma_{12})-\gamma & a(\gamma_{16}+\gamma_{26}) \\ a(\gamma_{16}-\gamma_{26}) & a(\gamma_{16}+\gamma_{26}) & 2a^2\gamma_{66}-\gamma \end{vmatrix} = 0, \quad \ldots\ldots(7)$$

which corresponds to eqn. (2). The two matrices

$$\left\| \begin{matrix} \frac{1}{2}(s_{11}+s_{22}-2s_{12}) & \frac{1}{2}(s_{11}-s_{22}) & \frac{1}{2}(s_{16}-s_{26}) \\ \frac{1}{2}(s_{11}-s_{22}) & \frac{1}{2}(s_{11}+s_{22}+2s_{12}) & \frac{1}{2}(s_{16}+s_{26}) \\ \frac{1}{2}(s_{16}-s_{26}) & \frac{1}{2}(s_{16}+s_{26}) & \frac{1}{2}s_{66} \end{matrix} \right\| \quad \ldots\ldots(8)$$

and

$$\left\| \begin{matrix} \frac{1}{2}(\gamma_{11}+\gamma_{22}-2\gamma_{12}) & \frac{1}{2}(\gamma_{11}-\gamma_{22}) & \gamma_{16}-\gamma_{26} \\ \frac{1}{2}(\gamma_{11}-\gamma_{22}) & \frac{1}{2}(\gamma_{11}+\gamma_{22}+2\gamma_{12}) & \gamma_{16}+\gamma_{26} \\ \gamma_{16}-\gamma_{26} & \gamma_{16}+\gamma_{26} & 2\gamma_{66} \end{matrix} \right\| \quad \ldots\ldots(8\,a)$$

are reciprocal.

(ii) *Improved Frequency Equation*

Taking Ekstein's (1944) solution for the three isolated longitudinal modes and Mähly and Trösch's (1947) solution for the shear mode (Bechmann 1951, table 1) and using Ritz's perturbation method, as employed by Ekstein, the frequency equation given below for the four contour modes of a free square plate was derived ($\alpha_2=\alpha_3=1$). The calculations cannot be given here because of their length. The corrections α_2, α_3 were introduced subsequently to obtain better agreement with experimental results and are discussed later in the paper.

$$\begin{vmatrix} \tfrac{1}{2}(\gamma_{11}+\gamma_{22}-2\gamma_{12})-\gamma & 0 & \alpha_3\dfrac{\sqrt{2}}{\pi}(\gamma_{11}-\gamma_{22}) & \alpha_4A(\gamma_{16}-\gamma_{26}) \\ 0 & \tfrac{1}{2}\alpha_2^2(\gamma_{11}+\gamma_{22})-\gamma & \dfrac{\alpha_2\alpha_3}{2}(\gamma_{11}-\gamma_{22})\left(1-\dfrac{8}{\pi^2}\right)^{1/2} & \alpha_2\alpha_4B(\gamma_{16}-\gamma_{26}) \\ \alpha_3\dfrac{\sqrt{2}}{\pi}(\gamma_{11}-\gamma_{22}) & \dfrac{\alpha_2\alpha_3}{2}(\gamma_{11}-\gamma_{22})\left(1-\dfrac{8}{\pi^2}\right)^{1/2} & \dfrac{\alpha_3^2}{2}\left(\gamma_{11}+\gamma_{22}+\dfrac{16}{\pi^2}\gamma_{12}\right)-\gamma & \alpha_3\alpha_4C(\gamma_{16}+\gamma_{26}) \\ \alpha_4A(\gamma_{16}-\gamma_{26}) & \alpha_2\alpha_4B(\gamma_{16}-\gamma_{26}) & \alpha_3\alpha_4C(\gamma_{16}+\gamma_{26}) & 2a^2\gamma_{66}-\gamma \end{vmatrix}=0 \qquad \ldots\ldots(9)$$

where

$$A=\frac{8\sqrt{2}}{\pi^2}\,\frac{kk'}{k^2-k'^2}(\kappa^2+2)^{-1/2}=-0{\cdot}896=-0{\cdot}981a,$$

$$B=\frac{32}{\pi^3}\,\frac{kk'}{k^2-k'^2}(\kappa^2+2)^{-1/2}\left(1-\frac{8}{\pi^2}\right)^{-1/2}\left(1-\frac{\pi^2}{16}\,\frac{k'^2}{k^2}\right)=0{\cdot}0537=0{\cdot}059a_0,$$

$$C=\frac{2}{\pi}\,\frac{k'}{k}\,\frac{k'^2}{k^2-k'^2}(\kappa^2+2)^{-1/2}=-0{\cdot}830=-0{\cdot}909a,$$

$$K=\frac{\pi}{l},\quad k'=\frac{2\kappa}{l},\quad \frac{k'}{k}=\frac{2\kappa}{\pi}=\sqrt{2}a_0,\quad a_0=0{\cdot}91327,\quad \kappa=2{\cdot}0288.$$

In eqn. (9), the four diagonal terms represent in order the three longitudinal modes 1, 2, 3 and the shear mode. This equation has four real solutions γ_i ($i=1, 2, 3, 4$). The corresponding frequencies can be derived from these solutions by the equation

$$\nu_i=\frac{1}{2l}\left(\frac{\gamma_i}{\rho}\right)^{1/2}, \qquad \ldots\ldots(10)$$

where l is the length of the square plate and ρ the density. In the case when all coupling vanishes, the γ_i are identical with the diagonal terms and the modes are easily defined. However when coupling exists, the resulting modes are combinations of the various types of vibration. It should be noted that there is no coupling between modes 1 and 2. In the case where the coefficients γ_{16} and γ_{26} are zero and $\alpha_2=\alpha_3=1$, eqn. (9) is identical, after suitable transformation, with eqn. (54) given by Ekstein (1944) for the three longitudinal modes.

It is interesting to compare the new eqn. (9), after cancelling the second row and column (mode 2) with the earlier approximation (7). The form is very similar and, apart from mode 3, differs only by small numerical changes of less than 10% in the coupling coefficients.

Consider particular conditions as discussed by Bechmann (1951):

$\gamma_{11}=\gamma_{22}$, $\gamma_{16}=\gamma_{26}\neq 0$ (condition 2). All coupling coefficients are zero and the four modes are isolated.

$\gamma_{11}=\gamma_{22}$, $\gamma_{16}=\gamma_{26}=0$ (condition 4). Modes 1 and 2 are isolated, but there is coupling between mode 3 and the shear mode.

$\gamma_{11}=\gamma_{22}$, $\gamma_{16}=-\gamma_{26}$ (condition in § 2 (iii)). Mode 3 is isolated and both modes 1 and 2 are coupled with the shear mode.

Equation (9) provides justification for the conditions for obtaining isolated modes, as already stated (Bechmann 1951).

The discussion of the isolated modes has shown that corrections are necessary for modes 2 and 3 and the shear mode to obtain an agreement between experimental and theoretical results. Similar corrections must be applied to eqn. (9) to obtain agreement for uncoupled modes. These corrections in eqn. (9) are:

For *mode* 2

$$\alpha_2=1/(1+D_2), \quad \ldots\ldots(11), \qquad D_2=0{\cdot}5(\tau^2+\tau^4) \quad \ldots\ldots(11\,a)$$

$$\tau=\frac{1}{(\gamma_{11}\gamma_{22})^{1/2}}[\gamma_{12}{}^2+\tfrac{1}{2}(\gamma_{16}{}^2+\gamma_{26}{}^2)]^{1/2}, \qquad \ldots\ldots(11\,b)$$

where (11 *b*) is a general expression which reduces to the form given previously for the special condition treated.

For *mode* 3. α_3 was derived from results given by Mähly (1945) and is included in the form of a curve plotted against Poisson's ratio (fig. 1).

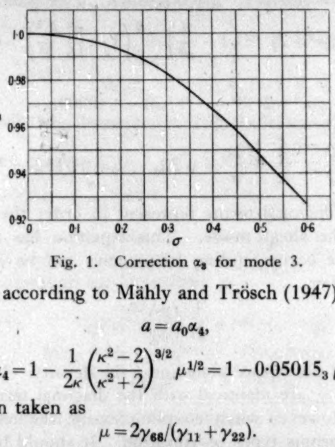

Fig. 1. Correction α_3 for mode 3.

For *shear mode*, according to Mähly and Trösch (1947),

$$a=a_0\alpha_4, \qquad \ldots\ldots(12)$$

where

$$\alpha_4=1-\frac{1}{2\kappa}\left(\frac{\kappa^2-2}{\kappa^2+2}\right)^{3/2}\mu^{1/2}=1-0{\cdot}05015_3\,\mu^{1/2} \qquad \ldots\ldots(12\,a)$$

and μ has now been taken as

$$\mu=2\gamma_{66}/(\gamma_{11}+\gamma_{22}). \qquad \ldots\ldots(12\,b)$$

The form of the frequency equations is unchanged for rotated plates, provided that the elastic coefficients s_{ik} or moduli γ_{ik} are replaced by their primed equivalents s'_{ik} or γ'_{ik}, denoting arbitrary orientation. The transformation of these coefficients is well known.

§ 3. EXPERIMENTAL RESULTS

Measurements of frequencies have been made on square plates of quartz, EDT and lithium sulphate monohydrate. The results on quartz, where the elastic constants are well known, were compared with values calculated from eqn. (9). In the case of EDT, eqn. (9) was used to improve the values for the elastic coefficients s_{55} and s_{13}, previously determined from eqn. (7), according to Bechmann (1950, §4). Equation (9) was also used to determine the coefficients s_{55} and s_{13} for lithium sulphate.

(i) *X-cut Quartz Plate*

The sides of the plate are parallel to the Y and Z axes. In order to use the previous equations it is necessary to make a cyclic transformation from Z to X. The suffixes of the constants are shifted by one place in the groups 1, 2, 3 and 4, 5, 6. The elastic moduli γ_{ik} calculated from the values s_{ik} given in the previous paper (Bechmann 1951) are: $\gamma_{22}=86{\cdot}12$, $\gamma_{33}=105{\cdot}56$, $\gamma_{44}=54{\cdot}32$, $\gamma_{23}=10{\cdot}94$, $\gamma_{24}=-19{\cdot}29$, $\gamma_{34}=-2{\cdot}45$, all values in $10^{10}\,\mathrm{dyn\,cm^{-2}}$. The corrections have the values $\alpha_2=0{\cdot}9862$, $\alpha_3=0{\cdot}9975$, $\alpha_4=0{\cdot}9622$. Poisson's ratio, which affects the correction α_3, is small ($\sigma=0{\cdot}16$). Results are given in table 1. The column a_{ii} refers to the diagonal terms in eqn. (9), γ_{calc} being roots of this equation. For comparison the roots are also calculated using eqn. (7), where a_{kk} are the diagonal terms of the cubic equation. From the observed values for the frequency constant, $N_{\mathrm{obs}}=\nu l$, the corresponding values γ_{obs} are calculated using eqn. (10). The percentage difference between the calculated and observed values of γ are given in the columns headed *D*. The agreement is quite satisfactory using eqn. (9).

Table 1. X-cut Quartz Plate

Modes	N_{obs} (kc/s mm)	γ_{obs}	Equation (9)		D (%)	Equation (7)		D (%)
			a_{ii}	γ_{calc}		a_{kk}	γ_{calc}	
shear mode	2400	61·15	83·88	61·66	0·83	83·88	60·34	−1·3
mode 2	2906	89·65	92·53	91·82	2·4	—	—	—
mode 1	3015	96·50	84·90	97·23	0·76	84·90	97·56	1·1
mode 3	3270	113·52	104·20	114·90	1·1	106·78	117·66	3·6

(ii) *Y-cut EDT Plate*

The sides of the plate are parallel to the Z and X axes. For this case the coefficients of the previous equations must be transformed from Z to Y. The suffixes in the corresponding expressions are shifted by two places. Equation (9) is used for a new determination of the elastic coefficients s_{55} and s_{13} where $s_{55}+2s_{13}=56{\cdot}5\times10^{-13}\,\mathrm{cm^2\,dyn^{-1}}$ (Bechmann 1950). The improved values are: $s_{55}=122$, $s_{13}=-32{\cdot}75\times10^{-13}\,\mathrm{cm^2\,dyn^{-1}}$ (the old values were 116·5 and −30). The moduli γ_{ik} are calculated from the values s_{ik} given by Bechmann (1950), and the two new values for s_{55} and s_{13}. The values for γ_{ik} are: $\gamma_{11}=59{\cdot}07$, $\gamma_{33}=19{\cdot}41$, $\gamma_{55}=11{\cdot}64$, $\gamma_{13}=22{\cdot}82$, $\gamma_{15}=13{\cdot}19$, $\gamma_{35}=7{\cdot}39$ (values in $10^{10}\,\mathrm{dyn\,cm^{-2}}$). The corrections are $\alpha_2=0{\cdot}6992$, $\alpha_3=0{\cdot}938$, $\alpha_4=0{\cdot}9727$. The results are given in table 2. The differences between observed and calculated

Table 2. Y-cut EDT Plate

Modes	N_{obs} (kc/s mm)	γ_{obs}	Equation (10)		D (%)	Equation (7)		D (%)
			a_{ii}	γ_{calc}		a_{kk}	γ_{calc}	
mode 1	1179	8·55	16·42	8·53	−0·23	16·42	8·44	−1·29
shear mode	1435	12·67	18·36	12·65	−0·16	18·36	12·68	+0·08
mode 2	1708	17·95	19·18	19·52	8·75	—	—	—
mode 3	3228	64·10	50·80	64·05	−0·08	62·06	75·72	18·1

values for modes 1 and 3 and the shear mode calculated from eqn. (9) are very small. There is a large difference for mode 2, where Poisson's ratio for this cut is unusually high ($\sigma=0\cdot49$) and may introduce uncertainty in the empirical correction for this mode. This correction reduces the value for the diagonal term a_{22} from 39·24 to 19·18. Using eqn. (7), the agreement for mode 1 and the shear mode is again quite close but mode 3 has a larger difference.

(iii) *Yψ-cut Lithium Sulphate Plates*

These plates are perpendicular to the Y axis and rotated through an angle ψ about it. The definition of the coordinate axes and the values for the elastic coefficients are taken from Bechmann (1952). The coefficients s_{55} and s_{13} were determined from frequency constants measured on Y_{0° square plates. These values are $s_{55}=64\cdot0, s_{13}=-7\cdot5\times10^{-13}\ \text{cm}^2\ \text{dyn}^{-1}$ where $s_{55}+2s_{13}=49\cdot0$, taken from longitudinally vibrating bars Yψ. The frequency constants for square plates Yψ ($\psi=22^\circ\ 30'$, 45°, $67^\circ\ 30'$) of lithium sulphate have also been measured and calculated from eqn. (9) using the well-known transformation equations for rotated coefficients. Curves of the calculated frequency constants for the four modes are shown in fig. 2, where they are compared with experimental values of a number of plates. The agreement between the two sets of values is quite satisfactory.

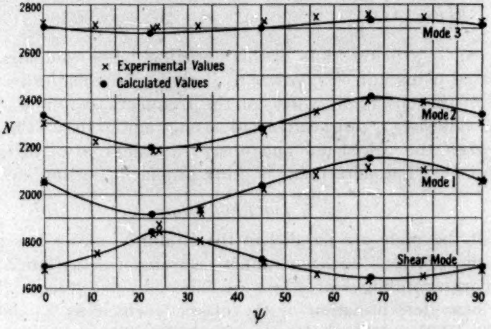

Fig. 2. Measured and calculated frequency constants for the four modes of lithium sulphate Yψ square plates.

ACKNOWLEDGMENTS

The author wishes to thank Mrs. S. Ayers (née Rodwell) for assistance in calculations and measurements.

Acknowledgment is made to the Engineer-in-Chief of the General Post Office for permission to make use of the information contained in this paper.

REFERENCES

Bechmann, R., 1941, *Z. Phys.*, **117,** 180 ; 1942, *Ibid.*, **118,** 515 ; 1950, *Proc. Phys. Soc.* B, **63,** 577 ; 1951, *Ibid.*, **64,** 323 ; 1952, *Ibid.*, **65,** 375.

Ekstein, H., 1944, *Phys. Rev.*, **66,** 108.

Mähly, H., 1945, *Helv. phys. Acta.* **18,** 248 ; 1951, *Ergebn. exakt. Naturw.*, **24,** 402.

Mähly, H., and Trösch, A., 1947, *Helv. phys. Acta*, **20,** 253.

Elastic and Piezoelectric Coefficients of Lithium Sulphate Monohydrate

By R. BECHMANN

Post Office Research Station, Dollis Hill, London

MS. received 22nd October 1951

ABSTRACT. A new determination has been made of the elastic and piezoelectric coefficients of lithium sulphate monohydrate and of their temperature coefficients.

---

§ 1. INTRODUCTION

LITHIUM sulphate monohydrate, $Li_2SO_4 . H_2O$, in the monoclinic sphenoidal class (C_2) is of practical interest because of its high longitudinal piezoelectric coefficient parallel to the two-fold symmetry axis. Its piezoelectric coefficients were measured by Spitzer (1938) and by Mason (1950), who also determined the elastic coefficients. A new determination of these coefficients has been made and compared with Mason's results.

§ 2. CRYSTALLOGRAPHIC DATA

A description of the crystallographic habit of lithium sulphate can be found in Groth (1908). A typical habit of a left-handed crystal is shown in fig. 1.

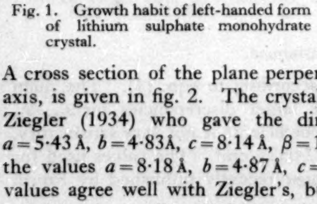

Fig. 1. Growth habit of left-handed form of lithium sulphate monohydrate crystal.

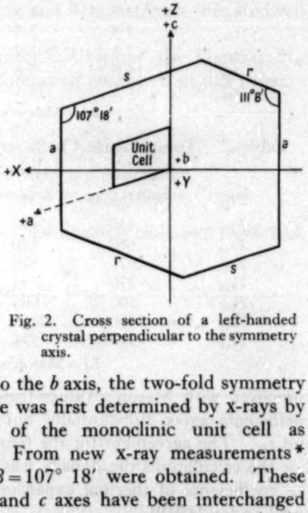

Fig. 2. Cross section of a left-handed crystal perpendicular to the symmetry axis.

A cross section of the plane perpendicular to the *b* axis, the two-fold symmetry axis, is given in fig. 2. The crystal structure was first determined by X-rays by Ziegler (1934) who gave the dimensions of the monoclinic unit cell as $a = 5{\cdot}43$ Å, $b = 4{\cdot}83$ Å, $c = 8{\cdot}14$ Å, $\beta = 107°\ 35'$. From new X-ray measurements* the values $a = 8{\cdot}18$ Å, $b = 4{\cdot}87$ Å, $c = 5{\cdot}45$ Å, $\beta = 107°\ 18'$ were obtained. These values agree well with Ziegler's, but the *a* and *c* axes have been interchanged making *c* the smaller axis in accordance with standards stated by the I.R.E. (1949).

* The measurements were made by Mr. G. T. Hollins.

The Y axis coincides with the symmetry axis, *b*, Z with *c*, and X is perpendicular to the Y and Z axes forming a right-handed coordinate system; X is 17° 18′ from the *a* axis in the *ac* plane.

Mason's (1950) coordinate system is in accordance with fig. 4 of the I.R.E. standards (1949), in which it appears that the *a* axis is shorter than the *c*. He based his system on Ziegler's unit cell, keeping the *a* and *c* axes as defined. The relation between the coordinates x', y', z' used by Mason and the coordinate system x, y, z used here is given by the scheme

$$\begin{array}{cccc} & x & y & z \\ x' & -\cos\theta_0 & 0 & \sin\theta_0 \\ y' & 0 & -1 & 0 \\ z' & \sin\theta_0 & 0 & \cos\theta_0 \end{array} \qquad \ldots\ldots(1)$$

where $\theta_0 = 107°\ 18'$.

§ 3. ELASTIC COEFFICIENTS

The determination of the elastic and piezoelectric coefficients was made in accordance with the earlier publication (Bechmann 1950) but the values for the elastic coefficients s_{55} and s_{13} were obtained using an improved frequency formula for square plates perpendicular to the symmetry axis (Bechmann 1952). The results of the new determination of the elastic coefficients* s_{ik} and their temperature coefficients Ts_{ik} are shown in tables 1 and 2. The new values are compared with Mason's values transformed according to eqn. (1). The main coefficients agree substantially but there are larger discrepancies for s_{55}, s_{13} and s_{25}. The agreement for the temperature coefficients is not very satisfactory. For the calculations the density was taken as 2·052 g/cm³. The values used for the coefficients of thermal expansion were those recently published by Smith and Landon (1949).

Table 1. Elastic Coefficients for Lithium Sulphate in 10^{-13} cm² dyn^{-1}

s_{ik}	New values	M	s_{ik}	New values	M
s_{11}	22·9	22·5	s_{55}	64·0	52·3
s_{22}	22·5	21·3	s_{66}	36·1	37·9
s_{33}	22·8	18·8	s_{15}	−2·1	−1·6
s_{12}	−5·4	−7·5	s_{25}	−8·3	−13·2
s_{13}	−7·5	−2·2	s_{35}	6·3	8·3
s_{23}	−4·6	−5·6	s_{46}	1·4	7·2
s_{44}	71·3	73·1			

M = Mason's values transformed.

Table 2. Temperature Coefficients of the Elastic Coefficients for Lithium Sulphate in 10^{-6} per °c

Ts_{ik}	New values	M	Ts_{ik}	New values	M
Ts_{11}	130	−76	Ts_{55}	400	370
Ts_{22}	680	520	Ts_{66}	500	344
Ts_{33}	920	870	Ts_{15}	−2900	−1010
Ts_{12}	−270	−93	Ts_{25}	670	204
Ts_{13}	500	685	Ts_{35}	2200	425
Ts_{23}	3900	2855	Ts_{46}	1800	1245
Ts_{44}	340	374			

M = Mason's values transformed.

---

[*] All new values for the coefficents have been determined at 20°c; Mason's values are given for 25° c.

§ 4. PIEZOELECTRIC COEFFICIENTS

The results of the new determination of the piezoelectric coefficients d_{ik} and their temperature coefficients Td_{ik} for a left-handed crystal are given in tables 3 and 4. For comparison Mason's transformed values for d_{ik} are given. Some of the values agree quite well but in other cases the values are completely different. Spitzer's (1938) value for d_{22}, the only value not affected by transformation, is $d_{22}=48\times10^{-8}$ e.s.u. dyn^{-1} which is close to the other results.

Table 3. Piezoelectric Coefficients for Lithium Sulphate in 10^{-8} e.s.u. dyn^{-1}

d_{ik}	New values	M	d_{ik}	New values	M
d_{14}	−11·6	−11·8	d_{23}	−5·15	−5·4
d_{16}	−9·3	18·4	d_{25}	−21·4	−23·3
d_{21}	−0·54	−0·70	d_{34}	−3·1	20·5
d_{22}	49	45	d_{36}	3·3	−15·8

Table 4. Temperature Coefficients of Piezoelectric Coefficients of Lithium Sulphate in 10^{-4} per °c

Td_{ik}	New values	Td_{ik}	New values
Td_{14}	61	Td_{23}	210
Td_{21}	−37	Td_{25}	−19
Td_{22}	<1·5	Td_{36}	−47

ACKNOWLEDGMENTS

The author wishes to thank Mr. P. L. Parsons for carrying out measurements of capacitance on a large number of specimens, and Mrs. S. Ayers (née Rodwell) for general measurements and calculations.

Acknowledgment is made to the Engineer-in-Chief of the General Post Office for permission to make use of the information contained in this paper.

REFERENCES

Bechmann, R., 1950, *Proc. Phys. Soc.* B, **63,** 577 ; 1952, *Ibid.*, **65,** 368.
Groth, P., 1908, *Chemische Kristallographie*, **2,** 362 (Leipzig : Engelmann).
Institute of Radio Engineers, 1949, *I.R.E. Standards on 'Piezoelectric Crystals'*, *Proc. Inst. Radio Engrs., N.Y.*, **37,** 1378.
Mason, W. P., 1950, *Piezoelectric Crystals and their Application to Ultrasonics* (New York : van Nostrand).
Spitzer, F., 1938, *Thesis*, Göttingen.
Smith, C. S., and Landon, H. H., 1949, *Phys. Rev.*, **75,** 1625.
Ziegler, G. E., 1934, *Z. Kristallogr.*, **89,** 456.

.B
55
52

The Absorption Spectra of Single Crystals of Lead Sulphide, Selenide and Telluride

By A. F. GIBSON

Ministry of Supply, Telecommunications Research Establishment, Great Malvern, Worcs.

Communicated by R. A. Smith; MS. received 13*th December* 1951, *and read before the Physical Society at Southampton on* 18*th December* 1951

ABSTRACT. The absorption spectra of single crystals of PbS, PbSe and PbTe have been examined in the temperature range from 20° K to 600° K. The spectra are characterized by a sharp absorption edge which coincides with the long wavelength limit of photoconductivity in each material. At longer wavelengths the absorption coefficient increases slowly with increasing wavelength, as in germanium and silicon.

§ 1. INTRODUCTION

A GREAT deal of experimental work has been carried out in recent years on the group of related substances PbS, PbSe and PbTe. This has arisen mainly because of the oustanding feature they have in common, namely marked photoconductivity in the infra-red. For many photoconductors and, in particular, elementary photoconductors there is a definite correlation between the long wavelength limit of photoconductivity and a marked decrease in absorption coefficient. In order to establish the relationship between absorption and photoconductivity in the PbS series, a study was made of the absorption spectra of thin evaporated layers such as are used in photoconductive detectors (Gibson 1950). The absorption coefficient is very large (greater than $10^5\,\text{cm}^{-1}$) in the visible and ultra-violet regions of the spectrum, but decreases rapidly in the near infra-red. This absorption 'edge' occurs at a position which corresponds to the energy gap between the highest filled energy band and the lowest empty energy band as determined from Hall constant data (Putley and Arthur 1951, Chasmar and Putley 1951). At longer wavelengths the absorption of thin films is still large, however (of the order of $10^4\,\text{cm}^{-1}$), and extends to much longer wavelengths than the photo-conductive sensitivity. In addition, there is no correlation between the temperature dependence of the long wavelength absorption and the well known shift in the photoconductive limit (Moss 1949). To explain this result it was assumed that the absorption giving rise to photoconductivity is masked in thin micro-crystalline films by additional absorption due to either (*a*) a very high density of impurities and free carriers within the micro-crystals, or (*b*) absorption characteristic of the structure of thin films, e.g. scattering by the micro-crystals. The first indication that the absorption at long wavelengths of single crystals might be much less than for evaporated layers was given by the measurements of Paul, Jones and Jones (1951) who studied the absorption spectrum of an abnormally transparent sample of natural galena of high purity. Until recently the only single crystals available to the writer were of natural galena containing about 2% impurity, such crystals being opaque even in very thin (~0·05 mm) sections. Now, however, large single crystals of PbS, PbSe and PbTe have been grown in this laboratory by W. D. Lawson (1951), and a study of their absorption spectra undertaken. It is found that the absorption coefficient at long wavelengths of these crystals is of the order of 100 times less than that of evaporated layers. The spectra are characterized by a sharp absorption edge which coincides with the long wavelength limits of photoconductivity at all temperatures. At wavelengths shorter than this edge the absorption coefficient rises to values comparable with those found in micro-crystalline layers. These experiments will now be described.

§ 2. EXPERIMENTAL METHODS

Polished or cleaved crystals were clamped between two copper rings, one of which was soldered to a copper-to-glass seal. The latter, upon which was wound an electric heater, formed the lower portion of the inner tube of a Dewar vessel. The outer portion of the Dewar vessel was fitted with two KRS-5 (thallium bromo-iodide) windows, a ground glass joint to facilitate opening to mount the crystal, and an evacuation tube.

Due to the large amount of copper in the system and the poor thermal contact between the crystal and holder, the crystal took some minutes to reach a steady temperature on cooling with, say, liquid oxygen. As, however, the transmission of a crystal at some wavelengths can change by as much as e^{100} or more on cooling from 290° to 90° K, it is not difficult to determine when a steady state has been reached. As far as could be determined, the incident radiation on the sample crystal did not appreciably increase the temperature.

Unless otherwise stated, a double monochromator fitted with a pair of NaCl prisms was used throughout. The crystal absorption coefficient at selected wavelengths was determined by transmission measurements at various crystal thicknesses. Because of the relatively small amount of energy transmitted by the crystals the monochromator slits had to be kept fairly wide open, resulting in poor resolution, particularly below $4\,\mu$. The resolution generally adopted was $0{\cdot}35\,\mu$ at $4{\cdot}0\,\mu$, $0{\cdot}19\,\mu$ at $8\,\mu$ and $0{\cdot}1\,\mu$ at $12\,\mu$.

The input beam to the monochromator was interrupted at 5 c/s and the transmitted energy detected by a Schwarz thermopile. The resultant signal was amplified at the interruption frequency in a bandwidth of about 0·5 c/s, using an amplifier designed by D. A. H. Brown (1949).

§ 3. PRESENTATION OF RESULTS

If the incident light intensity is J_0 and the transmitted intensity J, then the absorption coefficient k is given by

$$\frac{J}{J_0} = (1-R)^2\, e^{-kx} \quad \text{or} \quad \log\left\{\frac{J_0(1-R)^2}{J}\right\} = \frac{kx}{2{\cdot}3}, \qquad \ldots\ldots(1)$$

where R is the reflection coefficient and x is the thickness of the crystal. The above formula assumes that multiple reflections can be ignored. With the possible exception of the very thinnest samples used this seems to be justified (Becker and Fan 1951).

To determine the value of the reflection coefficient R, the quantity $\log(J_0/J)$ is plotted against the thickness x for various wavelengths. The intercept $\log(1-R)^2$ is then obtained. This is not an accurate method, but fortunately quite large errors in the determination of R have little effect on the determination of the value of the product kx if this is large, as is generally the case.

Determination of the value of the absorption coefficient k from the observable quantities J_0, J, $(1-R)^2$ and x necessitates two assumptions, namely (*a*) the validity of eqn. (1), (*b*) that the measurements are in no way limited by the finite resolution of the monochromator. The latter condition has not been achieved at short wavelengths, where kx varies very rapidly with wavelength. For this reason the observable quantity $\log\{J_0(1-R)^2/J\}$, which is proportional to k, has been plotted against the wavelength in figs. 1, 2 and 3. The value of R determined for each material is indicated in the appropriate diagrams. In subsequent figures, however, the value of k has been plotted to facilitate rapid appreciation of the results. It should be noted, therefore, that the value of k indicated in such diagrams may be in serious error when k is varying rapidly with wavelength.

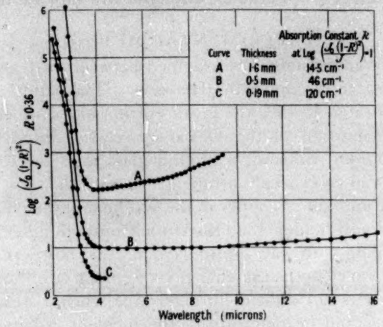

Fig. 1. PbS, n-type.

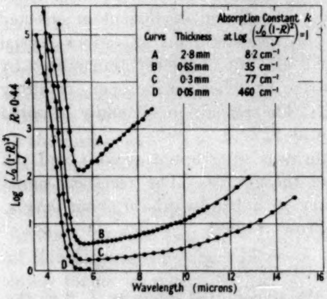

Fig. 2. PbSe, n-type.

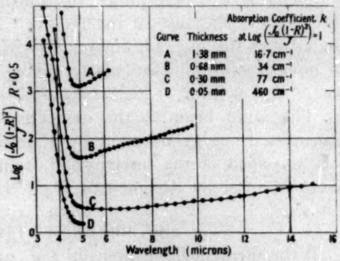

Fig. 3. PbTe, n-type.

§ 4. EXPERIMENTAL RESULTS, ROOM TEMPERATURE

The absorption spectra of n-type PbS, PbSe and PbTe are shown in figs. 1, 2 and 3 respectively. Each figure covers various thicknesses of the same specimen. The ordinate scale is proportional to the absorption constant k, and the appropriate scale factor for each curve is indicated on the diagram.

The curves shown in figs. 1, 2 and 3 are quite typical, and the same form is obtained for all specimens measured. The spectra are characterized by a sharp absorption edge occurring at about 3 μ for PbS, 5 μ for PbSe and 4 μ for PbTe. The edge is unchanged in position and apparent magnitude by variations in impurity concentration and is the same for p- or n-type samples of all three materials. The edge also remains unchanged when a sample of PbTe is converted from p- to n-type by neutron bombardment. The slope of the absorption edge is, however, independent of the thickness of the crystal sample, indicating that it is determined by the resolution of the monochromator, even for very thin specimens. Hence the absolute magnitude of the absorption coefficient within the edge remains in some doubt.

The position of the absorption edge in PbS and PbTe is in fair agreement with the known long wavelength limits of photoconductivity in these materials at room temperature. For PbSe, however, the edge occurs at a longer wavelength than previous photoconductivity measurements would suggest. This observation led to a re-examination of the photoconductivity of PbSe. Initially a PbSe photodiode was made, following the technique used for PbTe (Gibson 1952). The photoconductive spectrum of this cell is shown in fig. 4. Clearly the long wavelength limit of photoconductivity in this cell is in good agreement with the absorption spectrum. Subsequently photosensitive layers of PbSe having similar spectral characteristics were prepared by Dr. T. S. Moss of this laboratory. A note on these cells has already been published (Gibson, Lawson and Moss 1951).

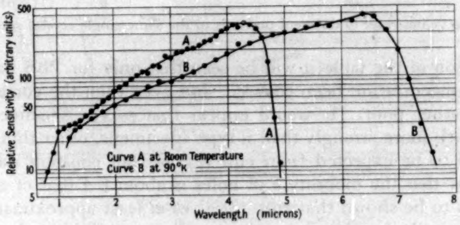

Fig. 4. Response of PbSe photodiode.

Following the absorption edge at short wavelengths, the absorption coefficient increases steadily with increasing wavelength to the limit of observation. The rate of change of k with wavelength λ is slow and no longer limited by the resolution of the instrument. A similar rise in absorption coefficient has been observed in Si and Ge by Becker and Fan (1949, 1950, 1951). These authors ascribe this absorption, in whole or in part, to the free electrons or holes in the material. Following a purely classical treatment, it can be shown that the absorption coefficient should be given by

$$k=\lambda^2\left[\frac{e^3N(\mu_0/k_0)^{1/2}}{nc^2m^2b}\right] \text{ in rationalized m.k.s. units, } \qquad \ldots\ldots(2)$$

where μ_0 and k_0 are the permeability and permittivity of free space, c the velocity of light, n the refractive index of the material and N, e, m and b the density, charge, effective mass and mobility of the carriers. According to the above equation the absorption constant should be proportional to λ^2, a result in good agreement with experiment, at least for Si. There is some correlation between k and N in these materials. The absolute magnitude of k is, however, in error by three orders of magnitude in Ge and one order of magnitude in Si.

In the absence of any better theory it seems reasonable to ascribe the long wavelength absorption in PbS, PbSe and PbTe crystals to the same cause. Inspection of the curves given in figs. 1, 2 and 3 shows that the λ^2 relation is approximately obeyed in all samples. In order to correlate variations in k with N a very wide range of values of N is required, and unfortunately these are not available. As in Si and Ge, the value of k can vary by as much as a factor of 10 without any appreciable change in N or b. This is illustrated in the following table. The carrier concentrations quoted are obtained from Hall constant data kindly supplied by Dr. E. H. Putley of this laboratory.

Substance	Type	Carrier density (cm^{-3})	k (cm^{-1}) at 8μ	Substance	Type	Carrier density (cm^{-3})	k (cm^{-1}) at 8μ
PbS	n	$\sim 10^{20}$	900	PbSe	n	2×10^{18}	71
	n	$\sim 5\times10^{19}$	300		n	$1{\cdot}5\times10^{18}$	215; 125*
	n	6×10^{18}	170		n	7×10^{17}	24; 45*
	n	$3{\cdot}5\times10^{17}$	37		p	4×10^{18}	350
	n	3×10^{17}	30				
	p	1×10^{18}	350	PbTe	n	6×10^{18}	88
	p	1×10^{18}	150		n	1×10^{18}	46
					p	2×10^{18}	220
					p	1×10^{18}	400
					p	1×10^{18}	108

* Two values refer to different portions of the same single crystal specimen.

From inspection of the table it will be seen that only for PbS has a sufficiently wide carrier concentration been covered, and even then the correlation between N and k is rather poor. It would appear that p-type specimens of all three materials absorb more strongly than n-type specimens, other things being equal. This result is to be expected from eqn. (2), as Hall constant data on all three materials show that the mobility b of holes is about 0·4 that of electrons.

It remains to be shown that eqn. (2) gives at least approximately the correct order of magnitude for the absorption coefficient. Taking the values for the quantities in eqn. (2): $N=10^{24}/\mathrm{m}^3$, $b=0{\cdot}1$ m/sec/v/m (n-type material), $m=$ free mass of electron, $\lambda=8\,\mu=8\times10^{-6}$ m, the absorption coefficient should be about 36 cm^{-1} for n-type crystals. With one exception all the observed values are appreciably greater than this. Thus the discrepancy between theory and experiment in these materials is in the same direction as in Ge and Si, though somewhat smaller, and suggests that there is some additional absorption unaccounted for.

§ 5. THE VARIATION IN THE ABSORPTION SPECTRA WITH TEMPERATURE

The absorption spectra of n-type PbS and PbSe and p-type PbTe at various temperatures are given in figs. 5, 6 and 7 respectively. For clarity results below room temperature are shown by broken curves. The general characteristics of all samples are the same as those shown. The features clear by inspection of the curves are as follows:

(*a*) The absorption edge at short wavelengths moves to longer wavelengths as the temperature is reduced. This is analogous to the shift in the long wavelength limit of photoconductivity with temperature (Moss 1949) and is the same as the latter in magnitude and direction. This observation confirms the view that the absorption edge is to be associated with the photoconductive limit.

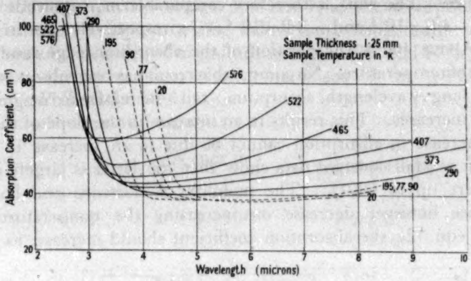

Fig. 5. PbS, n-type.

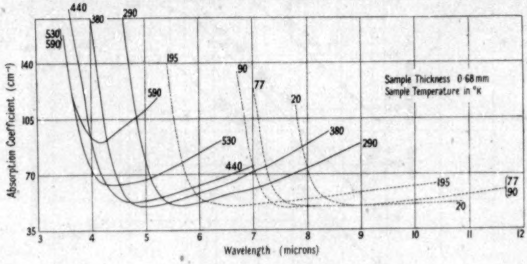

Fig. 6. PbSe, p-type.

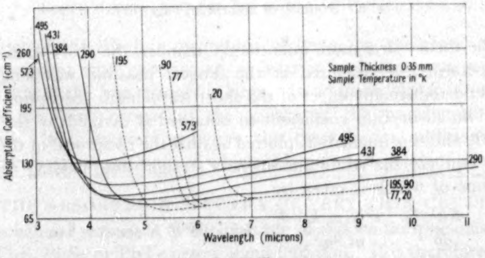

Fig. 7. PbTe, n-type.

As the absorption at short wavelengths is almost certainly due to some electronic transition requiring a minimum quantum of energy *E*, it seems appropriate to plot the position of the edge in electron volts against the absolute temperature. For this purpose the position of the edge has been arbitrarily defined as the wavelength at which $\log\{J_0(1-R^2)/J\}=4$. The resulting curves of minimum energy against temperature are given in fig. 8 for all three materials. It will be seen that the shift is linear with temperature below about 400° K down to 20° K. The actual value of dE/dT is slightly dependent upon the definition of the position of the absorption edge, but is approximately $+4{\cdot}0\times10^{-4}$ ev/° K for all samples. The shift is therefore comparable in magnitude with that in Ge and Si ($-4{\cdot}0\times10^{-4}$ and $-3{\cdot}0\times10^{-4}$ ev/° K respectively) but in the opposite direction. Above 400° K the position of the absorption edge tends to become independent of temperature. No comparable result has been observed in Ge or Si.

(*b*) The long wavelength absorption 'tail' increases in magnitude as the temperature increases. This results in an increase in the slope of the absorption tail. The increase in absorption cannot be due to an increase in free carrier concentration as Hall constant data show that the latter is largely independent of temperature up to 600° K. The mobility of electrons and holes in these materials does however decrease on increasing the temperature, and thus, according to eqn. (2), the absorption coefficient should increase, as observed.

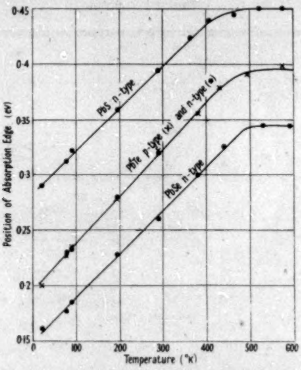

Fig. 8. Position of absorption edge (ev).

To test the theory in a more quantitative manner, the absorption coefficient at each temperature is measured at the longest possible wavelength. This condition should reduce any effect of the short wavelength absorption band to a minimum. The absorption coefficient so obtained is divided by the square of the wavelength, and this quantity is plotted against the reciprocal of the mobility. According to eqn. (2), the result should be a straight line, passing through the origin, the slope of which is given by

$$\frac{d(k\lambda^{-2})}{db^{-1}}=\frac{e^3N(u_0/k_0)^{1/2}}{nC^2m^2}\simeq 5{\cdot}5\times10^{-12}\,N\ \mathrm{sec}^{-1}\ \mathrm{v}^{-1}\ \mathrm{m}^{-1}.$$

Using the results shown in figs. 5, 6 and 7, the relevant curves are plotted in fig. 9. The mobility at each temperature and the carrier concentration are obtained from Hall constant data.* Unfortunately the mobility of holes in

---

* Kindly supplied by Dr. E. H. Putley.

PbTe is not known above about 350° K. Below this temperature, however, the mobility of holes and electrons are in a constant ratio, and it has been assumed that this ratio remains unchanged up to 600° K, thus allowing the hole mobility to be computed.

The curves given in fig. 9 are only approximately linear. In particular, the percentage deviation at low temperatures (near the origin of fig. 9) is very large. This is evident from inspection of figs. 5, 6 and 7, as the absorption coefficient does not decrease markedly on cooling below room temperature, whereas the mobility increases by an order of magnitude between 290° and 77° K.

The slopes of the curves given in fig. 9 are, in $\mathrm{sec}^{-1}\,\mathrm{v}^{-1}\,\mathrm{m}^{-1}$: PbS $2{\cdot}3\times10^{12}$, PbSe $8{\cdot}7\times10^{12}$, PbTe $3{\cdot}3\times10^{12}$.

The theoretical values of the slope are:

	N (per m^3)	Slope ($\mathrm{sec}^{-1}\,\mathrm{v}^{-1}\,\mathrm{m}^{-1}$)
PbS	$3{\cdot}5\times10^{23}$	$2{\cdot}0\times10^{12}$
PbSe	$1{\cdot}5\times10^{24}$	$8{\cdot}2\times10^{12}$
PbTe	1×10^{24}	$5{\cdot}5\times10^{12}$

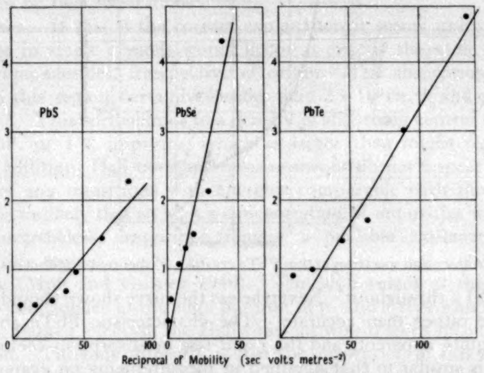

Fig. 9. Results obtained from figs. 5, 6 and 7: (*a*) PbS, (*b*) PbSe, (*c*) PbTe.

In respect of the absolute magnitude of the slope, therefore, the theory is in good agreement with experiment, at least at high temperatures, where the absorption due to the free carriers is large. In addition, the absorption constant is more nearly proportional to the square of the wavelength at elevated temperatures. This suggests, as before, that there is some additional absorption in these crystals, the magnitude of which is largely independent of temperature.

§6. THE ABSORPTION SPECTRA OF VERY THIN CRYSTALS

For mechanical reasons it is not possible to reduce the thickness of a single crystal of PbS, PbSe or PbTe below about 0·05 mm. It is therefore not possible to measure an absorption coefficient greater than about $2\times10^3\,\mathrm{cm}^{-1}$. To obtain thinner specimens evaporated films may be used, but for the reasons already stated it is unlikely that a measured absorption coefficient less than about $2\times10^4\,\mathrm{cm}^{-1}$ is characteristic of the crystal and not of the structure of the film.

Evaporated layers up to 0·05 mm thick have been prepared, the absorption spectra of which bear no resemblance at long wavelengths to the curves given in this paper.

It is clearly of considerable importance to obtain measurements of the absorption coefficient at wavelengths below the crystal edge, even if such measurements are of poor accuracy. Some very thin crystals of PbTe have been obtained by W. D. Lawson of this laboratory by evaporation on to a heated substrate of PbO on quartz. They are rectangular in shape and have an area of about 2 mm^2 or less. The impurity concentration and thickness are largely unknown.

The average absorption spectrum of two such samples is given in fig. 10. For these measurements a pair of LiF prisms were used, the resolution being better than 0·1 μ throughout. Nevertheless the curve shown should be considered as indicative rather than accurate. The characteristic PbTe absorption edge near 4 μ is quite apparent, and the rapid rise in absorption coefficient between 1 μ and 2 μ is similar to that obtained in measurements on evaporated films of PbTe. The thickness of these crystals can only be estimated by comparison with films when k is large and with the thinnest crystals available for small values of k, the latter being measured at the highest possible resolution. The estimated thickness of the crystals is about 1 μ and the derived values of k are indicated on the diagram. The variation of photosensitivity with wavelength of a PbTe cell 1 μ thick at room temperature can be predicted from this curve by assuming the quantum efficiency to be independent of wavelength. Such a curve is also shown in fig. 10.

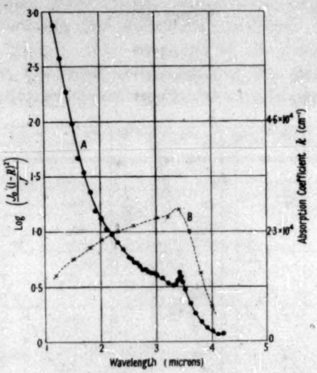

Fig. 10. (*a*) Absorption spectrum of thin PbTe crystal; (*b*) theoretical photosensitivity spectrum.

§ 7. DISCUSSION OF RESULTS

For convenience of discussion the following three wavelength regions can be distinguished: A, short wavelengths, less than about 1·5 μ; B, medium wavelengths, 1·5 μ to the edge at 3 μ, 4 μ and 5 μ in PbS, PbTe and PbSe respectively; C, long wavelengths.

The origin of the absorption in region C has already been discussed in some detail and has been ascribed, at least in part, to the free electrons or holes in the materials. This region will not be discussed further.

The absorption in regions A and B is almost certainly due to electronic transitions between allowed energy bands of the crystal. It is important to decide whether the same transition gives rise to absorption throughout both regions or whether there are two absorption bands overlapping one another. An experiment carried out by Chasmar and Gibson (1951) on optically sensitizable PbS cells tends to support the latter possibility. It was found that the sensitization spectrum of this type of cell coincides with the lattice absorption edge observed in PbS films. The sensitization efficiency falls to zero at about $1{\cdot}2\,\mu$, whereas photoconductivity extends to $3\,\mu$ as in normal cells. Hence the absorption giving rise to sensitization below $1{\cdot}2\,\mu$ cannot be due to the same transition as that giving rise to photoconductivity out to $3\,\mu$.

If this argument can be accepted it is natural to ascribe the absorption in region A to an electronic transition between the highest filled band and the conduction band, as assumed in the previous paper (Gibson 1950). This assumption is consistent with Hall constant measurements on PbS and PbTe and with the very high absorption coefficient in this region.

It remains, therefore, to explain the origin of the absorption band in region B. There appear to be two possibilities:

(*a*) ***Impurities.*** If this is the correct explanation it seems unlikely that the absorption edge in single crystals would occur at exactly the same wavelength for p- and n-type samples, irrespective of origin. The absorption coefficient is very high in this region, certainly greater than $2 \times 10^3\,\mathrm{cm}^{-1}$, and probably as high as $10^4\,\mathrm{cm}^{-1}$. This corresponds to a density of absorbing centres of the order of 10^{20} per cm^3, or 1% impurity, which is larger than might reasonably be expected. In addition, Hall constant measurements do not appear to indicate the existence of any transitions with energies comparable with those given in fig. 8. It seems unlikely that so high a concentration of impurities would escape detection. Nevertheless, impurities remain a possible explanation of the absorption in this region.

(*b*) *Excitons* (Mott and Gurney 1940). The high values of the absorption coefficient, the coincidence of the edge position in p- and n-type samples, and the absence of any marked effect on the Hall constant would seem reconcilable with this explanation. The only difficulty is that the absorption in this region gives rise to photoconductivity, at least in micro-crystalline layers of these materials. It is, however, possible to suppose that excitons may drift to the crystal surface and there dissociate (Apker and Taft 1951). The free electron and hole so produced will give rise to photoconductivity by a reduction in surface potential, as already envisaged (Gibson 1951, 1952). On this explanation there could be no long wavelength photoconductivity in single crystals of these materials. It is, of course, impossible to prove a negative result, but it may be stated that no volume photoconductivity has as yet been observed at any wavelength in single crystals of these materials.

§ 8. CONCLUSION

The absorption coefficient in PbS and PbSe covers a range of five orders of magnitude in the wavelength range from $0{\cdot}5\,\mu$ to $5\,\mu$. The high absorption ($k \gtrsim 10^5\,\mathrm{cm}^{-1}$) in the visible region of the spectrum can only be measured on evaporated or chemically deposited films (Gibson 1950). This absorption is probably due to electronic transitions between the highest filled band and the conduction band. At longer wavelengths up to the limit of photoconductivity the absorption coefficient remains large ($\sim 10^4\,\mathrm{cm}^{-1}$). This absorption may be due to exciton formation or possibly impurities. Beyond the photoconductive limit the absorption coefficient is small ($\sim 50\,\mathrm{cm}^{-1}$). This absorption is probably at least in part due to the free carriers in the crystal.

ACKNOWLEDGMENTS

The author is indebted to his colleagues at the Telecommunications Research Establishment for much help and advice, and particularly to Dr. E. H. Putley for the Hall constant data quoted. He is indebted to the Chief Scientist, Ministry of Supply, and to the Controller, H.M. Stationery Office, for permission to publish this paper.

REFERENCES

Apker, L., and Taft, E., 1951, *Phys. Rev.*, **81,** 698.

Becker, M., and Fan, H. Y., 1949, *Phys. Rev.*, **76,** 1530 ; 1950, *Ibid.*, **78,** 178 ; 1951, *Semi-Conducting Materials*, ed. H. K. Henisch (London : Butterworths Scientific Publications), p. 132.

Brown, D. A. H., 1949, *J. Sci. Instrum.*, **26,** 194.

Chasmar, R. P., and Gisbon, A. F., 1951, *Proc. Phys. Soc.* B, **64,** 595.

Chasmar, R. P., and Putley, E. H., 1951, *Semi-Conducting Materials*, ed. H. K. Henisch (London : Butterworths Scientific Publications), p. 208.

Gibson, A. F., 1950, *Proc. Phys. Soc.* B, **63,** 756 ; 1951, *Proc. Phys. Soc.* B, **64,** 603 ; 1952, *Ibid.*, **65,** 196.

Gibson, A. F., Lawson, W. D., and Moss, T. S., 1951, *Proc. Phys. Soc.* A, **64,** 1054.

Lawson, W. D., 1951, *J. Appl. Phys.*, **22,** 1444.

Moss, T. S., 1949, *Proc. Phys. Soc.* B, **62,** 741.

Mott, N. F., and Gurney, R. W., 1940, *Electronic Processes in Ionic Crystals* (Oxford : University Press).

Paul, W., Jones, D. A., and Jones, R. V., 1951, *Proc. Phys. Soc.* B, **64,** 528.

Putley, E. H., and Arthur, J. B., 1951, *Proc. Phys. Soc.* B, **64,** 616.

LETTERS TO THE EDITOR

Electrical Conductivity in the Compounds PbS, PbSe, PbTe

Measurements have been made in this laboratory of the conductivity σ and Hall coefficient R of polycrystalline ingots of lead telluride (Chasmar and Putley 1951) and of specimens of Sardinian galena (Putley and Arthur 1951). These measurements showed the existence of intrinsic conductivity in both PbTe and PbS. The object of this letter is to report that similar measurements have now been made on single crystals of PbS, PbSe and PbTe and to compare our results with the previous measurements and with those obtained recently by other workers.

Measurements on single crystals of PbTe and PbS in the intrinsic range have given values for R which are indistinguishable from those obtained from the polycrystalline specimens. The values found for σ, however, are higher than those found for the polycrystalline specimens by a factor of some 5 to 100. This is a result which one would expect because it is easy to show that R is not very structure sensitive while σ is very sensitive to imperfections in the specimen.

Measurements on single crystals of PbTe in the impurity range have enabled the mobility v of electrons and holes to be determined. Above 100° K results have been obtained which are independent of the crystal measured, and therefore it is assumed that in this case only lattice scattering is significant. The earlier measurements on polycrystalline PbTe gave mobilities which appeared to fit an exponential law of the form predicted by Mott and Fröhlich (1939), but the results now obtained using single crystals can be better represented by the power law $v=v_0\,T^{-5/2}$ where v_0 is a constant over the temperature range 100–700° K. The exponential law should only apply for T less than Θ, the Debye temperature. Recent measurements in our low temperature laboratory have shown that Θ is of the order of 150° K (D. H. Parkinson, unpublished) for both PbS and PbTe so that one should not expect the Mott–Fröhlich formula to apply to these mobility measurements. Above the Debye temperature the mobility is expected to vary as a power law, but theory predicts either $v\propto T^{-1/2}$ or $v\propto T^{-3/2}$ so that the observed $T^{-5/2}$ law is not explained. Below 100° K the mobility values obtained depend to some extent on the specimen and although some measurements have been made at 77° K and 20° K sufficient data are not yet available to determine the law of the variation of mobility with temperature.

At 77° K v is about 10 000–20 000 cm^2/v sec and at 20° K about 100 000 cm^2/v sec. These results were obtained from crystals containing about 10^{17}–10^{18} carriers/cm^3. It was found that in these crystals impurity scattering of the type found in silicon and germanium did not appear to be important.

The mobility in single crystals of PbS and PbSe has been found to behave in a manner similar to that described for PbTe. The number of crystals studied has been smaller. It has been found that some p-type crystals give higher mobility values than the best available n-type crystals. Since in the intrinsic range R is negative, the mobility of electrons must be greater than that of holes. These inconsistencies suggest that some of the PbS and PbSe crystals cannot be so perfect as the PbTe crystals.

The numerical data now obtained are summarized in the table. It is seen that the mobilities in single crystals are two or three times greater than the values reported for polycrystalline specimens (for example PbS, Eisenmann 1940, PbSe, Bauer 1940, PbTe, Chasmar and Putley 1951). Measurements of mobilities in thin films have given values in the range 0·5–50 cm^2 (Hintenberger 1941, Lothrop 1949). Moreover, the mobility in a layer falls rapidly as the temperature is lowered, which is opposite to the behaviour for single crystals. Thus it is clear that the structure of the layer has such a profound effect on its resistance that it is unwise to use the results of measurements on layers to attempt to deduce the band structure or other properties of single crystals.

Compound		PbS	PbSe	PbTe
Gap between full and empty bands (Mev)		1·17	—	0·63
Best values for mobilities at 290° K (cm^2/v sec.)	Electrons	640	1400	2100
	Holes	800	1400	840

The single crystals used were prepared by W. D. Lawson (1951) and we wish to thank him for his co-operation which was essential. We also wish to thank J. B. Arthur who assisted with some of the measurements. Acknowledgment is made to the Chief Scientist, Ministry of Supply, for permission to publish this Letter.

Telecommunications Research Establishment, E. H. Putley.
Great Malvern, Worcs.
25th February 1952.

Bauer, K., 1940, *Ann. Phys., Lpz.*, **38**, 84.
Chasmar, R. P., and Putley, E. H., 1951, *Semi-Conducting Materials*, ed. H. K. Henisch. (London : Butterworths Scientific Publications), p. 208.
Eisenmann, L., 1940, *Ann. Phys., Lpz.*, **38**, 121.
Hintenberger, H., 1941, *Z. Phys.*, **119**, 1.
Lawson, W. D., 1951, *J. Appl. Phys.*, **22**, 1444.
Lothrop, E. W., 1949, *Dissertation*, Northwestern University, Illinois.
Mott, N. F., and Fröhlich, H., 1939, *Proc. Roy. Soc.* A, **171**, 496.
Putley, E. H., and Arthur, J. B., 1951, *Proc. Phys. Soc.* B, **64**, 616.

The Spontaneous Magnetization of Magnesium Ferrite and Magnesium Ferrite-Aluminate Powders at Low Temperatures

X-ray diffraction studies (Barth and Posnjak 1932, Kingsnorth 1950, Kingsnorth and Welch 1952) on magnesium ferrite ($MgFe_2O_4$) suggest that it has the inversed spinel structure—half the Fe^{3+} ions occupying tetrahedral or A sites, and the remaining Fe^{3+} ions and the Mg^{2+} ions occupying octahedral or B sites. (In a normal spinel structure the Mg^{2+} ions would be in A sites and all the Fe^{3+} ions in B sites.) Since the Mg^{2+} ion is diamagnetic, this would result, according to Néel's theory (1948) of the magnetic properties of ferrites, either in complete antiferromagnetism or in ferromagnetic behaviour in which the saturation magnetization was zero at absolute zero, rose to a maximum, and fell again to zero at a higher temperature—as in curve L of Néel's paper. The observed ferromagnetism of magnesium ferrite, which was known to persist down to liquid air temperatures, has been explained by Gorter (1950), following Néel, by the suggestion that this ferrite might have an incompletely inverted spinel structure, that is, that some Mg^{2+} ions might occupy A sites. The magnetic balance between Fe^{3+} ions in A sites and B sites would then be upset; the necessary degree of reversion to the normal structure might not be detectable by x-ray analysis. There is supporting magnetic evidence (Pauthenet and Bochirol 1951) that the amount of partial reversion depends in a simple way on the temperature from which the magnesium ferrite has been quenched, and there appears to be some correlation (Kittel 1951) between the amount of the partial reversion and the frequency of the observed 'natural resonance' peak of permeability (Roberts 1951) in such materials.

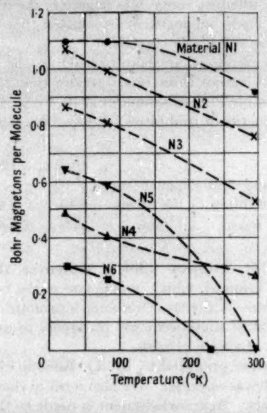

In order to investigate whether magnesium ferrite might not in fact behave at lower temperatures according to Néel's curve L (which does not appear to have been experimentally observed for any ferrite), we have extended measurements of the saturation magnetization of magnesium ferrite down to about 25° K. The results are shown in the curve of material N1 in the figure. It is clear that non-zero spontaneous magnetization must persist down to absolute zero, so that Néel's curve L does not represent the behaviour and some such explanation as that already given must stand.

We have carried out measurements also on five mixed ferrite-aluminates (solid solutions) of the following compositions (Nicks 1951, Nicks and Welch 1952): N2, $MgAl_{0\cdot2}Fe_{1\cdot8}O_4$; N3, $MgAl_{0\cdot4}Fe_{1\cdot6}O_4$; N4, $MgAl_{0\cdot6}Fe_{1\cdot4}O_4$; N5, $MgAl_{0\cdot8}Fe_{1\cdot2}O_4$; N6, $MgAlFeO_4$. As also shown in the figure, all these clearly have non-zero saturation magnetization at absolute zero. As will be seen, the magnetization decreases steadily as Al^{3+} ions replace Fe^{3+} ions—apart from minor unsystematic variations which may be due to the effects of heat-treatments.

Since spinel itself, $MgAl_2O_4$, has the normal spinel structure, with the Al^{3+} ions in B sites, a plausible assumption is that all the Al^{3+} ions in these mixed ferrites go into B sites, causing progressive reversion of the Mg^{2+} ions into A sites. The above values of saturation magnetization can then be accounted for by postulating in each case about 20% greater occupation of B sites than of A sites by the Fe^{3+} ions.

Our thanks are due to Mr. H. W. Hunter and Mr. D. G. M. Shirley for their assistance with the measurements, and to Dr. A. J. E. Welch, of the Department of Chemistry, Imperial College, London, for his kindness in supplying the ferrite sample materials.

One of us (G. O. J.) is indebted to the Department of Scientific and Industrial Research for a grant-in-aid, and to Imperial Chemical Industries, Limited, and the Central Research Fund of the University of London for the loan of apparatus.

Queen Mary College, G. O. JONES.
University of London, London E.1.
Post Office Engineering Department, F. F. ROBERTS.
Research Station,
Dollis Hill, London N.W.2.
20th February 1952.

BARTH, T. F. W., and POSNJAK, E., 1932, *Z. Kristallogr.*, **82**, 325.
GORTER, E. W., 1950, *Nature, Lond.*, **165**, 798.
KINGSNORTH, S. W., 1950, *Thesis*, University of London.
KINGSNORTH, S. W., and WELCH, A. J. E., 1952, *Trans. Faraday Soc.* (in the press).
KITTEL, C., 1951, *Phys. Rev.*, **82**, 565.
NÉEL, L., 1948, *Ann. Phys., Paris*, **3**, 137.
NICKS, P. F., 1951, *Thesis*, University of London.
NICKS, P. F., and WELCH, A. J. E., 1952, *Trans. Faraday Soc.* (in the press).
PAUTHENET, R., and BOCHIROL, L., 1951, *J. Phys. Radium*, **12**, 249.
ROBERTS, F. F., 1951, *J. Phys. Radium*, **12**, 301.

REVIEWS OF BOOKS

The Aurorae, by L. HARANG. International Astrophysics Series, Vol. 1. Pp. x + 166. (London: Chapman & Hall, 1951). 25*s*.

This volume is the first of a new series of 'authoritative volumes dealing with the main branches of Astrophysics and Radio-Astronomy'. They are intended both for specialists and for students, and 'some of the titles may have a wider and more popular appeal, but this will be secondary to their main purpose, which is to assist in teaching .... and the advancement' of their subjects.

The title of this volume has indeed a popular appeal, but the book itself is mainly of technical interest; little is given of the much that can be said on the spectacular aspects of this wonderful phenomenon.

To the professional or amateur scientist interested in the systematic observation and study of the aurora, the volume will prove helpful in many ways. The author is a distinguished auroral observer, who contributed much to our auroral knowledge while he was head of the Auroral Observatory at Tromsö, Norway. In writing on auroral classification and spectroscopy, on height determination and location of aurorae by simultaneous photography from two well-separated stations, he guides the reader from his store of practical knowledge.

Besides giving the main results of these researches, he discusses briefly the associations of aurorae with magnetic storms and disturbances of earth currents and the ionosphere. He gives also a concise account of Störmer's mathematical development of Birkeland's corpuscular theory of the aurora.

The volume is very well illustrated; its 157 pages of text include 152 photographs and diagrams. S. C.

Classical Mechanics, by H. C. Corben and Philip Stehle. Pp. xvii + 388. (New York: John Wiley; London: Chapman and Hall, 1950.) 52*s*.

Despite its appalling price for British purchasers, due partly to the doleful effect of devaluation, this work will amply repay those who can afford it, and should be in every university and college mathematical library.

For the benefit of students of dynamics who have passed well beyond the elementary stage and are primarily interested in the subject as an essential to the understanding of atomic physics, rather than in those aspects which are treated in the later chapters of Whittaker's *Analytical Dynamics*, this book can be whole-heartedly recommended. Recently there has been something of a renaissance in the writing of books on dynamics, and the authors of this book in particular are to be congratulated on their contribution to this revival.

The chief objectives of the authors are (i) to present classical mechanics so as to make clear exactly what it is about and to what it applies in nature, and (ii) " to help the reader sense the continuity in physical thought as he advances from classical mechanics to quantum mechanics and relativistic mechanics ".

Very wisely the authors begin with a set of introductory exercises, remarking that those students who cannot do them with comparative ease are well advised to study first some book or course in which " such problems are discussed in more detail than they are here ". The main body of the book is devoted to an excellent discussion of Lagrange's equations and their applications, the Hamiltonian theory, contact transformations, Poisson brackets and an introduction to special relativity theory. The final chapter is devoted to the motion of particles in high energy accelerators. Tensor methods which distinguish between covariant and contravariant components of vectors and tensors are employed throughout. The theory of real linear vector spaces is also discussed and applied.

At the end of each chapter there are a few exercises for the student to attempt. Any student aspiring to be a mathematical physicist would benefit greatly from a careful reading of this book. The print is clear and easy to read. The size of page is such that the book can be conveniently read in an armchair by older readers who are familiar with the main themes but wish to revise either the subject as a whole or special topics in their spare time.

G. J. WHITROW.

General Astronomy, by Sir Harold Spencer Jones. Pp. ix + 456. 3rd Edition, revised. (London: Arnold, 1951.) 30*s*.

This is the third edition of a well-known textbook, first published nearly thirty years ago at a time when it was still possible to compress a fairly comprehensive description of astronomy into one volume. The subject has grown out of all recognition since then, and all that can today be expected within such restricted space is a general introduction, with a summary of essential facts and generally agreed ideas. Viewed in this light, *General Astronomy* can still be recommended as a sound and reliable textbook.

The book has been reset and a number of new illustrations added. In general a conservative selection of material has been made, with a welcome bias in favour of ideas which are based on, or can be checked by, observation. Although a few small inaccuracies have been noted, this latest revision has for the most part been done thoroughly and with good judgment. Most specialists will doubtless find an occasional favourite item omitted, but that seems almost inevitable in a book of this length. For example, the present reviewer has missed any reference to the Lyot filter, the cinematography of prominences, radio stars (although radio observations of the Sun and of meteors are mentioned), Baade's stellar populations I and II, or to the direction of rotation of the spiral nebulae. Some readers may feel that the book is a little too attentive to older theories at the expense of the newer, but nevertheless the student who starts his astronomy with this as his text will learn a body of well-founded fact, very little of which he will have to discard as fashions change, as they inevitably will. There is room in astronomy for more books of this character.

R. O. REDMAN.

Isaac Newton, by S. I. WAWILOW. Pp. viii + 214. 1st German Edition. (Berlin: Akademie-Verlag, 1951.) 8.90 DM.

This book is the authorized translation from Russian into German of a biography of Isaac Newton written by a Russian scientist who, at the time of his death early in 1951, was President of the Academy of Sciences of the U.S.S.R. His own interests, which lay predominantly in the optical realm, had led him to analyse and translate into Russian the *Opticks* of Newton, the tercentenary of whose birth subsequently called forth this wider survey of the philosopher's life and achievements. It was first published by the Russian Academy in 1943 as one of a series of scientific works apparently intended for the serious general reader; and this translation is based upon the second edition of 1945.

Following a brief sketch of Newton's boyhood and student years, six chapters (comprising nearly two-fifths of the book) are devoted to his researches on light, in which the author recognizes the germ of all Newton's subsequent discoveries and the mature expression of his characteristic philosophy of physics. It was from optics that Newton passed to gravitational theory by way of speculations on the role of the aether. Wawilow recognizes the contributions which lesser men such as Borelli and Hooke made to the Newtonian synthesis; and he explains the criticisms to which the underlying assumptions of the *Principia* have been subjected by Einstein. The later chapters deal more briefly with Newton's work in mathematics and his controversy with Leibniz, his researches in chemistry, his theological writings and public life. There is a short classified bibliography but no index. The plates include eight likenesses of Newton (several of admittedly doubtful authenticity).

Wawilow obviously took pains to acquaint himself with the unfamiliar historical setting of Newton's career. His book is soberly written, free from bias, and even from the expected 'social-economic' emphasis. The author has made considerable use of L. T. More's biography of 1934, but he has taken account of more recent amendments to the traditional story. In the course of translation and re-translation the versions of passages quoted here have become noticeably free; also some errors have crept into the text. On page 5 Bath should read Bate; the date of Römer's determination of the velocity of light (page 24) was 1676; the Royal Society list reproduced in fig. 13 relates to 1675, not 1671; something has gone wrong with the formulation of Kepler's third law on page 99, and *Meshemami* on page 152 should presumably read *Masham*. A. ARMITAGE.

Modern Interferometers, by C. CANDLER, Pp. 502. (London: Hilger and Watts, 1951.) 57*s*. 6*d*.

The title of this book is rather misleading, since it suggests that there are early types of interferometer which are not described, whereas, in fact, the whole field seems to be treated. Evidence of this may be seen in the lists of references at the end of each chapter, the first few entries dating in most cases from the early years of the last century. The references are indeed very comprehensive, and they bear witness to the thoroughness with which the material for this book has been collated. Particularly valuable are the separate lists of Russian publications.

The treatment adopted will commend itself to users of interferometers. The author obviously has the 'feel' of the instruments he describes. Detailed accounts of the methods of adjustment, performance and sources of trouble are given.

The theory of interference is treated but sketchily. For example, only a qualitative treatment is given of the influence of the size of source on fringe visibility: the reader is referred to the work of Hansen. One would have thought that a full discussion of such a fundamental question would have been included in the text. It is welcome to find, on the other hand, insistence on the importance of group path differences and the group refractive index.

It is to be hoped that some day the author will provide an account of the developments that have taken place during the last few years in such fields as interference microscopes, interference filters and new techniques in the testing of gratings.

It may be remarked that the diffraction grating is regarded as an interferometer and more than 100 pages are devoted to ruling engines, mountings and the aberrations of gratings.

The book is well produced, and it will find a welcome place on many bookshelves.

H. H. HOPKINS.

The Conduction of Electricity through Gases, by K. G. EMELÉUS. Pp. x + 99. 3rd Edition, revised. (London: Methuen, 1951.) 5*s.* 6*d.*

This is the third edition of Professor Emeléus' little book. It differs from the first two editions, published in 1929 and 1936, only in that a number of minor alterations have been made to bring the subject matter up to date. The book cannot, of course, compare with the larger treatises, but is suitable for non-specialists or for those with little previous acquaintance with phenomena associated with electrical discharges in gases.

It gives a concise elementary exposition of the fundamental aspects of the subject. The explanations are clear, and brevity is largely achieved without resulting in inaccuracy.

Since the last edition was published the use of discharge lamps for lighting has become widespread, and, since this is the major application of electrical discharges through gases, it is a pity that space could not be found for some discussion on the spectral properties of the positive column.

V. J. FRANCIS.

Étude d'un champ aérodynamique par les ultrasons combinés à la strioscopie, by M. MERLE. Pp. x + 28. (Paris: Publications Scientifiques et Techniques du Ministère de l'Air, 1951.) 300 fr.

Détermination en soufflerie de la distribution de la circulation le long de l'envergure des ailes par la méthode des fumées, by J. VALENSI, H. PARIGI and M. REBONT. Pp. xii + 35. (Paris: Publications Scientifiques et Techniques du Ministère de l'Air, 1951.) 400 fr.

CONTENTS FOR SECTION A

PAGE

Dr. C. DOMB. On the Use of a Random Parameter in Combinatorial Problems . 305
Miss D. G. PADFIELD. The Range of Tensor Forces in the Deuteron Ground State 309
Mr. F. BOOTH and Mr. J. A. ENDERBY. On Electrical Effects due to Sound Waves in Colloidal Suspensions 321
Mr. V. L. NEWHOUSE. Discontinuities in the Variation of Magnetization with Temperature 325
Mr. R. E. SIDAY and Dr. D. A. SILVERSTON. The Construction and Testing of a Magnetic Prism β-Spectrograph of High Resolution, with a Note on the reported Fine-structure of certain Internal Conversion Lines of RaC.C′ . 328
Dr. D. A. SILVERSTON. The Re-investigation of some Photoelectron Lines of Thorium (B + C) 344
Dr. R. HILL. The Elastic Behaviour of a Crystalline Aggregate 349
Mr. D. J. HOWARTH and Prof. H. JONES. The Cellular Method of Determining Electronic Wave Functions and Eigenvalues in Crystals, with Applications to Sodium 355

Letters to the Editor:

- Mr. G. S. BOGLE and Dr. H. E. D. SCOVIL. Nuclear Spins of Samarium 147 and 149 368
- Mr. R. J. ELLIOTT and Dr. K. W. H. STEVENS. The Paramagnetism of Samarium Ethyl Sulphate: Theory 370
- Dr. E. R. ANDREW and Mr. R. G. EADES. Proton Magnetic Resonance in Solid Cyclohexane 371
- Mr. A. R. LANG. Wavelength Resolution of X-Ray Proportional Counters 372
- Mr. A. D. CAUNT and Dr. R. F. BARROW. The Ultra-Violet Spectrum of a Diatomic Hydride 373
- Dr. R. B. DINGLE. Derivation of the Velocity of Second Sound from Maxwell's Equation of Transfer 374
- Dr. R. A. BUCKINGHAM and Mr. R. A. SCRIVEN. Diffusion in Gaseous Helium at Low Temperatures 376
- Mr. S. J. WYARD. Intensity Distribution of Bremsstrahlung from Beta-Rays 377

Reviews of Books 379
Contents for Section B 382
Abstracts for Section B 383

ABSTRACTS FOR SECTION A

On the Use of a Random Parameter in Combinatorial Problems, by C. Domb.

ABSTRACT. Many problems in probability connected with n events occurring randomly in space can be substantially simplified by dealing first with an indefinite number of events distributed in a Poisson series. A combinatorial problem arising in cosmic-ray counting discussed recently by Schrödinger provides a good example, and several properties of the corresponding distribution are derived. A generalization of this problem is considered, and the method is also applied to the random division of a line.

The Range of Tensor Forces in the Deuteron Ground State, by D. G. Padfield.

ABSTRACT. A set of nuclear parameters (ranges and depths of potential wells) yielding the established values of the binding energy, quadrupole moment and magnetic moment of the deuteron, and consistent with the other experimental data relevant to the ground state of the neutron–proton system has been found.

On Electrical Effects due to Sound Waves in Colloidal Suspensions, by F. Booth and J. A. Enderby.

ABSTRACT. An expression is given for the potential differences set up in colloidal suspensions of solid particles by the passage of sound waves which is correct to the first power of the zeta potential of the particles. The question was examined in detail by Enderby in 1951. For a certain range of values of relevant parameters it was found necessary to introduce the simplification that the mobilities of the various ionic species in the electrolyte surrounding the colloidal particles were identical. In the present paper it is shown how the potential may be calculated quite generally without this restriction, by the use of vector methods.

Discontinuities in the Variation of Magnetization with Temperature, by V. L. Newhouse.

ABSTRACT. It is demonstrated that magnetic discontinuities accompany changes of temperature at constant field. The effect is investigated for hard-drawn iron and nickel and is accounted for in terms of two mechanisms, one associated with the decrease of coercivity with rise of temperature and the other associated with the disperse field due to the thermal oscillations of the carriers of magnetic moment.

The Construction and Testing of a Magnetic Prism β-particle Spectrograph of High Resolution, with a Note on the reported Fine-structure of certain Internal Conversion Lines of RaC.C$'$, by R. E. Siday and D. A. Silverston.

ABSTRACT. The first set-up of a very simple high resolution β-spectrograph is described. The instrument employs the focusing action of a magnetic prism with circular plane poles of 20 cm diameter. For this area of pole surface the dispersion is large, giving advantage to the width of source that may be used ; and the instrument can focus electrons with energies up to 4 Mev. It has been used with resolving powers $H\rho/\Delta(H\rho)$ up to 1 300 as measured from microphotometer traces on the plates. It appears to be the only instrument that has been operated at these resolutions as a spectrograph.

As a β-spectrometer, the resolving power should be 15% higher, but this has not yet been tested. As far as can be seen it has a luminosity roughly comparable with that of the ketron, but unlike that instrument it has considerable flexibility of experimental arrangement promising improved performance.

It has been used to look for the fine structure of the K-conversion line corresponding to the 1 414 kev γ-transition in the disintegration RaC.C$'$ reported by Latyshev and others. In agreement with the work of Bashilov and others who employed the ketron, and of Serebriskaya, Shpinel and Forafontov who used a spectrometer of completely novel design, this line was found to be highly monokinetic.

The Re-investigation of some Photoelectron Lines of Thorium $(B+C)$, by D. A. Silverston.

ABSTRACT. The β-ray spectrum of thorium (B+C) has been re-investigated using the β-ray spectrograph described by Siday and Silverston. The range 200 kev–300 kev was studied in detail using photographic recording and a previously unobserved γ-ray of energy 294·6 kev has been attributed to the transition thorium C.C″. The conversion lines of the γF ray of thorium B.C in the L_{I}, L_{II} electronic shells have been resolved and their relative intensities have been found using a Geiger counter. The conversion of the same γ-ray in the M_{I}, M_{II} electron shells has been measured and the lines have been partially resolved. The M photoelectron line associated with the transition thorium C″.D has been examined and its suspected doublet structure confirmed.

The Elastic Behaviour of a Crystalline Aggregate, by R. Hill.

ABSTRACT. The connection between the elastic behaviour of an aggregate and a single crystal is considered, with special reference to the theories of Voigt, Reuss, and Huber and Schmid. The elastic limit under various stress systems is also considered ; in particular, it is shown that the tensile elastic limit of a face-centred aggregate cannot exceed two-thirds of the stress at which pronounced plastic distortion occurs.

The Cellular Method of Determining Electronic Wave Functions and Eigenvalues in Crystals, with Applications to Sodium, by D. J. Howarth and H. Jones.

ABSTRACT. The eigenvalues and wave functions for the conduction electrons in metallic sodium are calculated for various points of high symmetry in the Brillouin zone. The method adopted is an extension of that used by von der Lage and Bethe in which boundary conditions are applied at a large number of points on the surface of the atomic polyhedron. Eigenvalues are obtained for states whose wave vectors lie at the ends of the 2-fold, 3-fold and 4-fold axes. The energy gap at the centre of a face of the zone is found to be 0·65 ev. A method of testing the results, of a more general nature than the empty lattice test of Shockley, is outlined and applied to certain cases.

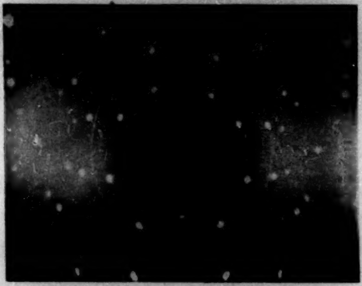

Fig. 2 (*b*). Cylindrical Laue photograph, radius 3 cm, showing diamond (Congo Cube). [110] vertical. X-rays along [100]. Cu radiation + Fe foil. 30 kv 15 mA. 2 hrs.

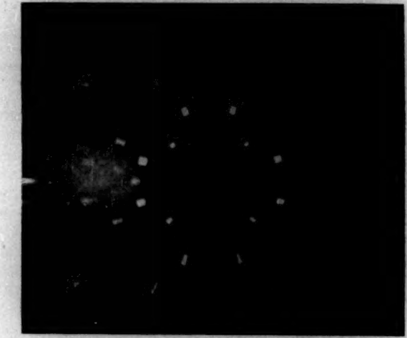

Fig. 3. Cylindrical Laue photograph, radius 3 cm, showing diamond. Mo radiation + SrO foil. Beam along [100]. [001] vertical. 50 kv 10 mA. 2 hrs.

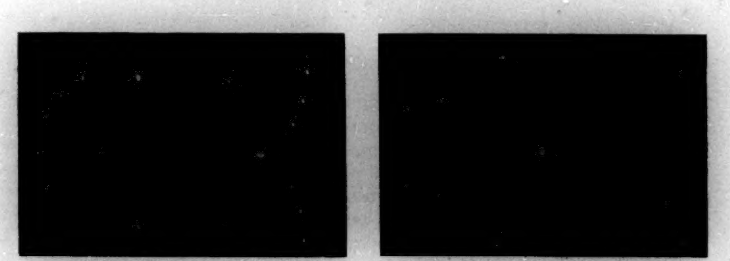

(*a*) (*b*)

Fig. 5 (*a*). Diamond [110] vertical. Cu radiation. Beam parallel to [111]. ($\theta_{111}-2\frac{1}{2}^\circ$ for CuKα) 30 kv 25 mA. 1 hr.

Fig. 5 (*b*). Diamond [110] vertical. Cu radiation. ($\theta_{111}-2\frac{1}{2}^\circ$ for CuKα.) Beam at $10\frac{1}{2}^\circ$ to [100]. 30 kv 12 mA. 1 hr.